New Mexico Geological Society

Downloaded from: https://nmgs.nmt.edu/publications/guidebooks/76



Second-Day Road Log: Northwest Albuquerque Basin: Rio Rancho and Ceja del Rio Puerco

Daniel J. Koning, Sean D. Connell, Jeremy K. Rugenstein, Spencer G. Lucas, and Geoff Rawling
2026, pp. 47-86. https://doi.org/10.56577/FFC-76.47

in:

Geology of the Albuquerque Region - Fall Field Conference 2026, Connell, Sean D.; Koning, Daniel J.;, New Mexico Geological Society 76th Annual Fall Field Conference Guidebook, 452 p. https://doi.org/10.56577/FFC-76

This is one of many related papers that were included in the 2026 NMGS Fall Field Conference Guidebook.

Annual NMGS Fall Field Conference Guidebooks

Every fall since 1950, the New Mexico Geological Society (NMGS) has held an annual Fall Field Conference that explores some region of New Mexico (or surrounding states). Always well attended, these conferences provide a guidebook to participants. Besides detailed road logs, the guidebooks contain many well written, edited, and peer-reviewed geoscience papers. These books have set the national standard for geologic guidebooks and are an essential geologic reference for anyone working in or around New Mexico.

Free Downloads

NMGS has decided to make peer-reviewed papers from our Fall Field Conference guidebooks available for free download. This is in keeping with our mission of promoting interest, research, and cooperation regarding geology in New Mexico. However, guidebook sales represent a significant proportion of our operating budget. Therefore, only *research papers* are available for download. *Road logs*, *mini-papers*, and other selected content are available only in print for recent guidebooks.

Copyright Information

Publications of the New Mexico Geological Society, printed and electronic, are protected by the copyright laws of the United States. No material from the NMGS website, or printed and electronic publications, may be reprinted or redistributed without NMGS permission. Contact us for permission to reprint portions of any of our publications.

One printed copy of any materials from the NMGS website or our print and electronic publications may be made for individual use without our permission. Teachers and students may make unlimited copies for educational use. Any other use of these materials requires explicit permission.

This page is intentionally left blank to maintain order of facing pages.

SECOND-DAY ROAD LOG:

NORTHWEST ALBUQUERQUE BASIN: RIO RANCHO AND CEJA DEL RIO PUERCO

DANIEL J. KONING[1], SEAN D. CONNELL[1], JEREMY K. RUGENSTEIN[2], SPENCER G. LUCAS[3], AND GEOFF RAWLING[1]

[1]New Mexico Bureau of Geology and Mineral Resources, 801 Leroy Place, Socorro, NM 87801; dan.koning@nmt.edu
[2]Department of Geosciences, Colorado State University, 400 University Ave., Fort Collins, CO 80523
[3]New Mexico Museum of Natural History and Science, 1801 Mountain Road NW, Albuquerque, NM 87104

Assembly Point: Parking lot for New Mexico Museum of Natural History and Science Annex (950 Eighteenth Street NW)
Departure Time: 7:30 AM
Distance: 68 miles
Stops: 2

Views, landmarks, and outcrops are given using the clock system, where 12:00 is straight ahead, 3:00 is to the right, and 9:00 is to the left. Driving distances are given in miles.

SUMMARY

The Day 2 agenda focuses on the Santa Fe Group in the northwestern Albuquerque Basin. We drive north on Interstate 25 and then use Paseo del Norte and Unser Boulevards to reach Rio Rancho. This rapidly growing city is now the third-largest metropolitan area in New Mexico. For its municipal needs, Rio Rancho is solely reliant on groundwater pumped from the Santa Fe Group regional aquifer, making understanding the stratigraphic and hydrogeologic character of its aquifer essential for efficient long-term water management (Koning et al., 2026a, 2026b, 2026c). From Rio Rancho, we drive west on Southern Boulevard across the Llano de Albuquerque ("llano" means plains in Spanish) to the Ceja del Rio Puerco, the latter being steep, west-facing slopes between the Ceja and the Rio Puerco. On this drive, we pass over several faults, including the east-down Zia fault that bounds the western side of the Montoya graben (sensu Koning et al., 2026a, 2026b, 2026c). Quaternary activity on these faults has allowed wedge-shaped sand deposits to accumulate on their immediate hanging walls (Connell et al., 2026).

Stop 1 is on Santa Ana Pueblo land about 5 km (3 mi) north-northwest from the west end of Southern Boulevard. **Note: unauthorized access is strictly prohibited, and the area is patrolled regularly by Santa Ana range patrol**. Here, we continue the "Nexus theme" of the 2024 Fall Field Conference and discuss the structural nature of the boundary between the Rio Grande rift and Colorado Plateau. Where exactly is the boundary, how is it defined, and how might faults affect groundwater recharge from the Colorado Plateau into rift basin fill? From the vehicles, we hike about 1.6 km (1 mi) south to Arroyo Benavidez, an area of exceptional exposure of the Zia Formation. Participants will alternate among five stations that exemplify the Piedra Parada, Chamisa Mesa, and Cañada Pilares Members of the Zia Formation. The goal is to interpret depositional environments and speculate what might be driving the change in these environments. Participants also observe an exposed fault zone of the Pilares fault, a normal fault offsetting the Zia Formation. We then climb a hill to view the lower Cerro Conejo Formation (Station 6), where we discuss a major unconformity near its base and recent studies that use the stable isotope record of authigenic carbonates to interpret paleoclimates.

Stop 2 is located 1 km (0.6 mi) south–southwest of the western end of Southern Boulevard. Here, we observe and discuss the upper Santa Fe Group stratigraphy and two rift-related faults that offset it: the Sand Hill and the San Ysidro faults. Another feature we can observe is a notable unconformity that separates the middle from the upper Santa Fe Group (late Miocene Arroyo Ojito Formation versus the Plio–Pleistocene Ceja Formation). We discuss the extent and genesis of this important rift feature.

In the topographic amphitheater north of Stop 2, ~30 m (~100 ft) of Quaternary sediment accumulated in a km-scale, wedge-shaped low on the proximal hanging wall of the San Ysidro fault. Referred to as Quaternary hanging wall wedge deposits (Qhwd), these sediments overlie a thick, cumulic, calcic soil developed on top of the Ceja Formation (minimum age for the Ceja is ~1.8–1.6 Ma here; Connell et al., 2013). The Qhwd here is characterized by 0.5–3-m (2–10-ft)-thick tabular units that commonly have calcic paleosols on their upper contacts, imparting a horizontally striped appearance to the unit. The Qhwd would not exist if it was not for the space created by over 1 My of movement on the fault. Here, we discuss how tectonics, paleoclimate, and landscape evolution affect the deposition of these post-Santa Fe Group deposits. Those willing to descend (and then ascend!) a steep slope can view the San Ysidro fault zone and various lithofacies of the Qhwd.

7:30 AM: Depart New Mexico Museum of Natural History and Science Annex parking lot in caravan.

8:45 to 10:00 AM: Stop 1. Hike to Arroyo Benavidez.

10:00 AM to 1:15 PM: Visit six stations at Stop 1. Topics include Zia and Cerro Conejo Formation stratigraphy, sedimentology, and paleoenvironments; fault zone architecture of rift normal faults; Miocene paleoclimate; 17–15-Ma rift-flank unconformity.

1:15 to 2:30 PM: Hike back to vehicles.

2:30 to 3:00 PM: Drive to Stop 2.

3:00 to 4:45 PM: Stop 2**.** Discussion and short hike regarding the Ceja Formation, Rincones paleosurface, and a 30-m (100-ft)-thick Quaternary hanging wall wedge deposit (Qhwd).

4:45 to 5:45 PM: Drive back to the New Mexico Museum of Natural History and Science.

6:30 to 10:00 PM: Indoor, semiformal banquet at New Mexico Museum of Natural History (1801 Mountain Road NW, Albuquerque).

Mileage Description *Distance to next entry*
[Waypoint, decimal degrees, World Geodetic System 1984]

0.0 **Waypoint 2.01 [N35.1016°, W106.6662°]**
Assemble caravan at the parking lot for the New Mexico Museum of Natural History and Science Annex, which is located across the street and northeast of the main museum (1810 Mountain Road NW, Albuquerque). You are parked on the latest Pleistocene–Holocene sedimentary fill of the Rio Grande, which is approximately 24 m (80 ft) thick across much of what is known as the inner valley of the Rio Grande. **Head west to parking lot exit, turning left (south) onto Eighteenth Street NW. ZERO ODOMETER AT THIS TURN.** *0.1*

0.1 **Turn right (west) onto Mountain Road NW.** *0.3*

0.4 **Waypoint 2.02 [N35.1047°, W106.6706°]**
Turn right at stoplight onto Rio Grande Boulevard and head north toward on-ramp to I-40. *0.4*

0.8 **At stoplight, merge onto eastbound I-40.** Quickly and safely move three lanes to the left to avoid local traffic congestion. *0.5*

1.3 Cross intersection of I-40 and Twelfth Street NW. Continue east on I-40. *0.7*

2.0 **Move right onto lane that feeds into the north-bound on-ramp to I-25** (Exit 159C toward Santa Fe). Approach the "Big I," the local name for the intersection of I-40 and I-25. *0.6*

2.6 **Waypoint 2.03 [N35.1050°, W106.6394°]**
Entrance to on-ramp leading to north-bound I-25. *1.1*

3.7 **Exit off-ramp leading to north-bound I-25.** *0.2*

3.9 **Merge left onto north-bound I-25.** *0.7*

4.6 Pass Comanche Road (Exit 227). *0.9*

5.5 Pass Montgomery/Montaño Boulevard overpass (Exit 228). *1.0*

6.5 Pass Jefferson Boulevard (Exit 229). *0.6*

7.1 Cross over north-trending Albuquerque Metropolitan Arroyo Flood Control Authority (AMAFCA) diversion channel. *0.3*

7.4 Pass San Mateo/Osuna Boulevard overpass (Exit 230). *0.5*

7.9 Pass San Antonio Boulevard (Exit 231). After crossing this road, get into the second-from-right lane. *0.5*

8.4 **Waypoint 2.04 [N35.1722°, W106.5840°]**
Exit I-25 onto on-ramp to west-bound Paseo del Norte Boulevard (State Road 423; Exit 232). *0.7*

9.1 **Waypoint 2.05 [N35.1787°, W106.6250°]**
Merge left onto west-bound Paseo del Norte Boulevard. *0.3*

9.4 Intersection of Paseo del Norte Boulevard and Jefferson Street. *0.1*

9.5 Centex American Gypsum Company processing plant to the left (south). *0.2*

9.7 We are traveling on a valley-border geomorphic surface that slopes west toward the Rio Grande, where it projects about 15–18 m (50–60 ft) above the floodplain. It is underlain by sand and gravelly sand corresponding to unit Qay of Connell (2008a). The Qay unit is Holocene to latest Pleistocene in age and overlies older Pleistocene deposits (e.g., the Duranes or Edith Formations). This unit locally is susceptible to soil hydrocompaction. *0.3*

10.0 Cross the AMAFCA North Diversion Channel. Note that the channel is trending north here whereas the Rio Grande flows south. This feat of engineering minimizes the length of the flood control channel across the flat floodplain since the Rio Grande at the terminus is near the eastern side of the floodplain while southward it lies near the western side. There is an added benefit to this placement. The Rio Grande is a losing stream here (e.g., Liu and Sheng, 2011; Bexfield et al., 2011; Rankin et al., 2013), and this diversion maximizes the amount of recharge into the Quaternary valley fill and Santa Fe Group aquifers from floodwaters. Bike and walking trails commonly are present alongside the structure. *0.6*

10.6 Paseo del Norte Boulevard descends off the Holocene terrace and crosses Edith Boulevard. On the east side of Edith Boulevard is a gravelly deposit called the Edith Formation. The Edith Formation is a middle Pleistocene terrace that is ~3–12 m (~10–40 ft) thick and is discontinuously exposed along the eastern side of the Rio Grande valley (Lambert,

1968; Connell et al., 2007, 2008a). It typically fines upward from a 2–8 m (6–26 ft) thick, quartzite-rich gravel (with abundant cobbles) to a yellowish-brown and reddish-brown mud (4–10 m [13–33 ft] thick) (Connell et al., 2007). The gravelly deposit is disconformably overlain by valley-border alluvial units, and its basal strath lies 12–24 m (40–80 ft) above the Rio Grande floodplain. In most places, the Edith is buried by the younger Duranes Formation (Connell et al., 2007). *0.1*

10.7 To the west lies the relatively flat, eastern floodplain of the Rio Grande and the community of Alameda. *0.1*

10.8 Paseo del Norte Boulevard passes over the Burlington Northern Santa Fe railroad tracks. This is the original line of the Atchison, Topeka, & Santa Fe Railroad, built in 1880. But now, most east-bound and west-bound freight on the railroad goes east of Belen on the Belen cutoff, constructed in 1903–1908 to avoid the problematic Raton Pass (Penner et al., 2014). Although the current north-south line north of Albuquerque receives little freight traffic, it does allow passenger trains like Rail Runner and Amtrak. *0.2*

11.0 Intersection of Second Street and Paseo del Norte Boulevard. *0.4*

11.4 Paseo del Norte passes over Fourth Street. *0.4*

11.8 Cross the acequia called the Chamizal Lateral. *0.3*

12.1 Cross the acequia called the Corrales Lateral. In this area, there are about subequal proportions of agricultural fields and house lots. *0.2*

12.3 Paseo del Norte Boulevard crosses over Rio Grande Boulevard. Beyond is the community called Los Manzanos ("the apple trees" or "apple orchard" in Spanish). *0.2*

12.5 Paseo del Norte Boulevard passes over an acequia, flanked on its western side by a deeper channel called the Albuquerque Drain. Beyond lies the undeveloped bosque (Spanish for woods), which in modern parlance generally conveys woods growing on a floodplain. These drains were installed by the Bureau of Reclamation in the 1930s to keep the groundwater table low enough for crops. Sedimentation in the Rio Grande channel would locally raise the groundwater table in the adjoining floodplain to such an extent that the ground would become marshy and/or the shallow groundwater would evaporate and leave salts. This topic is discussed at Stop 1 of Day 3. *0.3*

12.8 Cross the Rio Grande. Upstream (0.8 mi [1.3 km]) lies the diversion structure for the intake for the San Juan-Chama Surface Water Treatment Plant, operated by the Albuquerque Bernalillo County Water Utility Authority (Water Authority; Fig. 2.01). This facility withdraws and treats river water using a series of chemical and mechanical treatments (including coagulation–microfiltration, ozone, and chlorine) to produce water meeting drinking-water standards. This river water provides about half of Albuquerque's water needs (Water Authority, 2024). To the west lies a narrow sliver of riparian woodlands flanking the Rio Grande. *0.2*

13.0 Cross the western Corrales Riverside Drain that bounds the western side of the bosque. *0.5*

13.5 Off-ramp for north-bound Coors Boulevard. **Continue straight on Paseo del Norte Boulevard.** Ahead is a slight right bend in the road where we ascend small alluvial fans that rim the western margin of the floodplain. *0.2*

13.7 Paseo del Norte Boulevard passes over Coors Boulevard. *0.2*

13.9 Paseo del Norte Boulevard bends gently left and ascends a terrace deposit correlated to the "intermediate stream-valley alluvium" in Connell (2008a). This terrace fill consists mainly of sand and gravelly sand deposited by western tributaries to the Rio Grande. Preserved soils on these deposits exhibit up to Stage II+ to III+ carbonate morphology, but erosion in this area probably results in less developed soils. This fill is interpreted to be middle to late Pleistocene in age. *0.2*

14.1 **Waypoint 2.06 [N35.1812°, W106.6747°]** Paseo del Norte Boulevard and Eagle Ranch Road. **Turn right on Eagle Ranch Road and drive north.** *0.2*

14.3 **Waypoint 2.07 [N35.1838°, W106.6737°]** Paseo del Norte Boulevard and Paradise Boulevard. **Turn left on Paradise Boulevard and drive north.** We are in the southeastern corner of the study area of Koning et al. (2026a, 2026b, 2026c), who constructed a stratigraphic framework and conducted a permeability assessment of the Santa Fe Group aquifer in the northwestern Albuquerque Basin. This study interpreted four hydrostratigraphic units for the study area that approximate layers over length scales of about 5–30 km (3–20 km). The deepest unit could possibly be further



FIGURE 2.01. Photograph of the Rio Grande and the diversion structure for the San Juan-Chama Surface Water Treatment Plant. View to the east.

subdivided if more deep wells are drilled in the future. The basin fill is thickest in this part of the study area. The unit having groundwater with the lowest total dissolved solids (TDS) and highest hydraulic conductivities, the Upper Rio Rancho hydrostratigraphic unit, is also thickest in this part of the study area. Furthermore, because the potentiometric surface (approximating the groundwater table) slopes to the west away from the Rio Grande, this area (being closest to the river) has relatively high groundwater levels. Here, the saturated thickness of the Upper Rio Rancho hydrostratigraphic unit is >460 m (>1,500 ft; Koning et al., 2026a, 2026b, 2026c). *0.1*

14.4 We are driving northwest across a gently east-sloping erosional surface developed on the intermediate alluvium of Connell (2008a). *0.3*

14.7 Intersection of Paradise Boulevard and Davenport Street. A U.S. Post Office is on the southwest corner. West of here, the topographic surface becomes more gently sloping. *0.1*

14.8 This geomorphic surface slopes gently southward toward the Segundo Alto surface of Lambert (1968). This terrace tread (geomorphic surface corresponding to the top of a terrace) lies ~60 m (~200 ft) above the modern Rio Grande floodplain. *0.2*

15.0 Intersection of Golf Course Road and Paradise Boulevard. **Proceed straight on Paradise Boulevard.** The trailhead to the Piedras Marcadas Canyon Trail can be accessed by turning left (south) on Golf Course Road. This trail leads to numerous petroglyphs in Petroglyph National Monument (Fig. 2.02). *0.1*

15.1 Approximate west margin of a local geomorphic surface overlying the intermediate alluvial deposits. *0.1*



FIGURE 2.02. Photograph of petroglyphs at Piedras Marcadas. This site is a must see for people interested in history and Puebloan culture.

15.2 Basalt-capped ridge about 150 m (500 ft) to the left (south). This basalt is part of the Albuquerque volcanic field (Qb2 unit of Connell, 2008a). *0.2*

15.4 Road gently turns right and ascends a gentle east-dipping slope underlain by sandy sediment. *0.5*

15.9 Paradise Road turns gently left. *0.2*

16.1 Ascend onto a subhorizontal surface, where surficial sandy sediment is underlain by the Qb2 basalt flow of the Albuquerque Volcanoes. *0.1*

16.2 **Waypoint 2.08 [N35.1969°, W106.7033°]** Intersection of Paradise Road and Unser Boulevard. **Turn right on Unser Boulevard and proceed north.** *0.2*

16.4 Crest a slight topographic high in this urbanized area of northwest Albuquerque. Here, the Qb2 basalt flow likely underlies several meters of sandy surficial sediment. *0.3*

16.7 Descend into Arroyo de las Calabacillas. This ephemeral tributary to the Rio Grande has a watershed area of ~200 km² (~77 mi²) (AMAFCA, 2026). Arroyo de las Calabacillas and Arroyo de los Montoyas are the primary drainages developed in the northern Llano de Albuquerque and northern Rio Rancho. These arroyos generally drain southeastward, but in their downstream ends, near the Rio Grande, the arroyos take an easterly bend. At this road crossing, the Arroyo de las Calabacillas trends eastward and lies in a 15-m (50-ft)-deep valley. Looking back at 4:00, one can see a basalt flow, 3–4-m (10–13-ft)-thick, interbedded in sandy deposits (Fig. 2.03). The sand below is correlated to the intermediate alluvium of Connell (2008a), whereas the sand above is likely eolian and sheetwash. *0.1*

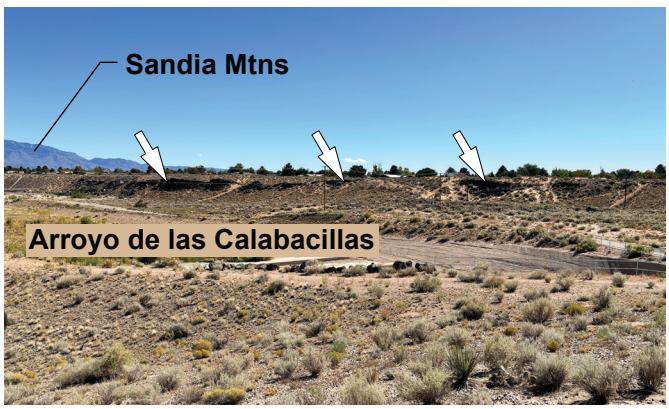


FIGURE 2.03. Photograph of the Qb2 flow of the Albuquerque volcanic field within sandy sediment on the south side of Arroyo de las Calabacillas, about 400 m (1,300 ft) east of Unser Boulevard. White arrows point to the top of the flow. The sand below the basalt is correlated to the intermediate alluvium of Connell (2008a). The uppermost part of this alluvium contains pebbles reworked from the Rio Puerco Member of the Ceja Formation. Above the flow, the sand is a mixture of eolian and sheetwash deposits. The basalt flow is 3–5 m (10–15 ft) thick, black, and vesicular, containing 10–15% plagioclase and 0.5–1% olivine phenocrysts.

16.8 Cross the active wash of Arroyo de las Calabacillas.

At a distance of 3.2 km (2.0 mi) to the east, on the northern flank of the valley, lies the Hunters Ridge monitoring well. It was drilled to 463-m (1,520-ft)-depth and consists of 5 nested piezometers. It encountered a 448-m (1,470-ft)-thick coarse-grained unit underlain by a notably finer-grained, clay-rich unit (Fig. 2.04). *0.1*

16.9 Unser Boulevard bends slightly right and ascends the northern slope of Arroyo de las Calabacillas. *0.2*

17.1 Cross the boundary separating Albuquerque (south) and Rio Rancho (north). Rio Rancho, the "City of Vision" per the welcome sign, is the third-largest metropolitan area in New Mexico and boasts a high rate of growth: 9.7% since the 2020 census (World Population Review, 2026). This population growth is probably driven by the availability and affordability of relatively new homes, and the fact that its crime rate is about one-half that compared with Albuquerque (City of Albuquerque, 2026; Neighborhood Scout, 2026; Meyers and Myers Real Estate, 2026). In contrast to Albuquerque, Rio Rancho lacks surface water rights to the Rio Grande and relies solely on groundwater for domestic and municipal water usage. Therefore, managing its groundwater resources to accommodate its population is both a priority and a challenge for the city. *0.3*

17.4 Intersection of Unser and McMahon Boulevards.

Continue north on Unser Boulevard. Structurally, we are on a south-dipping homocline bounded by two faults: the northwest-striking Coronado-Alameda fault to the east and an inferred east-down fault projecting north from Universe Boulevard that probably coincides with the "unnamed fault(s) near Star Heights" in the USGS Faults and Folds database

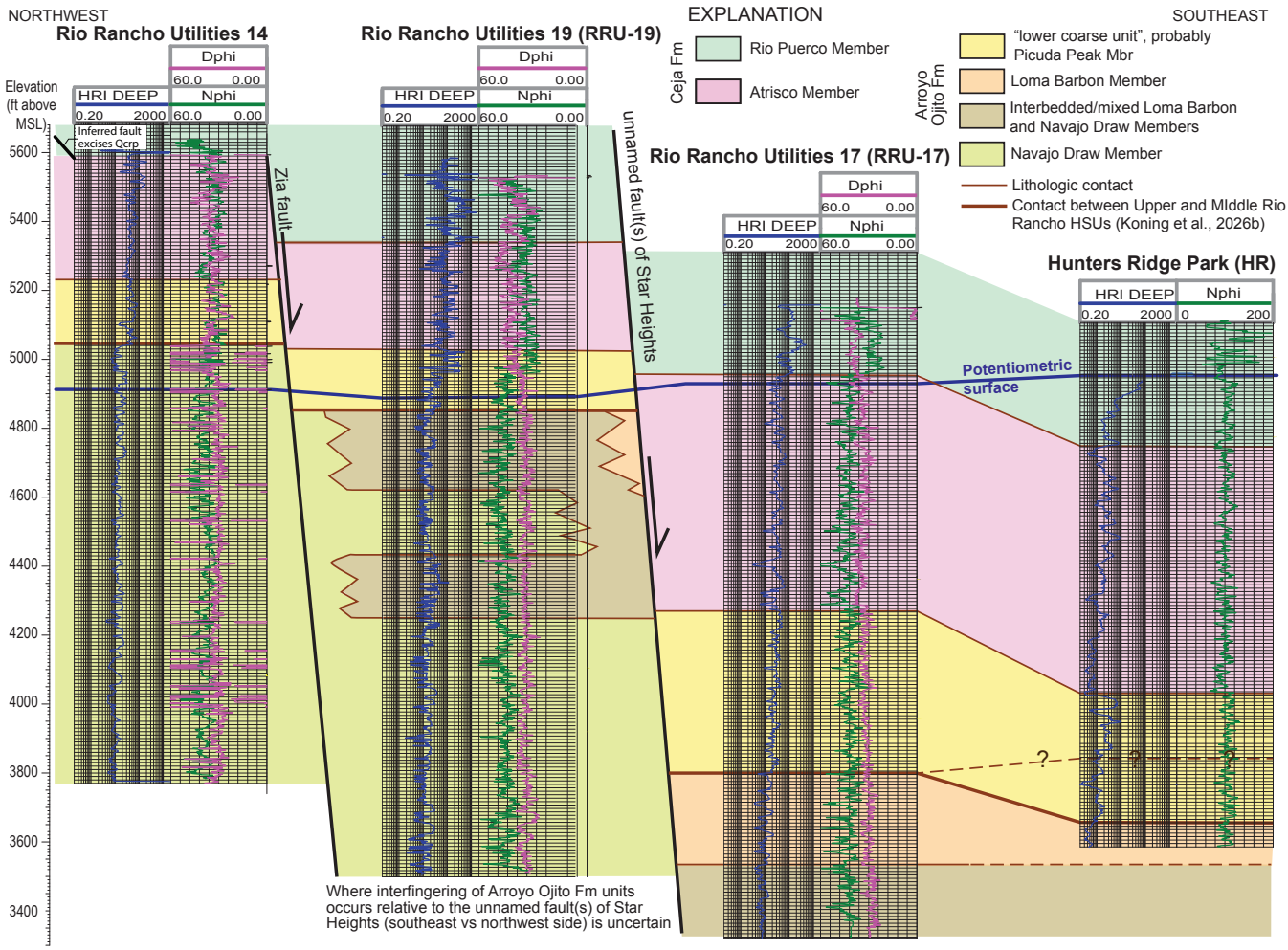


FIGURE 2.04. Subsurface stratigraphic correlation between Rio Rancho Utility wells RRU-14, RRU-19, RRU-17, and the Hunters Ridge Piezometer. The wells are aligned northwest–southeast and are shown in Figure 2.05. Depicted units of the Santa Fe Group belong to the Ceja and Arroyo Ojito Formations. Most of the "lower coarse unit" likely correlates to the Picuda Peak Member of the Arroyo Ojito Formation (sensu Connell, 2008b). Note how the Atrisco Member and the lower coarse unit thicken eastward across unnamed fault(s) of Star Heights, probably due to syndepositional, east-down faulting. The Navajo Draw Member observed in well RRU-14 interfingers eastward into the Loma Barbon Member, with a mixed/interbedded unit mapped in-between (brown shade). Abbreviations in the well headings: HRI_deep = deep induction curve (ohm-meters), D_phi = density porosity curve; N_phi = neutron porosity curve. Descriptions and wireline data are in Koning et al. (2026a). Note how the deep induction curve shifts to the right upsection in these wells, consistent with a general upward coarsening trend in the Santa Fe Group.

(Personius and Jochems, 2016a). We are on an unnamed geomorphic surface bounded on the west by steeper east-facing slopes near the West Paradise fault and to the east by steep slopes bordering the Rio Grande floodplain (east of the Intel facility). *0.1*

17.5 At 3:00 is an eastward view of the Sandia Mountains. *0.3*

17.8 Hill on the northern skyline is a landfill. The lower hill to its right is Loma Colorado de Abajo, which is adjacent to the Rio Rancho High School and the Loma Colorado Library. On the south-facing escarpment of Loma Colorado de Abajo, a reddish-brown and reddish-yellow sandstone of the Ceja Formation yielded tortoise and rodent fossils and numerous fossil rodent burrows, in the age range of 5–3 Ma (Morgan and Lucas, 2000; Morgan and Harris, 2015). *0.4*

18.2 Intersection of Unser and Westside Boulevard. Continue north on Unser Boulevard. At a distance 1 km (0.6 mile) to the west lies the Rio Rancho Utilities (RRU) 17 well (Fig. 2.05). *0.6*

18.8 Intersection of Unser and Cabezon Boulevards. Continue north on Unser Boulevard. North end of the unnamed geomorphic surface described at mile 17.4. *0.6*

19.4 Waypoint 2.09 [N35.2312°, W106.6969°]

Turn left onto Southern Boulevard at the intersection of Unser and Southern Boulevards and REZERO THE ODOMETER. We are in the middle of the Rio Rancho metropolitan area. Rio Rancho is a relatively new city compared with most New Mexico towns and cities. For example, Santa Fe and Albuquerque were established 300–400 years ago, but Rio Rancho had its beginnings in the early 1960s. At that time, the AMREP Corporation purchased 55,000 acres of the Koontz Ranch. Originally called Rio Rancho Estates, AMREP marketed their planned community development to people (primarily retirees) from the Midwest and the eastern United States. The first homes were built in 1966, and by 1977, there were 5,000 residents. AMREP purchased and platted an additional 35,000 acres in 1971. Rio Rancho was incorporated in 1981, and at that time, it had a population of 10,000. Several years later, the city began offering low-interest home loans and Rio Rancho changed from what was initially a retirement community to a town attractive to younger families. Nearly 80% of these arrivals came from Albuquerque. A big boost to the local economy was the construction of a large manufacturing plant by Intel in 1981. In 2023, Intel announced a $3.5 billion expansion to enable manufacturing of cutting-edge semiconductor technologies (Albuquerque.com, 2026; Rio Rancho, 2026).*0.4*

0.4 Cross an unnamed arroyo draining to the south–southeast, which, at the time of writing of the road log, was undergoing flood control-related construction. *0.2*

0.6 Cross a flood-control channel draining southeast. To the west, the surface slopes more steeply to the east, in part due to east-down movement along a north-striking, normal fault system correlated to "unnamed fault(s) near Star Heights" (Fig. 2.06; Connell, 2008a; Personius and Jochems, 2016a). Structural contouring of the fault system suggests approximately 100 m (300 ft) of vertical offset of a 5-Ma stratigraphic contact and 150 m (500 ft) of vertical offset of a ~10-Ma contact (Koning et al., 2026a, 2026b). *0.3*

0.9 Cross the West Paradise fault. Although the Quaternary Faults and Folds database (Personius and Jochems, 2016b) indicates a west dip direction, the topographic surface slopes eastward (Fig. 2.06). *0.4*

1.3 The slope increases slightly to the west, and in this location of slope steepening an east-down normal fault was mapped (Connell, 2008a) that was called "Unnamed faults near Star Heights" in the USGS Faults and Folds Database (Fig. 2.06; Personius and Jochems, 2016a). *0.2*

1.5 Ascend onto the east edge of a mesa-like feature on the larger Llano de Albuquerque. Intersection of Southern Boulevard and Baltic Avenue. Strongly developed calcic soils can be seen in Google Earth imagery at the crest 160 m (530 ft) to the south, and these calcic soils are also evident in the white silt and sand exposed in roadcuts on either side of Southern Boulevard. To the east, the notably lower geomorphic surface coinciding with Unser Boulevard can be seen (Fig. 2.07). *0.3*

1.8 Continue west across a gently west-sloping cuesta. Ahead is the valley of the Arroyo de las Calabacillas (Fig. 2.08). Puesta del Sol Elementary School is to the south. From the entry road to this school, one has a nice view of the northern end of the Albuquerque Volcanoes (Fig. 2.09). *0.1*

1.9 Rainbow Park to north. Cross small arroyo draining southward into Arroyo de las Calabacillas. *0.3*

2.2 Intersection of Southern and Rainbow Boulevards. Continue on Southern Boulevard. About 1.1 km (0.7 mile) to the north lies Rio Rancho Utility Well 19 (RRU-19; Figs. 2.04 and 2.05). Structurally, we are in the middle of a north-trending graben called the Montoya graben by Koning et al. (2026a, 2026b). The Montoya graben is bounded by the Ziana horst to the northeast and the east-down Zia fault to the west (Fig. 2.05). *0.8*

3.0 Waypoint 2.10 [N35.2416°, W106.7513°]

Cross the sandy bed of Arroyo de las Calabacillas. Leave the Rio Rancho and enter a region of where houses and trailers occupy larger acreages outside of city limits. The city does not generally provide water to these houses, so homeowners either have to drill deep wells (water table here is ~230 m [~750 ft] deep) or truck in water. *0.2*

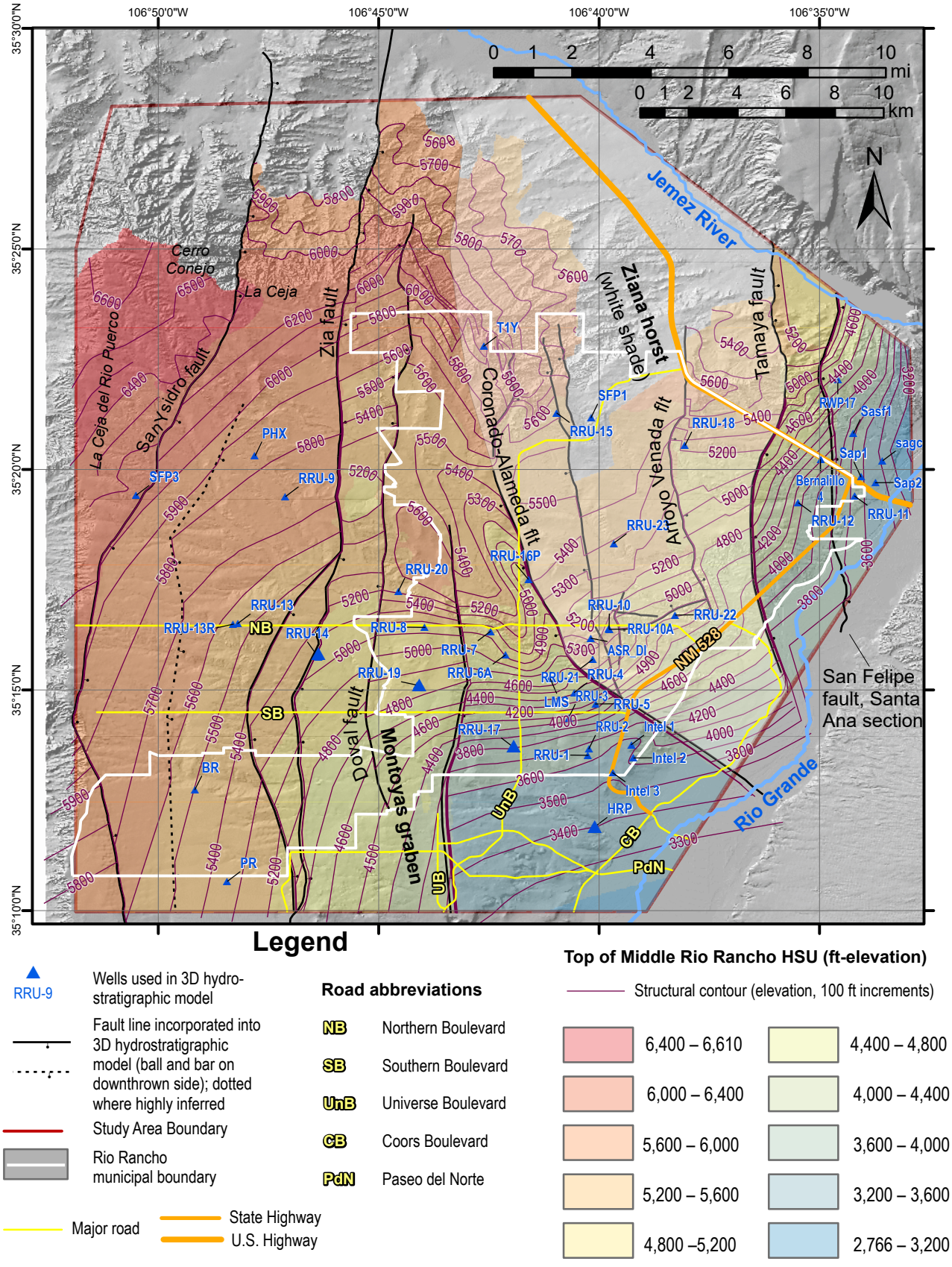


FIGURE 2.05. Map showing structural contours of the contact between the Upper and Middle Rio Rancho hydrostratigraphic units (HSUs). Of these two, the Upper HSU has higher hydraulic conductivities, but the Middle HSU is thicker (Koning et al., 2026a, 2026b, 2026c). The location of wells RRU-15, RRU-19, RRU-17, and the Hunters Ridge piezometer nest (HRP) (Fig. 2.04) are emphasized by depicting their locations as larger blue triangles.

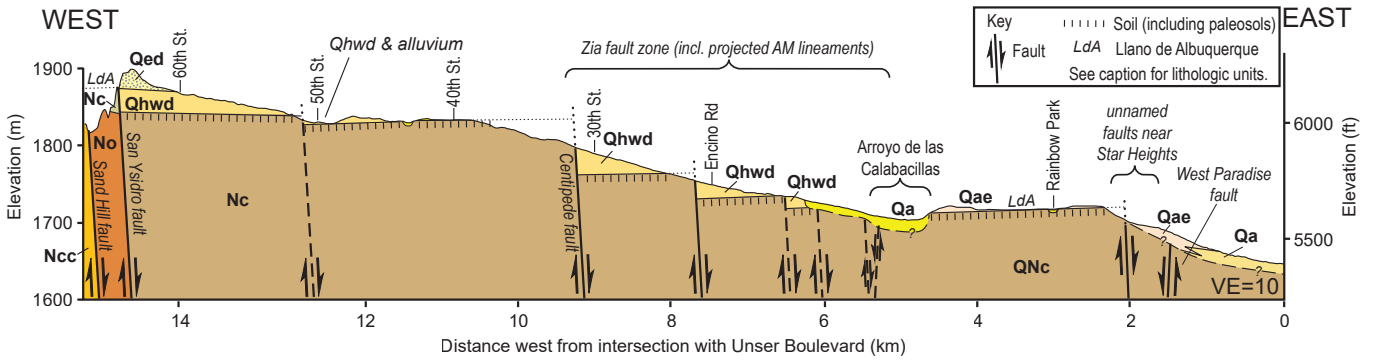


FIGURE 2.06. Topographic profile along Southern Boulevard between its western end and Unser Boulevard. Units include the following: Ncc = Cerro Conejo Formation; No = Arroyo Ojito Formation; QNc = Ceja Formation; Qhwd = Quaternary hanging wall wedge deposits (i.e., Pleistocene eolian, colluvial, and sheetwash deposits); Qae = Quaternary alluvium and eolian sediment, undivided; Qa = Quaternary alluvium.

3.2 Cross a west-down fault inferred by Koning et al. (2026a, 2026b), correlated to the Doval fault of Connell (2008a). *1.2*

4.4 Cross an unnamed, southeast-flowing arroyo that is a tributary to Arroyo de las Calabacillas. North of here (2.3 km [1.4 mi]) lies the Rio Rancho Utilities Well 14 (RRU-14), whose correlation with deep wells to the south–southwest is shown in Figure 2.04. *0.2*

4.6 Intersection of Southern Boulevard and Encino Road. The latter parallels a northwest-trending powerline. *0.2*

4.8 Cross the east strand of the Zia fault (Fig. 2.06; Connell, 2008a), which has a very subtle topographic expression here. The Zia fault is a major east-down normal fault zone that extends ~60 km (~37 mi) north–south in the western Albuquerque Basin. The southern extension of this fault is the County Dump fault (see Day 3 road log), with an ill-defined boundary separating the two near the northern end of the Albuquerque Volcanoes. West–northwest of Rio Rancho, the Zia fault defines the western edge of the Montoya graben of Koning et al. (2026a, 2026b). Structural contouring by Koning et al. (2026a) suggests 60 m (200 ft) of vertical displacement of a 5-Ma contact and ~110 m (~350 ft) of vertical displacement of a 10-Ma contact. Topographic profiles suggest 12–15 m (40–50 ft) of vertical displacement of the Llano de Albuquerque surface. *0.9*

5.7 Cross the Centipede segment of the Zia fault (Fig. 2.06; Connell, 2008a). A topographic profile across this fault segment suggests ~10 m (~33 ft) of east-down vertical displacement since abandonment of the 1.5-Ma Llano de Albuquerque surface. However, this east-facing scarp is quite eroded and it is difficult to disentangle faulting from erosion by Arroyo de las Calabacillas and its tributaries. The eroded topography reveals the gravelly sand substrate correlated to the Rio Puerco Member of the Ceja Formation. The gravels are generally subrounded-rounded pebbles composed of basaltic–intermediate volcanics, granite, various cherts (including the whitish and mottled Pedernal Chert), and sandstone. *0.5*

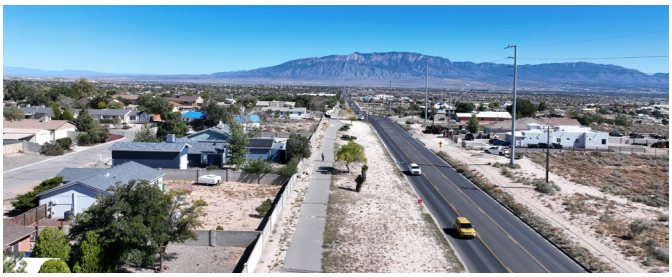


FIGURE 2.07. Photo looking eastwards down Southern Boulevard near Rainbow Park (2.9 km [1.8 mi] west of Southern Boulevard). The steepened slope of Southern Boulevard is likely due to faulting (i.e., the fault zone called "Unnamed faults near Star Heights" in Personius and Jochems, 2016). In the foreground, note the white color along the shoulder of Southern Boulevard that is due to multiple stacked calcic and petrocalcic paleosols (likely >2 m [>6 ft] thick here). These soils are developed on the Ceja Formation or surficial sediment (i.e., eolian deposits, sheetwash deposits, or colluvium) overlying this formation.



FIGURE 2.08. Photo looking west down Southern Boulevard near Rainbow Park. The topographically low area about 1.6 km (1 mi) distant is Arroyo de las Calabacillas, whose western flank corresponds to the east-down Zia fault zone.



FIGURE 2.09. View to south–southwest of Albuquerque Volcanoes from Puesta del Sol Elementary School, located 2.9 km (1.8 mi) west of the intersection of Unser and Southern Boulevards. The low area in the middle ground is Arroyo de las Calabacillas. The gently rolling vegetated topography is characteristic of the eolian sand-capped Llano de Albuquerque.

6.2 Pavement ends. **Continue driving west** on the continuation of Southern Boulevard. *1.4*

7.6 Ascend a small knoll, from which the TAG Solar field can be seen stretching north–south just below the skyline. The skyline here corresponds to the Ceja del Rio Puerco (Fig. 2.10). *0.2*

7.8 Cross a low-order, ephemeral arroyo draining to the south. Another similar drainage is 0.3 km (0.2 mi) to the west. *0.4*

8.2 Rolling topography in this area is mantled by a sandy surficial unit. The sand is generally massive. The upper few decimeters of the sediment is commonly loose, but below this interval there are generally soils characterized by subangular blocky peds and weakly developed calcic horizons (Fig. 2.11). *0.8*

9.0 **Waypoint 2.11 [N35.2416°, W106.8563°]**
Just before the north–south powerlines, turn right (north) on the wide dirt road corresponding to Sixtieth Street NW—but don't expect to see a street sign! On a clear day, there are great views of the Albuquerque Basin from here. *0.1*

9.1 Communication building on left (west). *0.4*

9.5 Drive northward on grassy, relatively gentle topography on the west side of the Llano de Albuquerque. To the left (west) is vast acreage of solar panels belonging to TAG Solar. *0.6*

10.1 Intersection of Sixtieth Street NW with the west end of Sandia Boulevard. Continue on Sixtieth Street NW. *1.1*

11.2 Intersection of Sixtieth Street NW with the west end of Northern Boulevard. Continue straight. *0.9*

12.1 North end of the solar panel field belonging to TAG Solar. *0.5*



FIGURE 2.10. The last house on Southern Boulevard. The irregular horizon is due to eolian sand dunes that formed along the top of the Ceja del Puerco.

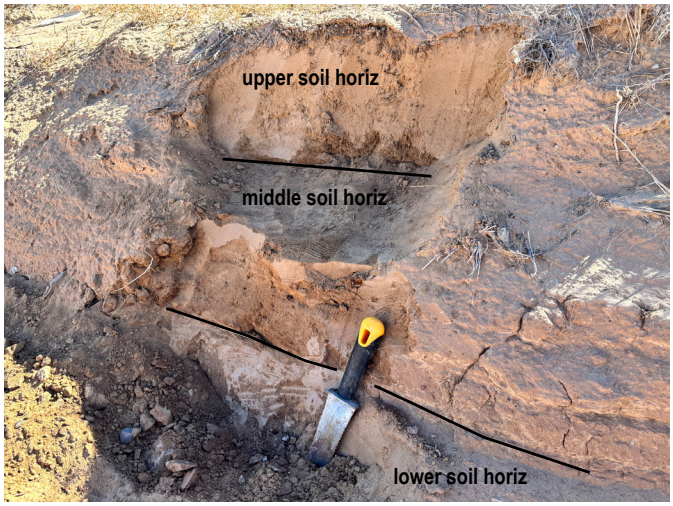


FIGURE 2.11. Annotated photograph of the surficial sand mantling rolling topography alongside Unser Boulevard, ~1.6 km (~1 mi) east of the Ceja del Rio Puerco escarpment. The upper soil horizon (32 cm [12.6 inch] thick) consists of massive, loose, fine- to medium-grained sand that is strong brown to reddish yellow. The middle soil horizon (16 cm [6.3 inch] thick) is a strong brown to yellowish brown, fine sand with weak, coarse, subangular blocky peds (no clay films). The lower horizon is >10 cm (>3.9 inch) thick and composed of brown, slightly clayey-silty, fine-grained sand with subangular blocky ped development. A minor amount of calcium carbonate has accumulated in all three units. Knife is 13 cm (5 inch) long.

12.6 **Waypoint 2.12 [N35.2940°, W106.85755°]**
A confusing network of roads leads to the left (west) from a dirt road corresponding to Twenty-First Street NW (unsigned). **Follow the northernmost of these roads** to a gate at the eastern boundary of the former King Ranch, which was later acquired by the Santa Ana Pueblo.

Note: This gate is typically locked to prevent trespassing and vandalism on the lands of Santa Ana Pueblo. Official permission is required to access Santa Ana Pueblo land to the west. The pueblo indicated to the authors of the road log that such access is unlikely to be granted in the future, so appreciate what you see on this field trip. Furthermore, no samples or artifacts are allowed to be taken.

Drive west through the gate and follow the wide dirt road down off the top of the Ceja del Rio Puerco escarpment. *0.1*

12.7 Descend off the west edge of the Llano de Albuquerque. The gravelly sand on the roadcut to the left (south) is the Rio Puerco Member of the Ceja Formation. The Rio Puerco Member has a distinct gravel assemblage that includes brown to red to black cherts, mottled white and gray chert correlated to the Pedernal chert, cemented sandstone, reddish granite, quartz and quartzite, and intermediate volcanic rocks. Straight ahead lies a distinctive butte, called Tamaya Kwii Kiinii Puu by Santa Ana Pueblo, that is capped by Upper Cretaceous Gallup Sandstone. Beyond Tamaya Kwii Kiinii Puu lies the south end of the much-larger, basalt-capped Mesa Prieta. *0.2*

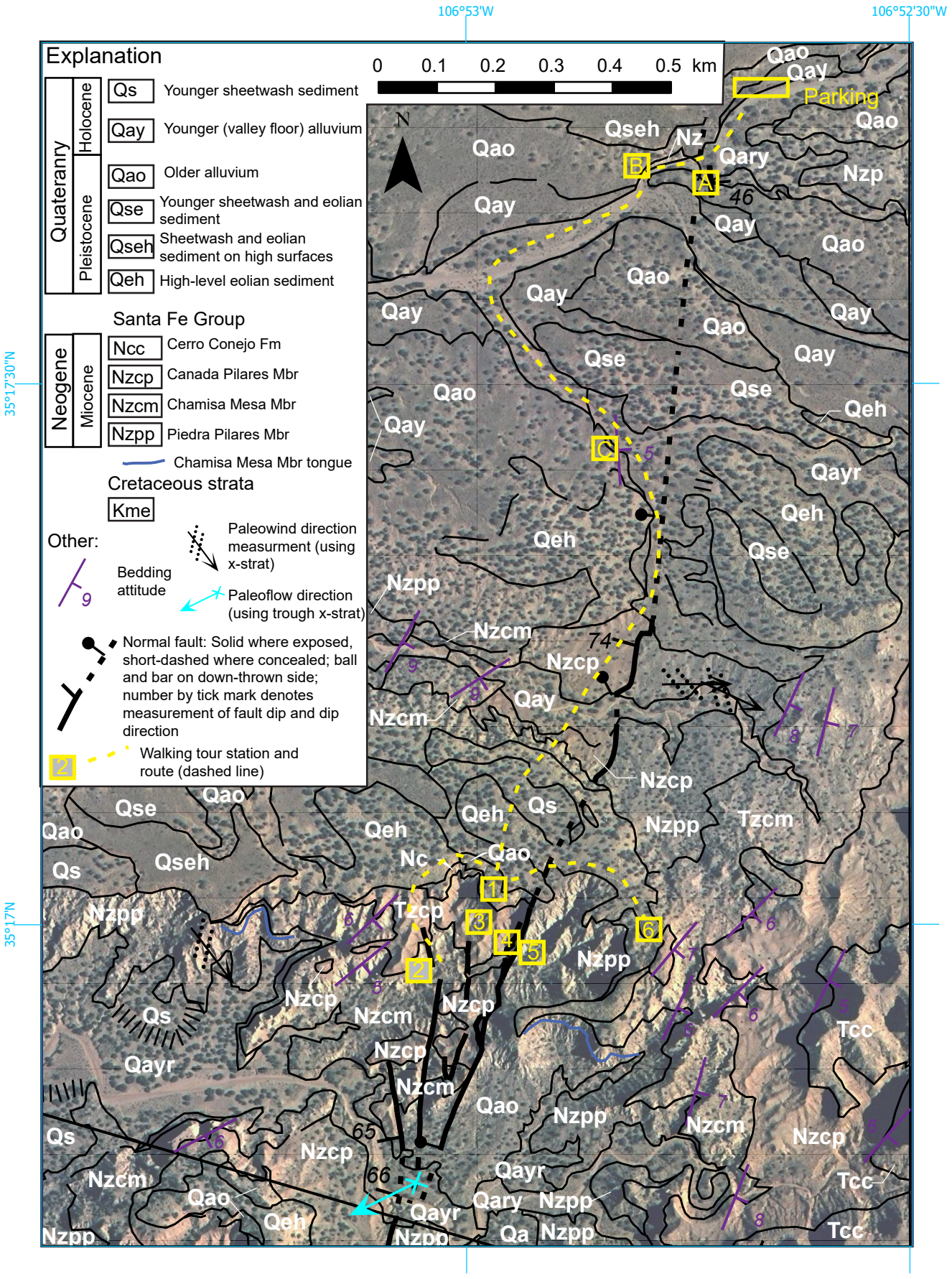


FIGURE 2.12. Annotated satellite image showing walking route and stations of Stop 1, as well as geologic features (from Koning and Rawling, 2017).

12.9 On left (south) roadcut is a ~3-m (~10-ft)-tall outcrop of gravely sand correlated to the Rio Puerco Member (Ceja Formation). A yellowish-brown sand on lower right contains fewer than 5% pebbles. *0.1*

13.0 The light yellowish-brown, well-bedded mudstone and sandstone on the lower, western end of the left (south) roadcut (~2-m [~6 ft]-tall) is correlated to the Navajo Draw Member of the Arroyo Ojito Formation. To the left (east), gravelly alluvium of possible middle Pleistocene age lies against the Navajo Draw across a buttress unconformity. *0.3*

13.3 Cross the northward projection of the Sand Hill fault (east-down normal fault). *0.1*

13.4 On the west side (footwall) of the Sand Hill fault lies readily erodible, poorly exposed sands of the Zia Formation (lower Miocene). *0.2*

13.6 Cross an unnamed arroyo. *0.1*

13.7 Ascend onto a broad surface capped by 0.5–3.0 m (1.5–10 ft) of fine- to medium-grained sand (unit Qseh of Koning and Rawling, 2017), which in many places is overprinted by a cumulic paleosols characterized by subangular blocky to prismatic ped development, clay illuviation, and calcium-carbonate accumulation (generally Stage I to II carbonate morphology). This sand represents eolian deposits that have been locally reworked by sheetfloods and subjected to bioturbation and pedogenesis. This sand overlies upper Pleistocene alluvium composed mainly of sand and pebbly sand. **After ascending onto the top of the high-level piedmont surface, park on the right (north) side of the dirt road.** *1.1*

Waypoint 2.13 [N35.2963°, W106.8791°]

STOP 1: Walking Tour of the Lower Santa Fe Group and Pilares Fault

Cross the road (to the south) and then turn left to descend into an unnamed, west-southwest-flowing arroyo using a side road that parallels the main dirt road.

INTRODUCTION

We will hike 1.6 km (1 mi) southward to an excellent exposure of the lower Santa Fe Group in Arroyo Benavidez (Fig. 2.12). Well-exposed outcrops of the lower Santa Fe Group in the Albuquerque Basin are restricted to the northwestern edge of the basin at the northern Ceja del Rio Puerco escarpment and near San Ysidro and Zia Pueblos (permission is needed to visit outcrops on pueblo land). After a brief overview of the area's geographic and geologic context (Station 1), participants hike into a small tributary canyon of Arroyo Benavidez to examine sedimentologic features of three lithostratigraphic units, corresponding to members of the Zia Formation, and use these features to infer depositional environments for the lower Santa Fe Group (Stations 2, 3, and 5). Additionally, there is a well-exposed deformation zone of the north-striking, intrabasinal Pilares fault (Station 4; Fig. 2.12). After examining these exposures, we hike to a nearby hilltop for lunch (Station 6; Fig. 2.12) and take in a view of the lower Cerro Conejo Formation (lower to middle Miocene), which is about 300 m (1,000 ft) thick here. After lunch, we discuss how the stratigraphy of the lower Santa Fe Group and associated intraformational faults might influence groundwater flow and possible hydrologic connections between the Santa Fe Group aquifer and Colorado Plateau.

Hike to Station 1

The main goal of the walking tour is to examine a nicely exposed area of the lower Santa Fe Group, located about 1.6 km (1 mi) south of the parking area (Stations 1 through 6). Along the way, we pass small exposures of the same lithologic units as seen in this large exposure. Here, we summarize these small outcrops in case people choose to stop briefly to inspect them.

0.1 mi Waypoint 2.14 [N35.2948°, W106.8788°]
Outcrop A: Piedra Parada Member of the Zia Formation

An exposure of whitish sandstone lies on the left (southern) side of the first, relatively sharp, rightward bend in the arroyo (Fig. 2.13). The sandstone in this exposure is mainly medium-grained and exhibits lamina to very thin beds that dip relatively steeply (15–20°) to the east. This sandstone is correlated to the Piedra Parada Member of the Zia Formation, which is the lowest unit of the Santa Fe Group (Galusha, 1966; Gawne, 1981a, 1981b; Tedford, 1982). *0.1 mi*

0.2 mi Waypoint 2.15 [N35.2949°, W106.8800°]
Outcrop B: Pleistocene alluvium overlying Zia Formation

At a leftward bend of the arroyo, a low set of arroyo-cut exposures exhibit a subtle downsection progression (to the west because strata are east dipping) from Chamisa Mesa Member to the Piedra Parada Member. On the left (east) end of the exposure, strata are slightly orange, fine-grained sandstone containing local beds of clayey sandstone, consistent with the Chamisa Mesa Member. On the west end of the exposure, the sand is coarser grained and grayer in color and likely correlative to the Piedra Parada Member. A north–northeast striking fault is interpreted to coincide with the northwest-trending arroyo between Outcrops A and B, and its west-down throw explains the presence of Chamisa Mesa strata at Outcrop B. At the far western end of the exposure, weakly consolidated, pebbly sand (~2 m [~6 ft] thick) disconformably overlies ~1 m (~3 ft) of the Piedra Parada Member of the Zia Formation. This pebbly sand is interpreted to be upper Pleistocene alluvium derived mainly from erosion of the Ceja Formation (unit Qao of Koning and Rawling, 2017).

A tributary from the southeast joins the main arroyo just south of Outcrop B. **Follow the main arroyo downstream to the southwest**. *0.2 mi*

0.4 mi Waypoint 2.16 [N35.2931°, W106.8788°]
Juncture of arroyos

A relatively large tributary arroyo enters from the southeast. T**urn left and follow this tributary upstream toward the southeast.** *0.2 mi*

0.6 mi Waypoint 2.17 [N35.2908°, W106.8806°]
Outcrop C: Chamisa Mesa Member of the Zia Formation.

A low outcrop of sandstone is seen on the south side of the arroyo. The sandstone is relatively massive, pinkish white to white (7.5YR 8/2 and 7/3–4), and its grain size is fine-lower to medium-lower. These strata are correlated to the Chamisa Mesa Member of the Zia Formation. The cemented bed on the east end of the outcrop is a slightly coarser sandstone (medium-lower to medium-upper) and has a nodular-cemented top (where the nodules are about 5 mm in diameter). The enhanced cementation here is probably due to its slightly coarser texture and to bioturbation slightly after deposition (both would be expected to increase permeability and allow increased flux of groundwater chemical constituents). **Just beyond this outcrop, keep right at the next arroyo junction and follow the southern tributary to the southeast.** *0.1 mi*

0.7 mi Waypoint 2.18 [N35.2908°, W106.8806°]
Arroyo juncture and well(?)

On the low Holocene terrace to the right (southwest) is a ~4–5 m (~15-ft)-diameter depression that is the remains of a 6–10-m (20–30-ft)-deep hole that was backfilled by Santa Ana Pueblo personnel. Presumably, this hole may have been a historic attempt by local ranchers to obtain groundwater from a hand-dug well. **At this well, turn left and walk southeast up a small gully.** *0.15 mi*

0.85 mi Waypoint 2.19 [N35.2880°, W106.8799°]
North end of cross-country hike from arroyo to Station 1

Leave the arroyo/gully and walk cross country southwest (220°) across slightly dissected terrain underlain by reddish sands and clays of the Cañada Pilares Member of the Zia Formation. This unit is better exposed at Stations 1 and 3 and are described below in the walking log. After 200 m (800 ft), we ascend a steep slope southward to the top of the mesa, which is capped by eolian sand. Once on top of a mesa, proceed 215 m (700 ft) along a bearing of 205° south to a small peak at the south edge of the mesa. *0.35 mi*

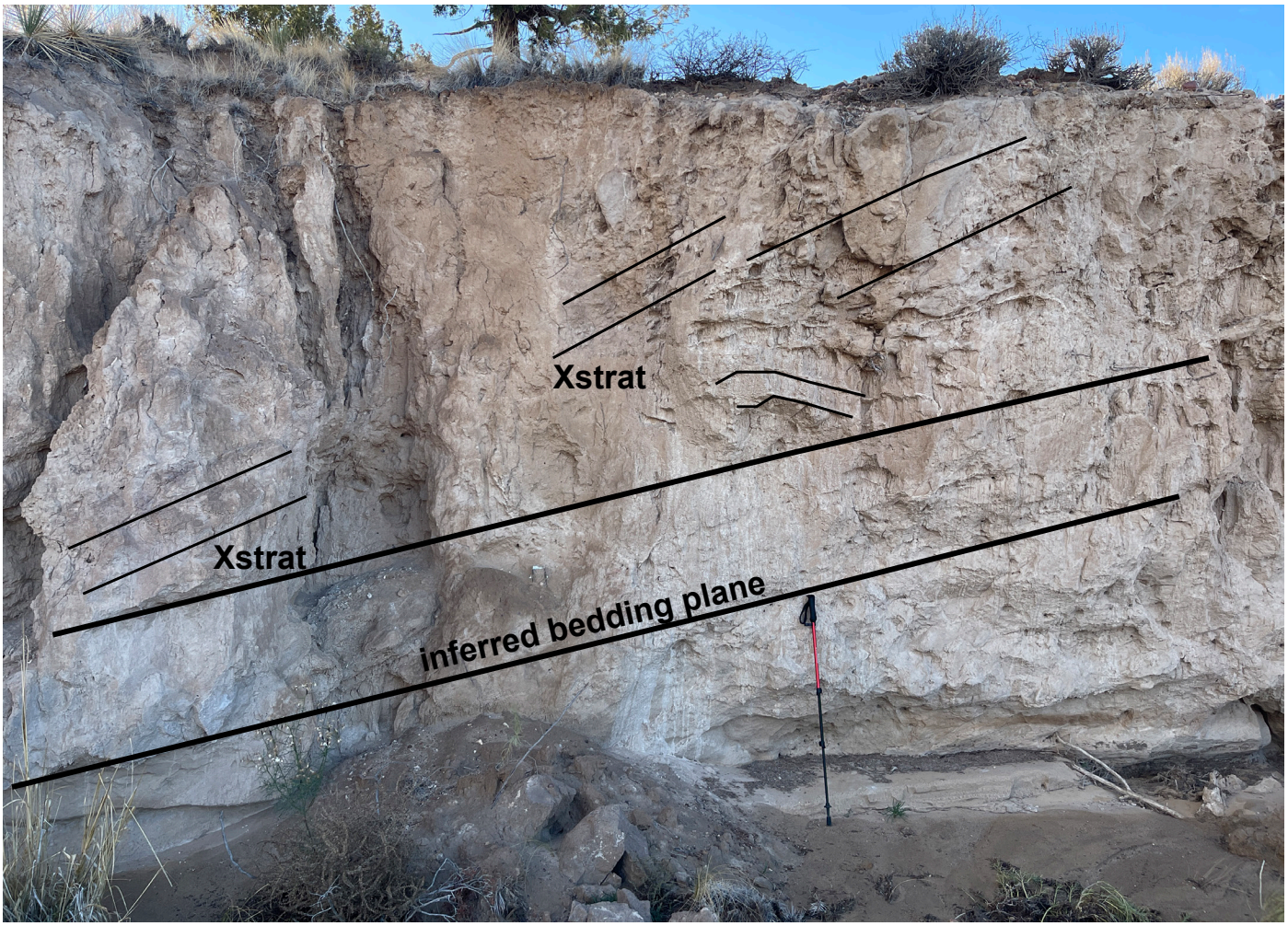


FIGURE 2.13. Exposure of Outcrop A. View to north. This is a whitish sandstone correlated with the Piedra Parada Member of the Zia Formation. Note annotation of local bedding planes and cross-stratification (Xstrat). The sand is white to light gray (10YR 8/1–7/2), mainly medium-grained, subrounded, and moderately sorted.

1.2 mi Waypoint 2.20 [N35.2838°, W106.8829°]

Station 1: Western Rift Margin and Lower Santa Fe Group

Congregate at a small peak overlooking, to the south, a topographic amphitheater eroded out by a small tributary drainage to the west-flowing Arroyo Benavidez, the latter being located 0.5 km (0.3 mi) to the south of this peak (Figs. 2.12 and 2.14). Before exploring this elucidative exposure, we discuss the physiographic and geologic context of this area (Fig. 2.15). Physiographically, we are about 1 km (0.6 mi) east of the boundary separating the Colorado Plateau (to the west) and the Rio Grande rift (to the east). A line representing this boundary on a map could reasonably be placed where basal rift-basin fill (Santa Fe Group) onlaps onto Cretaceous rocks about 920 m (3,000 ft) west of here. The geologic nexus of the 2024 NMGS Fall Field Conference, where the Colorado Plateau and Rio Grande rift physiographic provinces meet the southern end of the Rocky Mountains, is located about 27 km (17 mi) to the north (Fig. 2.15; Karlstrom et al., 2024). A nexus is a connection linking two or more things. Near the town of San Ysidro, three physiographic provinces, approximating tectonic provinces, come together and share many aspects of their respective geologic histories (Karlstrom et al., 2024). Below, we discuss the geology of the southeastern Colorado Plateau, Rio Grande rift, and the nature of the boundary between the two.

Colorado Plateau

The Colorado Plateau is relatively high in elevation (average of ~2 km, [~6,500 ft]) and exhibits relatively low topographic relief. The core of the plateau is underlain by relatively thick lithosphere (100–125 km [60–78 mi] thick). However, the southern and eastern edges of the plateau, including the part of the southeastern plateau that can be seen from here, is thinner (<80 km [<50 mi]; Karlstrom et al., 2024). Above basement lies a ~3.5-km (2.2-mi)-thick succession of Paleozoic to Upper Cretaceous strata. Upper Cretaceous strata are preserved at the surface over the majority of the southeastern Colorado Plateau. But tectonic subsidence in the San Juan Basin in the northwest corner of the state has resulted in preservation of a ~1-km (~0.6-mi)-thick section of Paleogene strata overlying uppermost Cretaceous strata, as was observed in the 2025 Fall Field Conference.

Immediately west of the structural boundary of the rift, Cretaceous strata include (in ascending stratigraphic order) the Dakota Sandstone (more precisely, an interbedded Dakota–Mancos succession), the lower interval of Mancos Shale, Gallup Sandstone, Mulatto Member of the Mancos Shale, Crevasse Canyon Formation (Dalton Sandstone and Gibson Coal Members), Satan Tongue of the Mancos Shale, Point Lookout Sandstone, and the Menefee Formation (see stratigraphic chart on back cover of guidebook). These formations mainly represent offshore and nearshore depositional environments, but the Gibson Coal Member (Crevasse Canyon Formation) and the Menefee Formation were deposited on coastal plains. Deposition of these strata reflects four transgressive-regressive depositional cycles of the Late Cretaceous Western Interior Seaway, which took about 20 million years (~100–80 Ma) of Cenomanian–Campanian time (Molenaar, 1983). Cretaceous strata typically erode to produce a low-relief landscape, where low mesas and cuestas are underlain by sandstone and low areas are commonly underlain by shales.

Notable topographic features of the Colorado Plateau that can be observed from Station 1 include Mount Taylor and the Rio Puerco Valley. The volcanic edifice of Mount Taylor, the focus of the 2021 Fall Field Conference, stands boldly at the south end of the basalt-capped Mesa Chivato, 40 km (25 mi) west-southwest of here. Mount Taylor is a stratovolcano composed of alkalic lavas ranging primarily from basanite to trachybasalt to trachydacite; minor rhyolite is also present. Eruptions that built the stratovolcano occurred in three phases spanning 3.72–2.50 Ma. Scattered mafic volcanism on its flanks continued to 1.26 Ma (Goff et al., 2015).

Much closer to us is the south-trending middle Rio Puerco Valley, formed by Pleistocene erosion of the Rio Puerco. The meandering channel of this river lies about 8 km (5 mi) to the west. The 2024 Fall Field Conference explored terraces and geologic features ~35 km (~22 mi) upstream of here (Koning et al., 2024a; Koning, 2024). During cooler (and possibly wetter) climates and higher river discharges during the 1700s to 1800s, Hispanic pioneers established several small farming/ranching villages here that depended on irrigation from the Rio Puerco (Bryan, 1928; Sánchez, 2008). Extreme post-1885 incision of the Rio Puerco, perhaps facilitated in this part of the valley by a failure of a man-made dams (Love, 1997), made irrigation extremely difficult, and the settlers turned to ranching before migrating elsewhere.

To the northwest, about 6 km (4 mi) distant, lies the relatively small butte called Tamaya Kwii Kiinii Puu by Santa Ana Pueblo (~300 m [~1,200 ft] diameter), and beyond (about 10 km [6 mi] to the northwest) is Mesa Prieta (Fig. 2.16). Tamaya Kwii Kiinii Puu is capped by the resistant Gallup Sandstone. The Gallup Sandstone is an Upper Cretaceous nearshore sandstone,

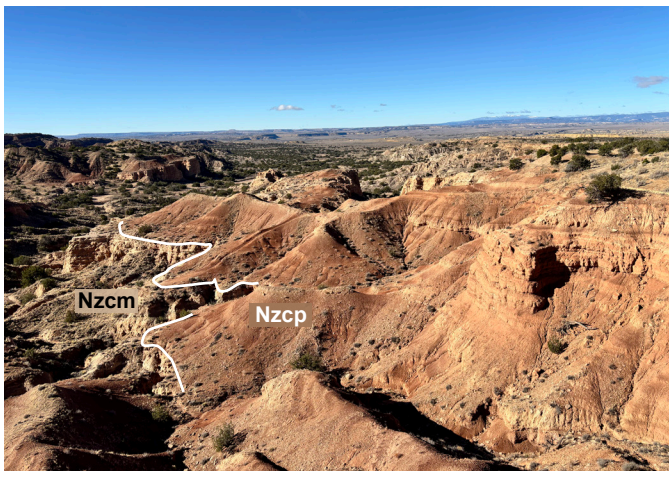


FIGURE 2.14. View to the southwest from the overlook at Station 1. Exposed sediment belongs to the Zia Formation of the lower Santa Fe Group. The reddish brown, clay-rich strata correspond to the Cañada Pilares Member (Nzcp) and the underlying, cliff-forming, lighter-colored sandstone correlates to the Chamisa Mesa Member (Nzcm).

stratigraphically sandwiched between tongues of the offshore Mancos Shale, that marks the former location of the 90-Ma southwestern shoreline of the Western Interior Seaway (Molenaar, 1983; Nummedal and Molenaar, 1995). This sandstone unit extends from the Four Corners region southeast to Ruidoso, New Mexico. Most of the lowlands around San Felipe Mesa are underlain by the lower tongue of the Mancos Shale (between the Dakota Sandstone and the Gallup Sandstone).

Mesa Prieta is capped by two lower Pleistocene basalt flows locally underlain by thin (<10-m [<30-ft]-thick) river gravel. The lower was dated at possibly 2.2 ± 0.03 Ma (Armstrong et al., 1976) and the upper at 2.05 ± 0.13 and 2.36 ± 0.30 Ma (Hallett et al., 1997). This gravel and overlying basalt may have filled a shallow paleovalley whose formerly higher margins have been eroded, an example of inverted topography. The somewhat younger ages of the mesa-capping basalts relative to topographically lower basaltic eruptive centers (i.e., the Puerco volcanic necks) suggests the paleovalley associated with the Mesa Prieta lava flows was not fully graded to the main Rio Puerco valley (Koning et al., 2024a, fig. 2.83).

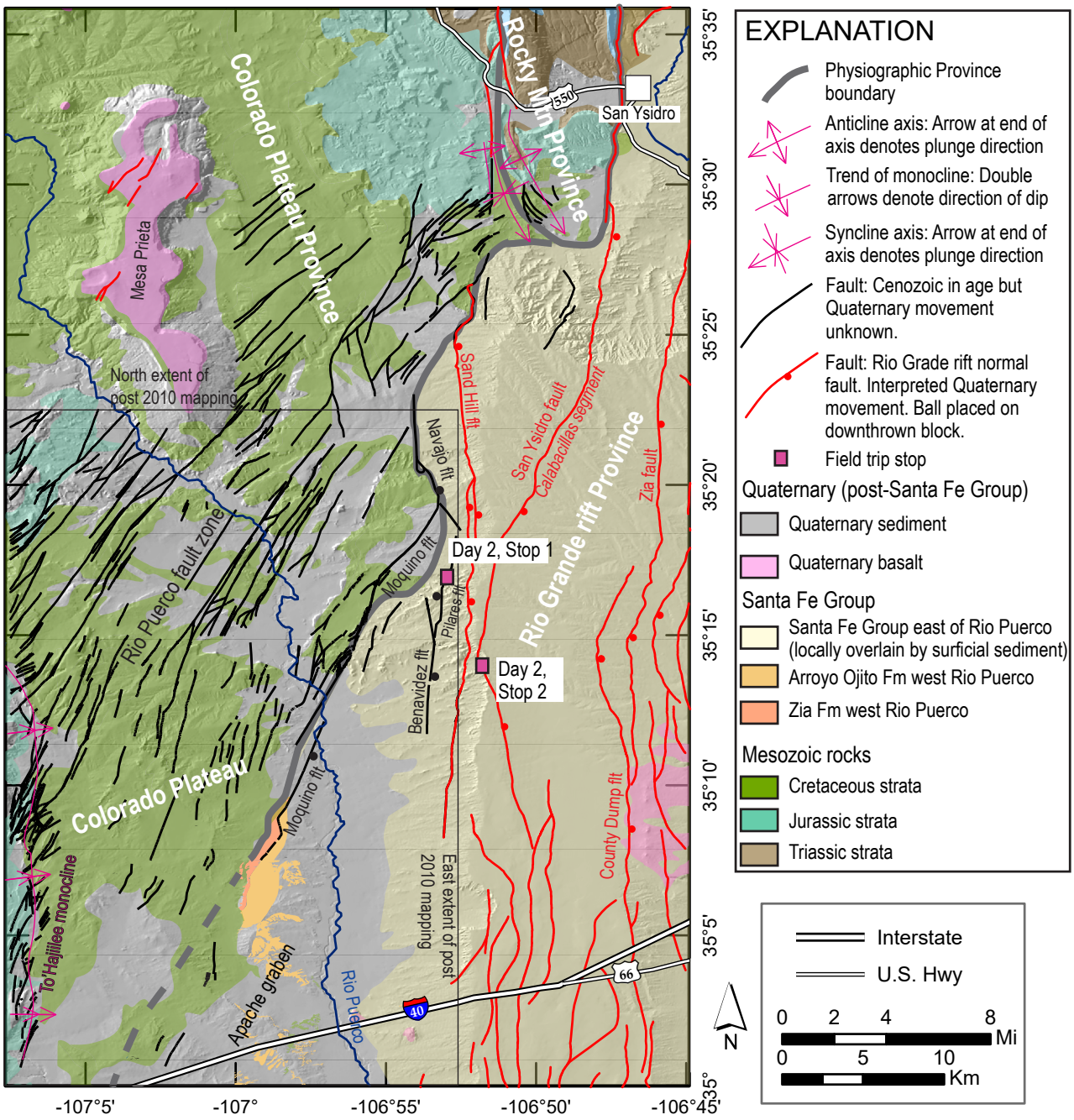


FIGURE 2.15. Regional map showing the major physiographic provinces (thick dark-gray lines) and faults near Stop 1. Stop 1 lies in the border zone between the Rio Grande rift and Colorado Plateau physiographic provinces. Faults mapped in this border zone are shown as thin black lines. Rift faults with demonstrable Quaternary activity are in red (Quaternary faults and folds database (USGS, 2024). Note that west of the Rio Puerco, the Santa Fe Group is both in depositional and fault contact against Cretaceous sedimentary rocks.

Rio Grande rift

Subsidence of the Rio Grande rift preserved a thick sequence of sand-dominated, clastic sediment assigned to the Santa Fe Group (Spiegel and Baldwin, 1963). The stratigraphy of the Santa Fe Group in the Albuquerque Basin is reviewed by Connell (2004, 2008b, and references therein) and Connell et al. (2013). The extent of the Santa Fe Group approximately marks the boundary of the Rio Grande rift. Deposition of the Santa Fe Group and concomitant rift tectonism occurred during late Oligocene time and continues through the present (van Wijk et al., 2018). Subsidence rates and sediment accumulation rates were higher prior to the latest Miocene and lower during the Pliocene and Quaternary (Connell et al., 2013, fig. 21; Van Wijk et al., 2018). Although most workers would agree that tectonic extension rates are slower today, the ubiquitous presence of faults offsetting Quaternary sediments reminds us that earthquakes hazards exist for the area (Fig. 2.15).

The lower Santa Fe Group is generally deeply buried across the Albuquerque Basin (deeper than >95% of water wells), but the topographic amphitheater below us exposes a condensed section of these strata. Three lithologic units are readily recognized and listed in ascending stratigraphic order: Piedra Parada, Chamisa Mesa, and Cañada Pilares Members of the Zia Formation (Fig. 2.17). Strata strike northeast and dip 5–6° to the southeast. An obvious north-striking fault, called the Pilares fault, has west-down throw and juxtaposes the Piedra Parada Member on the east (footwall) against the Cañada Pilares Member on the hanging wall to the west (Fig. 2.18). The 21–18-Ma Piedra Parada Member of the Zia Formation (~80 m [~260 ft] thick) consists mainly of white to light gray to light-tan, medium-grained, cross-stratified sand deposited mainly by eolian processes, whose foresets dip, on average, to the northeast (Fig. 2.19). The Piedra Parada Member becomes slightly coarser-grained to the southwest, where it locally contains sparse pebble beds (Rawling and Koning, 2020) and is partly of fluvial origin in that direction. The 19–18-Ma Chamisa Mesa Member (35–30 m [115–100 ft] thick) is a tabular bedded, light-pink to light-orange, very fine- to medium-grained sandstone containing local rhizoliths and paleoburrows (Figs. 2.20 and 2.21). The 18.5–17.5-Ma Cañada Pilares Member (~38 m [~125 ft] thick) is a slope-forming, reddish brown, clay-rich mudstone interbedded with tongues of predominately fine- to medium-grained sandstone (Figs. 2.18, 2.20, and 2.22). Above the Cañada Pilares Member lies the 200–330-m (650–1,080-ft) thick Cerro Conejo Formation (Fig. 2.17), which will be discussed further at Station 6.

Lower Santa Fe Group strata are exposed in several other places of the Rio Grande rift and offer a useful comparison to the facies interpreted in this area. In the Tano Formation of the northern Albuquerque Basin (Santo Domingo subbasin), conglomerates grading upward into mudstone and sandstone are interpreted to represent basin-floor and distal-piedmont deposition in a closed basin in the latest Oligocene to early Miocene (Connell et al., 2002). Farther north in the Española Basin, conglomeratic alluvial-slope (piedmont) sediment, shed from the Sangre de Cristo Mountains, flanked the eastern Española Basin but retrograded around 20–18 Ma, roughly coincident with the start of the Middle Miocene climatic optimum (Koning et al., 2002; Spaur et al., 2025). In the Socorro Basin, early rift sedimentation was also relatively conglomeratic and graded north–northwestward into sandstones and mudstones of a playa lake in the southwestern corner of the Albuquerque Basin (near the modern Rio Salado; Koning et al., 2024b). In general, during early rifting (25–16 Ma) the central Rio Grande



FIGURE 2.16. View to the west-northwest of Mesa Chivato and Mesa Prieta, as viewed from the parking area of Stop 1. Both are capped by 3–2 Ma basalts. In the center of the photograph is Tamaya Kwii Kiinii Puu. This butte's upper yellowish resistant layer corresponds to the Cretaceous Gallup Sandstone.

rift was characterized by topographically and hydrologically closed basins, where fine-grained playa lakes graded outward to coarse-grained fans. It was much later, in the late Miocene and early Pliocene, that an axial-fluvial system became established in the central and southern rift (Connell et al., 2005; Repasch et al., 2017; Koning et al., 2024b).

Rio Grande rift–Colorado Plateau structural boundary

The boundary between the Rio Grande rift and the Colorado Plateau near Stop 1 can be characterized by either onlap of the Santa Fe Group or by faults. About 1.1 km (0.7 mi) west of here, the Piedra Parada Member disconformably overlies the Menefee Formation (Upper Cretaceous) with up to 10 m (30 ft) of paleotopographic relief (Koning and Rawling, 2017). The Menefee Formation (~550 m [~1,800 ft] thick in this area) is characterized by grayish to grayish-brown, fine-grained floodplain deposits (mudstone, siltstone, and very fine- to fine-grained sandstone) interbedded with 15–30% sandstone channel-belt fills (Koning and Rawling, 2017). The Menefee just below the unconformity may locally be affected by paleoregolith formation, as exemplified by the upper ~10 m (~30 ft) weathering into a very light-green massive sandstone with local, strongly cemented sandstone bodies. At the base of the Piedra Parada Member, draped on the disconformity, is a lag of pebbles consisting of rounded–subrounded chert (brown to black) with 1–30% monolithic, light gray, hornblende-biotite dacite, 10% quartz, and trace petrified wood. Of the dacite clasts, 1% are cobble size (up to 17 by 15 cm [6.5 by 5.9 inch]). To the north, the dacite cobbles on the unconformity are ventifacted (shaped into smooth, multifaceted, semipyramidal forms) by wind action, but similar examples of ventifacts are not seen in Arroyo Benavidez. One of the dacite cobbles was dated by the $^{40}Ar/^{39}Ar$ technique and returned ages of 33.7 ± 1.0 Ma (Peters, 2018); similar dacitic clasts in this stratigraphic position along the Ceja del Rio Puerco have returned ages of 31.8 ± 1.8 Ma, 33.03 ± 0.02 Ma, and 33.24 ± 0.24 Ma (Kelley et al., 2013, p. 119). These intermediate-volcanic gravels may broadly correlate to the volcaniclastic interval called the Gilman Conglomerate of the southern Jemez Mountains (Kelley et al., 2013). But $^{40}Ar/^{39}Ar$ dating of four clasts in the Gilman conglomerate returned a distinctly younger population of 29.7–28.7 Ma (Kelley et al., 2013). In Arroyo Benavidez, the other gravel types occurring with the dacite were sourced from the Colorado Plateau north of a large volcaniclastic fan that flanked the northern Mogollon-Datil volcanic field (Koning et al., 2021). So, it is reasonable to assume that this dacite was also sourced from a vent complex to the northwest or reworked from an older alluvial deposit; however, no eruptive center of similar composition is known.

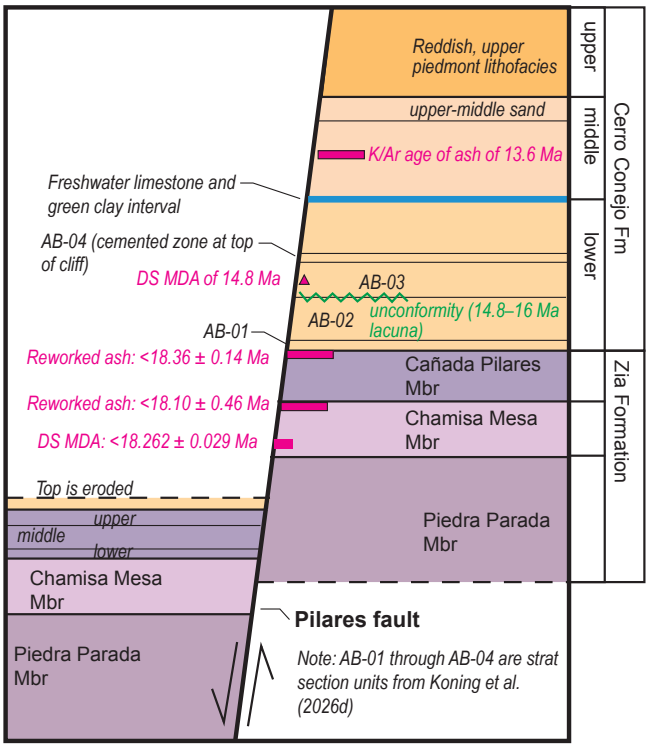


FIGURE 2.17 Stratigraphy of the lower Santa Group at Stop 1. DS MDA = detrital sanidine maximum depositional age.

The boundary between the Colorado Plateau and Rio Grande rift in the modern Rio Puerco Valley commonly corresponds to the traces of normal fault zones that commonly exhibit down-to-the east throw. Two particularly prominent normal faults include the Navajo fault to the north and the Moquino fault to the west and southwest (Fig. 2.15). The Moquino fault has experienced 300–550 m (1,000–1,800 ft) of east-down throw (Koning and Rawling, 2017). The juxtaposition of the top of the Cerro Conejo Formation against Cretaceous strata across the Navajo fault suggests 300–400 m (1,000–1,300 ft) of east-down stratigraphic displacement on that structure (Koning and Rawling, 2017). Two other large faults 3–5 km (2–3 mi), inboard (east of) the Moquino and Navajo faults include the Sand Hill fault and Calabacillas section of the Jemez-San Ysidro fault, each of which have 200–300 m (660–1,000 ft) of east down throw (Fig. 2.15; Connell, 2008b, 2011; Koning et al., 2026a, 2026b).

Several northeast-striking faults with lengths of several kilometers have been mapped in Cretaceous strata west of the Moquino and Navajo faults (Fig. 2.15), corresponding to the Rio Puerco fault zone of Slack (1975) and Slack and Campbell (1976). Many of these faults are inferred to have formed during northwest-orientated Laramide compression, during which they experienced right-lateral slip or right-lateral oblique slip (Slack, 1975; Slack and Campbell, 1976). This compression also formed northwest-striking folds near San Ysidro (Woodward and Reutschilling, 1976). By the end of the Laramide orogeny, there were numerous small, northeast-trending normal faults that formed a series of grabens and horsts (Slack, 1975). At least some faults were reactivated during east–west Rio Grande rift extension, and across the border region near Stop 1, most vertical displacement accrued during this extension. Additional confirmation of oblique slip was locally measured on these faults (Rawling and Koning, 2019, 2020) and Rawling and Jochems (2018), but for the most part, it is not known whether these relate to extension or earlier Laramide movement. In summary, the Rio Puerco fault zone likely began as a transpressional fault structure in the Laramide, where lateral movement was likely greater than vertical movement (based

on comparison to the Nacimiento fault; Cather et al., 2006), and many of these faults were later strongly reactivated during Rio Grande rifting—resulting in a structural inversion.

To the southwest of Stop 1 (~30 km [~20 mi]), subsidence along these northeast-striking faults has locally preserved Santa Fe Group as far as 10 km (6 mi) west of the Rio Puerco (Fig. 2.15; the Apache graben of Wright, 1946; Campbell, 1967). In this area, the basal Santa Fe Group onlaps Cretaceous strata (commonly the Menefee Formation) in many areas.

Collectively, the distribution of lithologic units and faults west of the Moquino fault in the Rio Puerco Valley indicates that the margin between the Rio Grande rift and the Colorado Plateau encompasses a relatively wide zone of northeast-striking faults (Fig. 2.15). We consider the western rift-margin fault zone near Stop 1 to extend from the Calabacillas section of the San Ysidro-Jemez fault zone westward to the To'Hajiilee monocline (name proposed herein), a width of approximately 20 km (12 mi; Fig. 2.15). We maintain that this structural margin should be viewed as a wide, complex zone of extension that accommodates strain between the Colorado Plateau and the Albuquerque Basin. A similarly diffuse zone of extension is recognized in the Chama Basin, northwest of the town of Abiquiu (Koning et al., 2006). We find no evidence that the western margin of this zone is progressively extending westward into the Colorado Plateau over time. Specifically, faults of the Rio Puerco fault zone do not appear to offset Pleistocene deposits, whereas many faults to the east, in the Albuquerque Basin, do show evidence of movement in the late Quaternary (Fig. 2.15).

Stations 2 Through 4: Stratigraphy of Lower Santa Fe Group

After the overview at Station 1, we hike ~200 m (~600 ft) along the main ridge westward and then follow a former dirt-bike track southward ~200 m (~600 ft) to access the exposures of the lower Santa Fe Group (see route in Fig. 2.22). There,

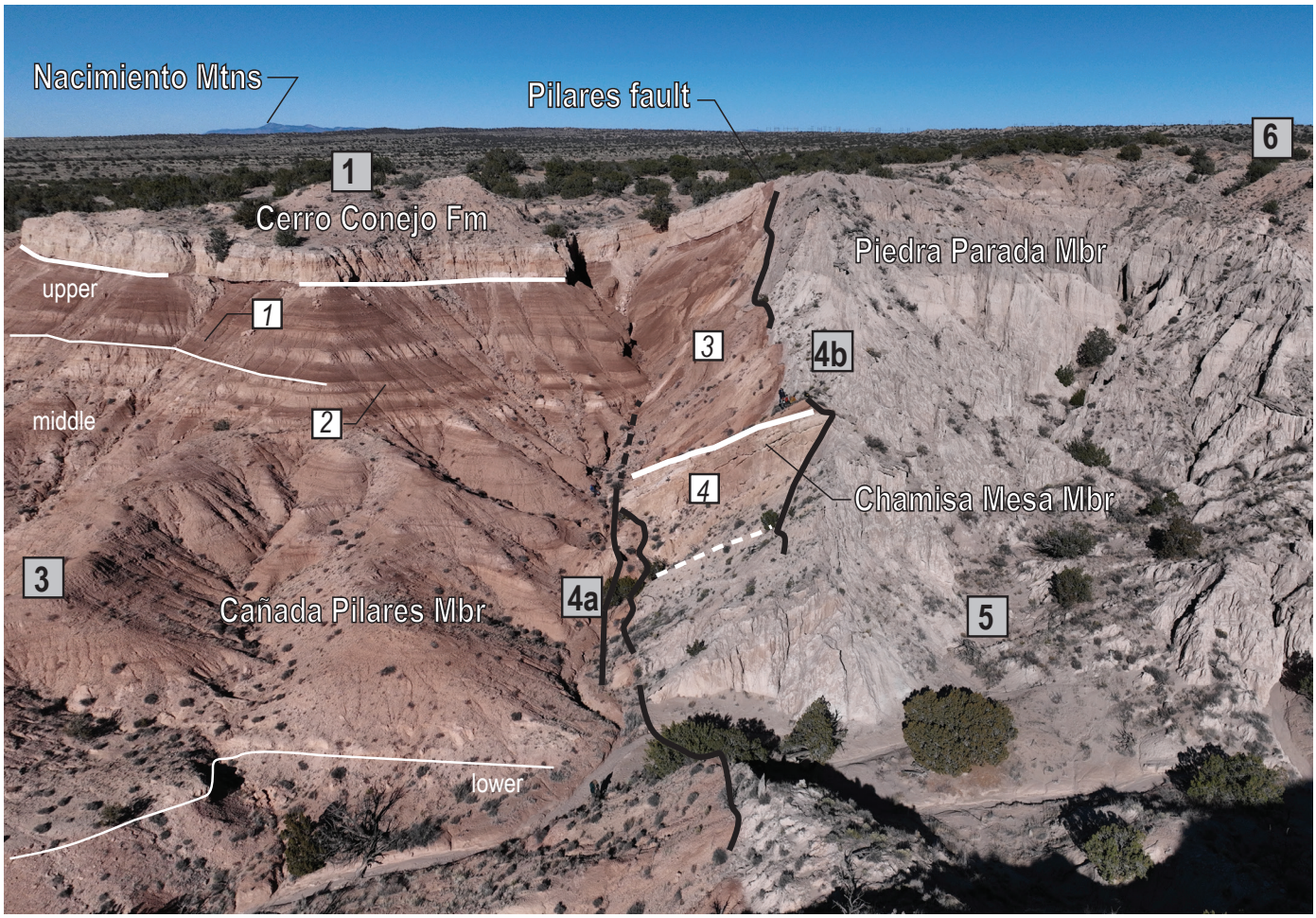


FIGURE 2.18. View north of the Pilares fault zone (black line) and surrounding Miocene strata. The Piedra Parada, Chamisa Mesa, and Cañada Pilares Members are part of the Zia Formation (note the Chamisa Mesa Member directly underlying the Cañada Pilares Member is out of the field of view). The Cañada Pilares Member is subdivided into lower, middle, and upper units. Stations of Stop 1 are shown in the gray boxes. Features of interest are labeled in the white boxes and include the following (1) thinning of light-colored sandstone in the upper Cañada Pilares Member that may be due to scour before deposition of overlying reddish-brown clay (scoured contacts are relatively common in the Cañada Pilares Member); (2) sand bed pinches out to the right (east), probably reflective of a sandy fan toe (of the nearby western piedmont slope) retrograding westward due to the associated playa lake briefly filling with water; (3) above lies normal drag of Cañada Pilares strata near the trace of the Pilares fault; and (4) NNW-dipping pinkish sandstone of the Chamisa Mesa Member lies between two right-stepping fault strands. This dip is consistent with a north-dipping ramp structure.

participants split into two groups that independently visit Stations 2 through 5 (Fig. 2.22). Stations 2, 3, and 5 pertain to the lower Santa Fe Group (i.e., the Zia Formation), whereas Station 4 showcases the Pilares fault zone. Stations 2 through 5 offer participants an opportunity to examine (1) proportions of lithologies (clay, silt, very fine–fine sand, medium–coarse sand) and any upsection trends in lithologic texture; (2) bedding character (e.g., geometry and thickness) and any upsection trends; (3) color; and (4) paleontological features, including trace fossils left by roots and animal burrows.

Each of the three members of the Zia Formation represents a unique depositional environment. The goal is to examine outcrop features, including upsection changes and Walther's Law, and to interpret the paleodepositional environments/facies represented by the three members. Potential depositional environments include piedmont (proximal, medial, distal), alluvial flat, floodplain, axial river, playa lake, relatively perennial lake, and eolian. Auxiliary questions are what factors caused the depositional environments to change: tectonics, paleoclimate, or autogenic drivers? We will discuss paleoenvironmental interpretations and these drivers before we leave for Station 6. In the following text and figures, we describe Stations 2 through 5 from west to east and emphasize features that give clues to the depositional environment of a given unit. Our preferred depositional environment interpretations are given in Koning et al. (2026d). *0.25 mi*

1.45 mi Waypoint 2.21 [N35.2825°, W106.8843°]

Station 2: Chamisa Mesa Member of the Zia Formation

Station 2 is a several-meter-tall exposure of pinkish to tannish, tabular-bedded, very fine- to medium-grained sandstone (Figs. 2.20 and 2.21). Lower strata are very thickly bedded, but thin to medium beds become more common upsection, particularly in the upper 2–3 m (6–10 ft), where there are locally light-greenish beds. The interiors of beds are typically massive to horizontal planar laminated. This outcrop is capped by a 20–30-cm (8–9-inch)-thick, white, well-cemented bed that is an ashy fine sand. Intervals, <0.5 m (<1.6 ft) thick, with abundant rhizoliths or burrows are locally present. One such bed is moderately cemented and exposed at the level of the arroyo ~20 m (~65 ft) to the north. Finer, more intricate rhizoliths are seen in the upper 2–3 m (6–10 ft) of the unit (Fig. 2.21, top). The thick to very thick beds of sandstone continue as one travels down the arroyo (downsection). Near the mouth of the tributary canyon, there is a ~0.5-m (~1.6-ft)-thick, strongly burrowed, strongly cemented sandstone that shows signs of strong bioturbation (Fig. 2.21, bottom). This bed lies 2–3 m (6–10 ft) above a gradational contact between the Chamisa Mesa and Piedra Parada Members. Examine the sand in the pinkish, tabular beds with your hand lens and estimate the proportion of dark lithic grains (commonly ~10%), which we will compare with the older Piedra Parada Member at Station 5. Also, as we walk up the arroyo, take note of sedimentologic features and grain size variations in the upper few meters of the Chamisa Mesa Member.



FIGURE 2.19. Foresets of a northeast-facing eolian dune in the Piedra Parada Member. The whitish to light gray color, cross-stratification, and medium- to coarse-grained sand texture is characteristic of the member. Also, sand grains are subrounded to rounded and contain 15–30% lithic grains (mostly volcanics and lesser chert). Exposure is located 0.5 km (0.3 mi) south of Stop 2.





FIGURE 2.20. Top photo: Light-orange, tabular-bedded, ledge-forming Chamisa Mesa Member at Station 2. Softer (more erosive), brown to reddish-brown clay above and to the right is the Cañada Pilares Member. The Chamisa Mesa cliff to the right side of the arroyo is ~10 m (~30–35 ft) tall. View is to the southwest. Bottom photo: Upper 5 m (15 ft) of the Chamisa Mesa Member upstream from Station 2. The white bed near the map board (noted by the gray arrow) is a volcanic ash bed.

The preferred interpretation of the depositional environment is one of a retrograding toe of an alluvial fan or piedmont slope (Koning et al., 2026d). Rather than cross-stratified channel forms, there is a predominance of tabular beds that are internally massive or horizontal-planar laminated. Rhizoliths are commonly present. These support the interpretation of predominately unconfined flow in a relatively vegetated area, which is expected at the toe of an alluvial fan grading into a basin floor. We discuss the age of the Chamisa Mesa Member in Station 6. *0.1 mi*

1.55 mi Waypoint 2.22 [N35.2830°, W106.8834°]

Station 3: Cañada Pilares Member

In this local area, the reddish-brown, clayey Cañada Pilares Member is subdivided into three units based on the proportion of sandstone beds (Figs. 2.23–2.25). These units are layers at the scale of this outcrop and include (1) the clay-rich lower unit (5–6 m [15–20 ft] thick), (2) sand-dominated middle unit (13 m [43 ft] thick), and (3) clay-rich upper unit (9–10 m [30–33 ft] thick). Sandstone beds are lighter colored compared with reddish-brown clayey strata. Sandstone beds appear to make up less than 50% of the outcrop area in the upper and lower subunits but are more than half of the middle subunit. Individual sandstone and claystone beds are typically 10–200 cm (4–80 inches) thick. The interior of sandstone beds is massive to vaguely planar laminated. Are there vertical trends in the sandstone succession, and what is the nature of their upper and lower contacts? Note the sand in these beds is not obviously finer than the Chamisa Mesa sand, but rather is commonly fine- to medium-grained with sparse coarse-grained sand. The upper contacts are relatively abrupt and planar but exhibit local gradation in the form of (1) clay interlaminations become more abundant in the upper ~10 cm of the underlying sandstone bed, and (2) the lower few decimeters of the overlying clay often are sandy but grade up into purer clay (Figs. 2.26A and 2.26B). However, some of the sandstones have scoured upper contacts (Fig. 2.26C).

The middle unit is mostly composed of tabular sandstone beds <50 cm (<20 inch) thick (Figs. 2.25 and 2.28) that are separated by thinner clayey beds. As elsewhere, the sandstone is internally massive or horizontal-planar laminated, but locally cross-stratification is present with clay rip-up clasts (Fig. 2.27). An exposure in Benavidez indicates that clay locally fills shallow channel forms (Fig. 2.28). At Station 3, there is at least one decimeter-thick zone in sandstone that displays local reddening and paleosol development.

Although the middle unit mostly consists of sandstone, there are lateral changes in the proportions of sandstone beds. This is best seen in the butte to the northwest ("Interfingering butte" in Figs. 2.24 and 2.25). This butte is mostly composed of tabular sandstones. A clayey bed near the base has notable northeast-directed cross-stratification about 30-cm (~12-inch)-tall, where there is intercalation of sand and clay (Fig. 2.25, white arrow). To the northeast, the sandstone beds decrease in proportion and thickness concomitantly with an increase in clay beds (Figs. 2.24 and 2.25)—in the same northeast direction as the paleoflow obtained from the aforementioned cross-stratification.

The interpretation of the Cañada Pilares is challenging. The abundance of thick, massive clay beds indicates steady rates of



FIGURE 2.21. Rhizoliths are locally common in the Chamisa Mesa Member. Top photo: In the uppermost Chamisa Mesa strata, erosion has concentrated a rhizolith lag on the surface. Pencil for scale. Bottom photo: A few meters above its basal contact is a laterally extensive, tabular, strongly cemented sandstone with abundant bioturbation (roots and burrows). Pen for scale.

suspended-clay settling from slow moving or standing water. Scour features, local-channel forms, and intraformational claystone clasts demonstrate tractive paleocurrent currents and erosion at the base of channel belts. In at least one location, a paleosol is developed in a sand bed (middle unit). These features are consistent with a floodplain deposit, and that was the

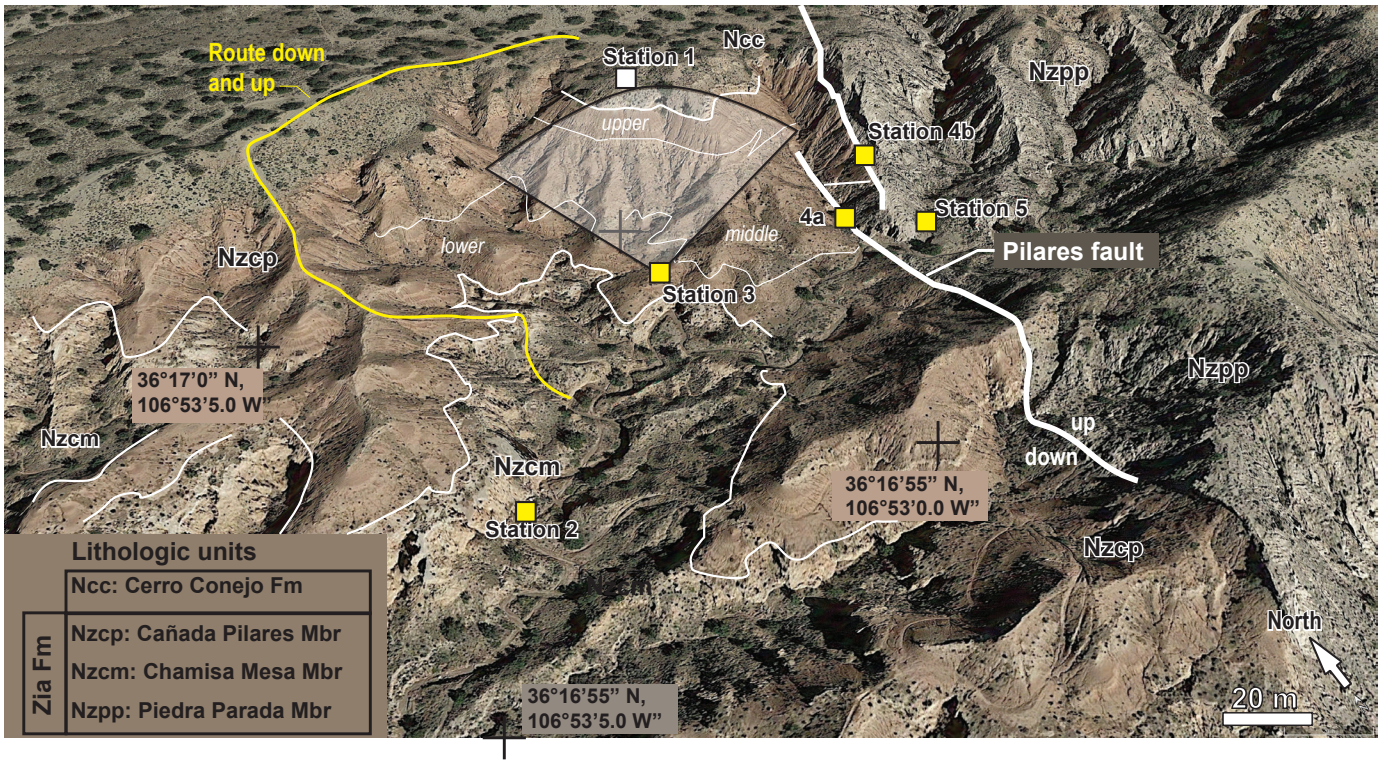


FIGURE 2.22. Annotated Google Earth imagery showing the geology of Stop 1 and locations of Stations 1 through 5. Basemap image from Google Earth, © 2018 Landsat/Copernicus.

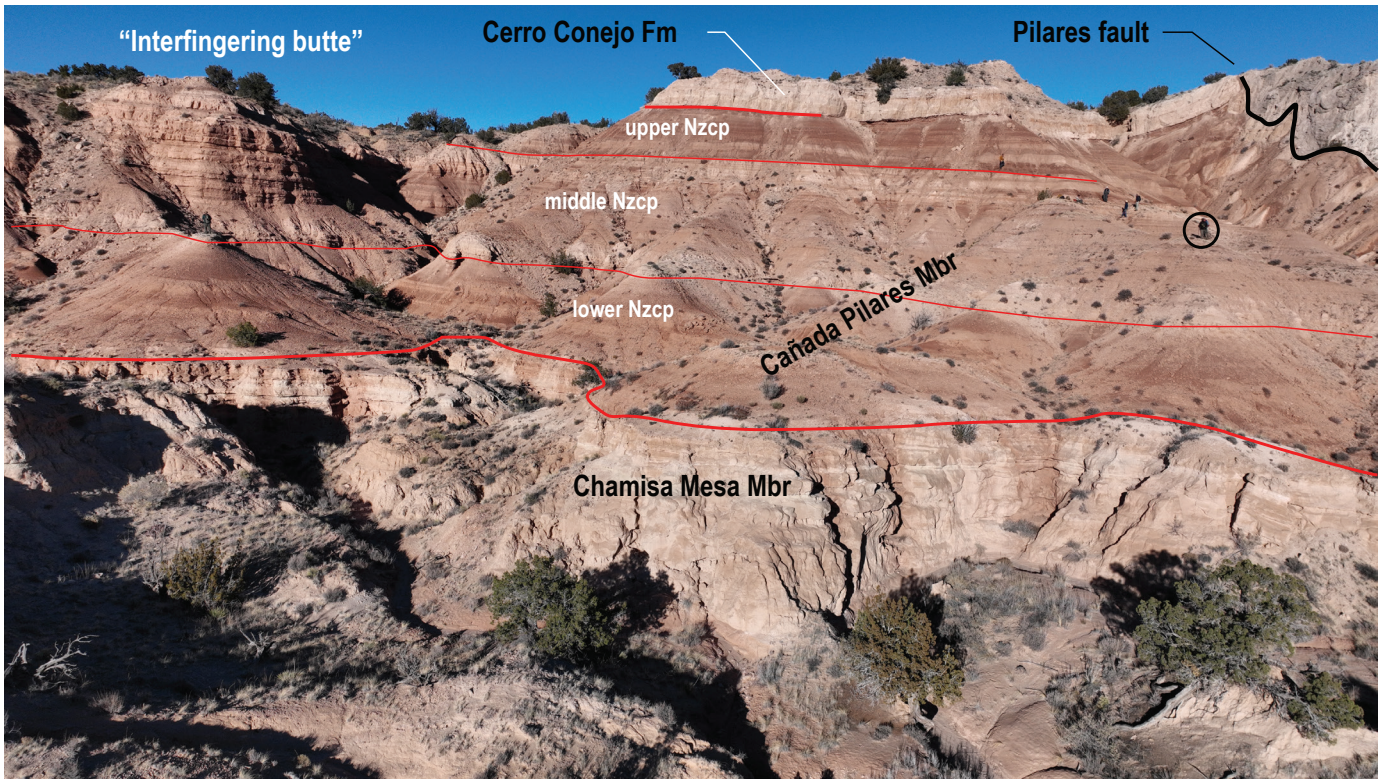


FIGURE 2.23. View to north of Station 3, showing the lower, middle, and upper units of the Cañada Pilares Member (Nzcp). "Interfingering butte" is to the left (middle, sandy tongue) and the Pilares fault is on the right. A person is in the black circle on the right.

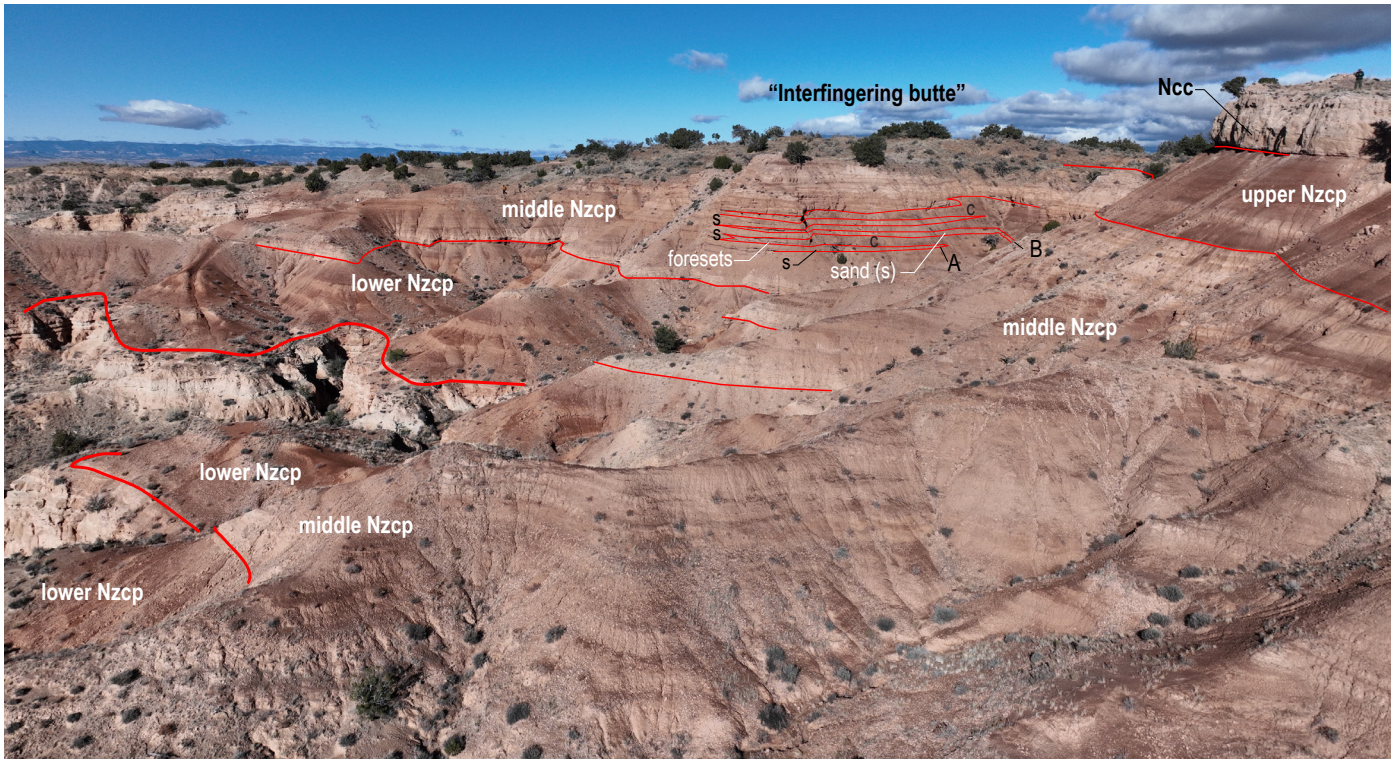


FIGURE 2.24. View to WNW of Cañada Pilares Member and three local units. Note that three sand beds at Interfingering butte pinch out or thin to the NNE. The two lower of these beds are labeled A and B. Two clayey beds are labeled C.

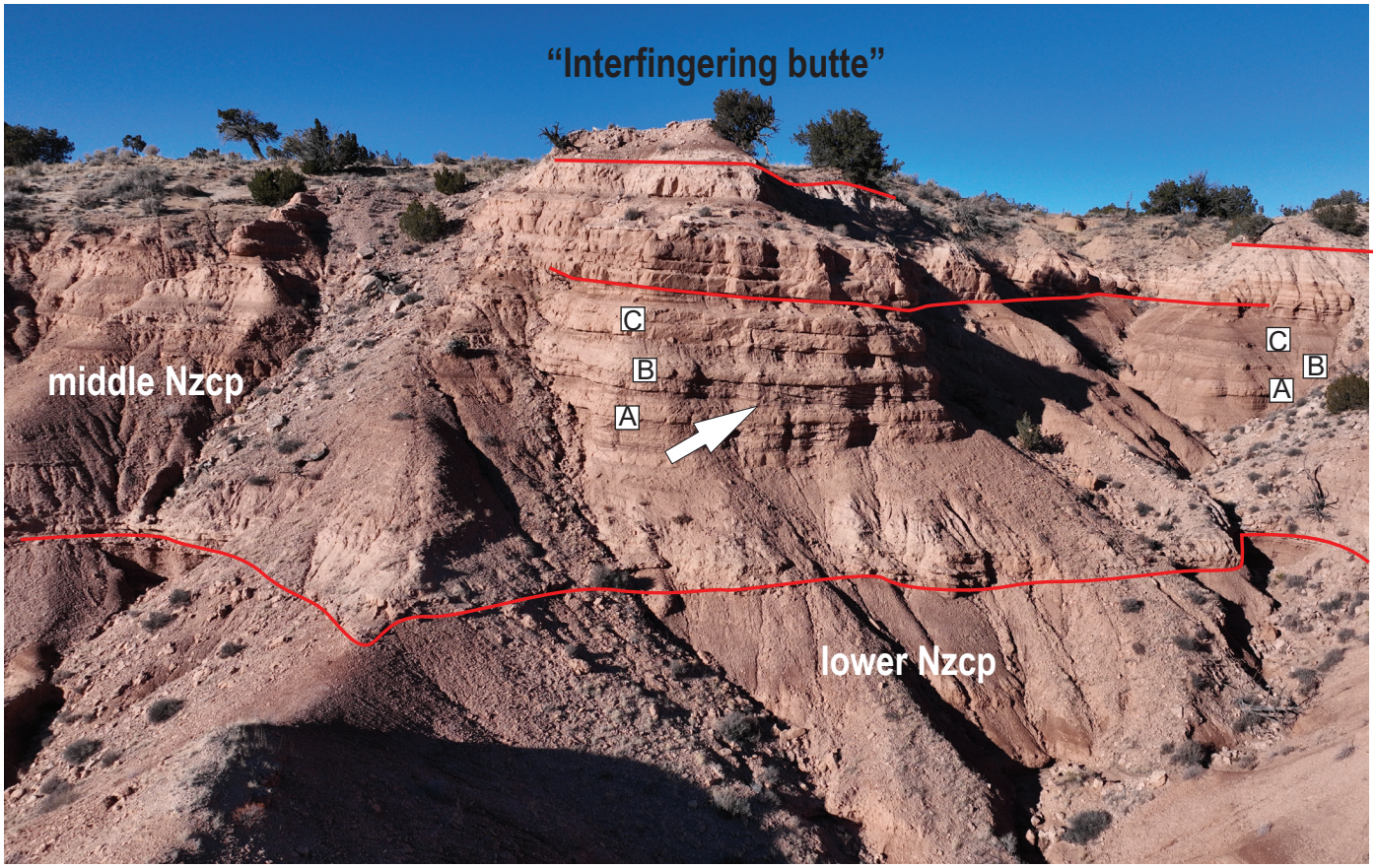


FIGURE 2.25. View to northwest of the lower and middle units of the Cañada Pilares Member (Nzcp) at "interfingering butte." The white arrow demarcates cross-stratified, intercalated clayey sediment and sands. Sandstone interfingers with clays to the right, increasing the proportion of clay to the northeast (see annotations of these interfingering beds in Figure 2.25). Three of these beds are labeled A, B, and C.

first working hypothesis of the lead author when mapping this unit. The preferred interpretation was changed to a playa lake based on the following:

1. tabular sand beds and tongues that commonly pinch out laterally (Figs. 2.24 and 2.25)
2. intercalation of clay and sand foresets (Fig. 2.25, white arrow), suggesting pulsating input of sand (probably from a channel mouth) into standing water;
3. stratigraphic intervals of interbedded sand and clay that grade laterally from sand-dominated to clay-dominated over a short distance, as exemplified at "Interfingering butte" and also an exposure to the south (Figs. 2.24 and 2.25; Koning et al., 2026d), suggestive of a relatively abrupt transition from a playa margin into playa interior, the latter having more chance of standing water;
4. relatively intricate intercalation of sand and thinner clay suggesting periodic deposition of subaerial sand sheets that were then covered by clay in a subaqueous environment (Figs. 2.26A, 2.27, and 2.28);
5. the lack of a thick or extensive cross-stratified, sandstone-channel-fill complex in or stratigraphically adjacent to the Cañada Pilares Member (e.g., if this was a floodplain, there should be river deposits, unless this river constantly stayed east of here).

We propose that these features can be explained by a playa lake that generally was dry and only held appreciable water after high runoff from adjoining piedmont drainages (mainly to the west) during intense precipitation events. Initial discharge delivered sand sheets that extended across a formerly dry playa surface, creating tabular beds (containing horizontal-planar laminations) that pinched out toward the center of the playa lake (#2 in Fig. 2.18 and Fig. 2.24). Discharge was sufficient to create scour features and shallow channels on the playa surface, and in these channels, cross-stratification could be preserved (Fig. 2.27). As the playa lake filled with water, sand sheets retrograded and graded upsection relatively abruptly into clayey sands and then clays (Fig. 2.26). This rise in water depth also allowed clay to be deposited in formerly exposed channels (Fig. 2.28). Pulsating discharge (typical in semiarid ephemeral drainages) created intercalation of clay and sand lamina and very thin foresets or planar beds (Figs. 2.26A and 2.28). *0.05 mi*

1.6 mi Waypoint 2.23 [N35.2829°, W106.8826°]

Station 4: Pilares Fault

Station 4 allows a close look at a well-exposed damage zone in the Pilares fault, in addition to the larger complexities (scales of several meters length) of a fault zone that formed in clastic basin fill. The Pilares fault is west dipping and, at this exposure, juxtaposes claystone-rich Cañada Pilares strata on the west (hanging wall) against light-colored, medium-grained sands of the Piedra Parada Member on the east (Fig. 2.18). The marked steepening of Cañada Pilares strata on

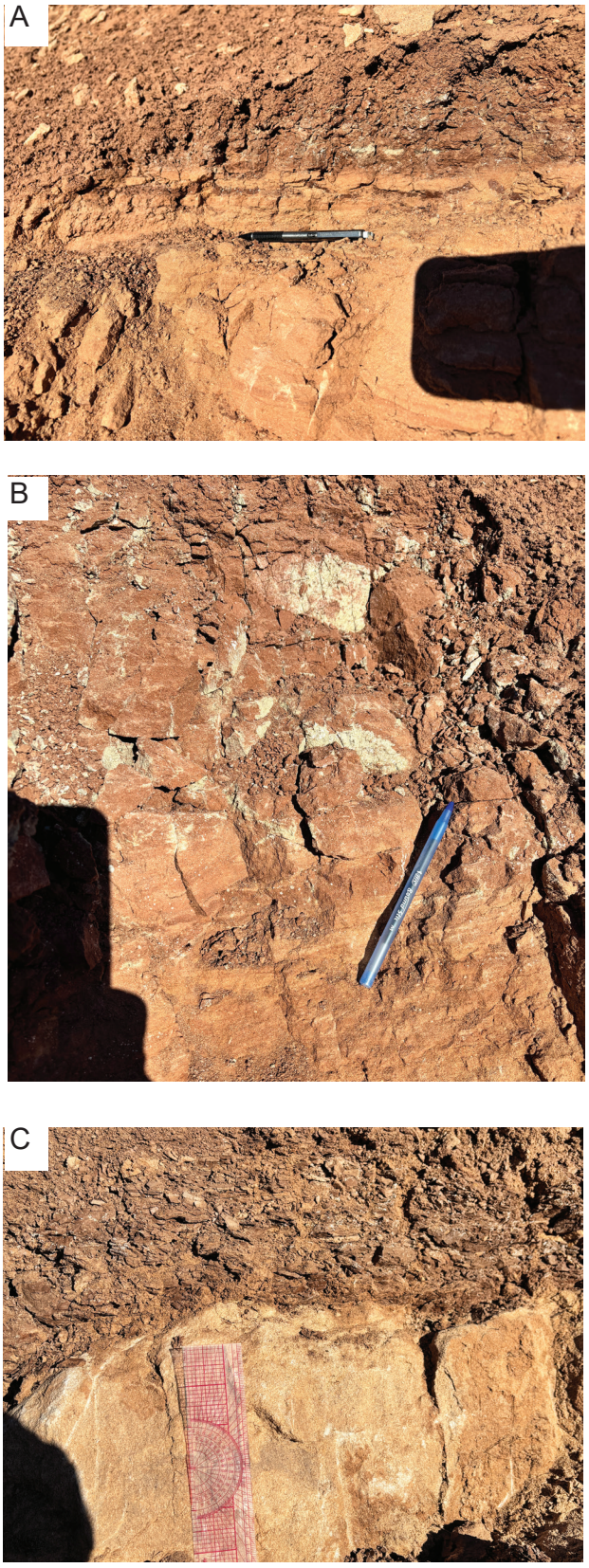


FIGURE 2.26. Photos showing different styles of the upper contact of sandstone beds in the Cañada Pilares Member. A: Abundant clay lamina in upper ~10 cm (~4 inches) of the underlying sandstone bed with silvery mechanical pencil for scale; B: Sand grading up into clayey sand-sandy clay near the blue pen; C: Slightly wavy (scoured) surface. Ruler is 15 cm (5.9 inch) long.



FIGURE 2.27. Cross-stratified sandstone bed in the middle sandy unit of the Cañada Pilares Member, exposed ~0.5 km (~0.3 mi) south of Station 3. Note the clay rip ups near the pen. This sand was likely associated with a prograding leeward side of a fluvial sand bar. Progradation ended abruptly, water level rose, and settling of suspended clay in the turbid playa lake water formed a clay drape on the bar face formed a clay drape on the bar face observed ~10 cm above the pen.

the immediate west side of the fault is an example of normal drag (Fig. 2.18). This, combined with local fault-plane slicken-striae, indicate that this fault primarily exhibits normal dip slip. Note that the fault zone is several meters wide and consists of a stepover between two fault strands, as illustrated in Figure 2.18. Between two terminating fault strands, strata dip to the north-northwest analogous to a relay ramp.

Two substations (4a and 4b) make up this station (Fig. 2.29). Substation 4a is in the arroyo bottom, where there are multiple exposures of a damage zone in the eastern strand. Features at this station illustrate how such a damage zone is formed. This damage zone is a few tens of centimeters wide and contain deformed mudstone and sandstone. Figure 2.29 shows a schematic figure of a fault zone in basin fill. Common to all basin-fill faults is the damage zone, which is typically 10–100 cm (4–40 inch) wide but can be wider (up to several meters) in large-displacement faults. In the damage zone, the original sedimentary fabric is notably disrupted by shear that approximately parallels the fault plane. If the host sediment is composed of sandstone, then deformation band faults develop in the early stages of faulting. A mix of sand and clay typically results in a clayey sand-damage zone. Disruption and shear of the damage zone typically lessens outward from the interior of the fault zone. Depending on the clay content of the host rock, a clay core can develop in the damage zone (usually in the middle or to one side or another). Clay cores in faults with small- to moderate-displacements in the Santa Fe Group (as observed by the authors) are typically a few millimeters to a few centimeters thick, but thicknesses locally can be up to a few decimeters. Such clay is not formed by cataclasis (i.e., mechanical breakdown) of sand grains. But rather, water-saturated clay is often drawn into the clay core (or wider damage zone) when low pressure pockets are created during rupture events (Caine and Minor, 2009). This phenomenon may explain the sliver of clay extending up from the top of the Cañada Pilares into the fault zone seen at the top of the exposure (Fig. 2.30). Note that in the upper part of the exposure, a sandstone block a couple meters long is bound by two faults in the fault zone. With continued displacement, one can imagine this sandstone being progressively disaggregated within the fault zone and mixed with the clay being drawn into fault zone, resulting in a mixed zone composed of sand and clay (Rawling et al., 2001; Rawling and Goodwin, 2006).

Substation 4b is upslope and to the right (east) and is best accessed by climbing up along the Cañada Pilares–Chamisa Mesa contact in the aforementioned relay ramp (Fig. 2.18). Here, one can look closely at the eastern strand of the Pilares fault zone, where reddish-brown clay (Cañada Pilares Member) is juxtaposed against light gray to white sand of the Piedra Parada Member (Fig. 2.30). Fine laminations parallel to the main fault make up a shear zone of coalesced deformation bands on the immediate footwall of the Pilares fault, a few tens of centimeters orthogonally away from the center of the fault zone (Fig. 2.31). Is there a similar shear fabric in the clay on the immediate hanging wall?

Subdued ridges on the cemented sandstone immediately underlie the fault plane, raking close to 90° (Fig. 2.31). One may be fooled into thinking these ridges and intervening grooves are slicken-striae, which are linear features produced by various phenomena related to fault slip. While there are nearby polished surfaces with slicken-striae, these ridges/grooves indicate subvertical paleogroundwater flow that was controlled by the shear fabric (Mozley and Goodwin, 1995). Consistent with this interpretation, locally these ridges are observed to bend relatively abruptly 90° (e.g., locally on the cemented fault outcrop south of the main arroyo), which would be an unusual fault-slip vector. *0.05 mi*

1.65 mi Waypoint 2.24 [N35.2830°, W106.8822°]

Station 5:
Piedra Parada Member of the Zia Fault

On the east side of the Pilares fault lies sculptured, badland topography underlain wholly by white to light tan, moderately consolidated, and weakly cemented sandstone (Fig. 2.32). The sand is medium-lower to coarse-lower, subrounded to rounded, and composed of quartz, minor plagioclase, and sanidine, 10–15% lithic (volcanic grains and chert), 5–7% orangish-colored quartz and potassium-feldspar grains, and 1–3% mafic grains. The sand mostly looks massive, but locally there is sparse cross-stratification. Near Station 4b, on the fault footwall, related foresets are >1 m (>3 ft) thick. The total sand thickness is greater than 50 m (160 ft) and mudstone interbeds are lacking. Cross-stratification generally faces east–northeast. This unit has previously been interpreted as eolian dunes, sand sheets, and interdune areas with considerable bioturbation (Gawne, 1981a, 1981b; Tedford and Barghoorn, 1999; Koning et al., 2026d).

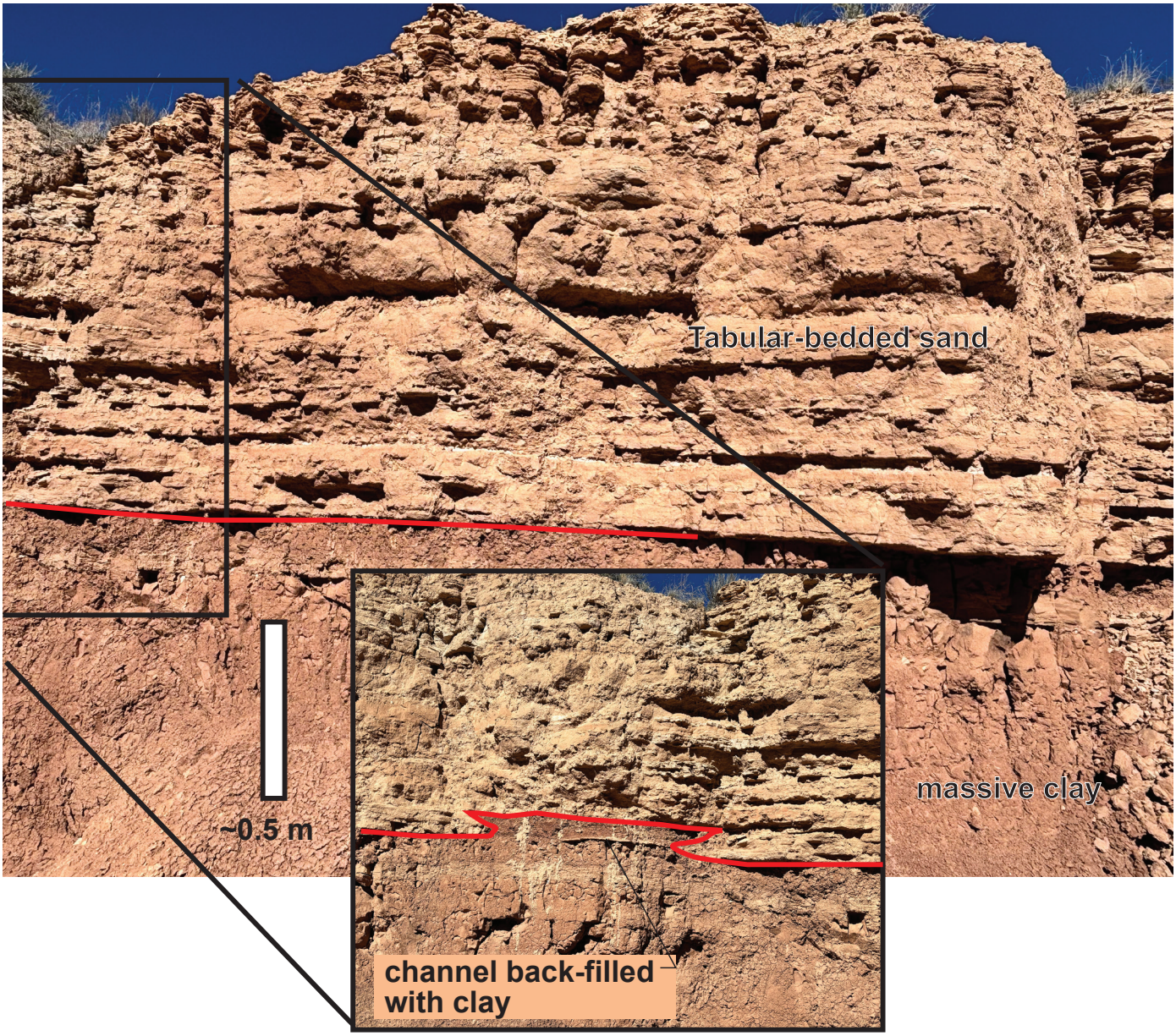


FIGURE 2.28. Very thin to medium tabular-bedded sandstones of the middle unit. View to the north. Note the sharp and planar basal surface of the sandstone interval (red line). Above the red line, the recess-forming very thin beds are silty-clayey sandstone or sandy claystone. Below the red contact lies massive sandy reddish-brown claystone. The inset photograph shows the area just left of the left border of the main photograph, where a shallow channel is filled by claystone.

Route to Station 6

Leave the amphitheater following the same route that we came (Fig. 2.15). Return to Station 1 and continue east on the mesa capped by eolian sand, following a dirt-bike path. At about 300 m (1,000 ft) east of Station 1, turn slightly right and ascend a low peak (Station 6). *0.55 mi*

2.2 mi Waypoint 2.25 [W35.2838°, W106.8829°]

Station 6:
Cerro Conejo Formation, Paleoclimate Trends in the Lower–Middle Santa Fe Group, and How Faults Influence Groundwater Flow

Stratigraphy

This peak at Station 6 offers a nice view of the cliff-forming, lower part of the Cerro Conejo Formation to the east. In the foreground are the Chamisa Mesa and the Cañada Pilares Members of the Zia Formation—the same strata that were the focus of Stations 2 through 5. Here, these strata lie on the footwall (east side) of the Pilares fault (Station 4), conformably overlying the Piedra Parada Sandstone viewed at Station 5. In this area, a stratigraphic section was recently measured for the purpose of lithostratigraphic study and for sampling authigenic carbonates for paleoclimate studies (Fig. 2.33; Koning et al., 2026d; Rugenstein et al., 2026).

At a distance of 250 m (800 ft) to the east–southeast, the Cañada Pilares Member is overlain by 60 m (200 ft) of

cliff-forming sandstone (Fig. 2.34). This sandstone was mapped as the lower Cerro Conejo Formation by Koning and Jochems (2014) and Koning and Rawling (2017). The cliff landform is due to a protective, several-meter-thick cap of strongly cemented sandstone (unit 4 in Fig. 2.34).

Of interest is the contact between the Zia and the Cerro Conejo Formations (Fig. 2.34). Whereas the contact between the two formations is scoured at Station 3, here the contact alternates between a scour to a gradation (Fig. 2.35). Elsewhere, meter-scale interfingering between sandstone of the Cerro Conejo Formation and underlying strata of the Cañada Pilares has been noted, such as 3.5 km (2.2 mi) to the southeast (Koning and Rawling, 2017; Koning et al., 2026d). The interfingering nature of the contact was also noted by Tedford and Barghoorn (1999).

The cliff-forming, lower part of the Cerro Conejo Formation contains a stratigraphic succession shown in Figure 2.33. The Cerro Conejo Formation is composed of sandstone that is similar for all units: moderately to well sorted, subrounded to rounded, and composed of quartz, minor plagioclase and sanidine feldspar, and roughly 10–17% lithics (chert and lesser volcanics). Thin-section analyses of a single sample (on the Benavidez Ranch quadrangle to the south) indicates the following mineral distribution: 50% quartz, 14% feldspar, and 36% lithic grains, with about subequal feldspar and plagioclase. The lithic fraction contains (from most to least): volcanic, chert, and fragments of siltstone and very-fine-grained sandstone (Koning et al., 2021, appendix 2, BR-198-140304-djk). Unit 1 is 5 m (16 ft) thick and consists of tabular-bedded, fine-upper to coarse-lower sandstone interbedded with 5–7% clayey sandstone. The sandstone beds are medium to thick (with horizontal-planar lamina common), whereas the clayey sand beds are very thin and erode more readily. Unit 2 is 27 m (90 ft) thick and exhibits very thickly bedded, tannish, primarily medium-grained sand. Locally, cliff exposures indicate broad channel forms. Beds are internally massive, cross-stratified, or display horizontal planar laminations. Tedford and Barghoorn (1999) note that camel fossils occur in this unit that are correlated to species from the late Hemingfordian North American Land Mammal Age. Unit 3 is 22 m (70 ft) thick and contains mainly thick to very thick beds of fine- to medium-grained sand and clayey fine sand (sand size ranging from very fine-lower to medium-lower). Beds are mostly internally massive, but there are 1% that contain 10–30-cm (4–12-inch)-thick intervals of horizontal-planar laminated, medium-lower to coarse-upper sandstone that locally fine upward. Unit 4 is 4 m (13 ft) thick and consists of a strongly cemented, interbedded succession of sandstone and minor siltstone and 5–10% clayey mudstone. Beds are distinctive and very thin to thick and tabular, with 10% channel forms. Within a given bed, sand is moderately to well sorted (e.g., very-fine- to fine-grained sand or medium- to coarse-grained sand).

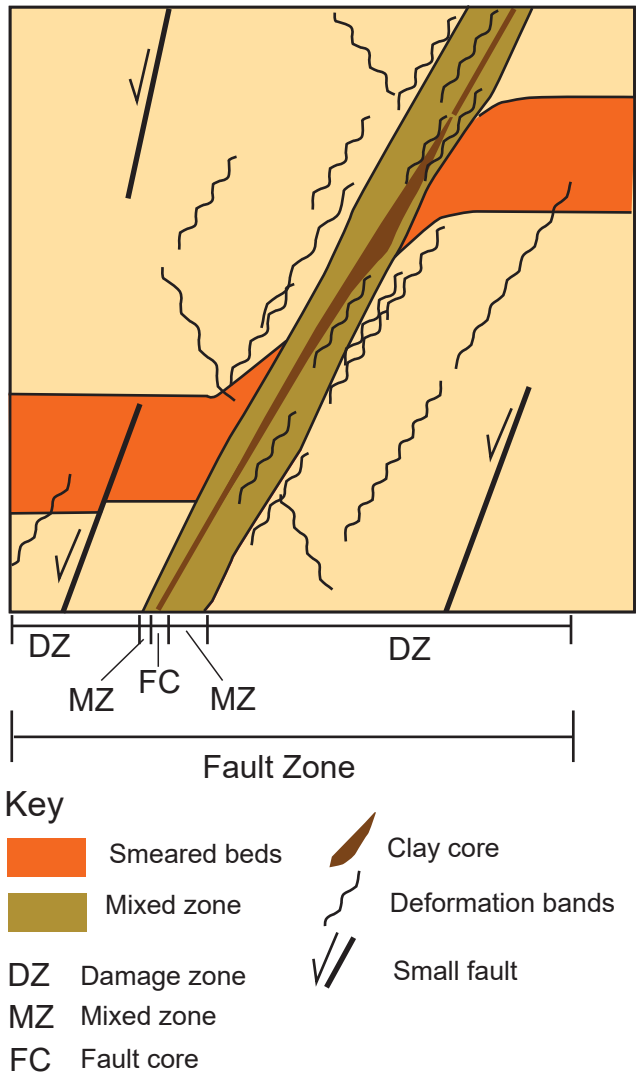


FIGURE 2.29. Schematic diagram illustrating fault zone elements that include a fault core, mixed zone, and damage zone (modified from Loveless et al., 2011, fig. 1a). Clay is commonly observed in the fault core, and deformation bands are present throughout.

Units 1 through 4 are broadly similar to sands of the Chamisa Mesa Member, particularly in color and tabular bedding. All these sands are interpreted to be alluvium deposited on the distal parts of a former piedmont (or the bajada of coalescing alluvial fans) sloping southeast from the Colorado Plateau, and locally including the adjoining basin floor (Koning et al., 2026d). Differences that proved useful in mapping were the higher proportion of coarse sand grains in the lower Cerro Conejo Formation and the higher abundance of rhizoliths in the Chamisa Mesa Member (Zia Formation). Unit 2 of the Cerro Conejo Formation is also relatively distinctive and was interpreted to be eolian by Tedford and Barghoorn (1999). However, the presence of local clay interlamination and broad channel forms suggests a complex mixture of eolian sand and fluvial cross-stratification for unit 2 (Koning et al., 2026d).

Age

The Piedra Parada Member, outcrops of which are observed west of the peak, contains fossil mammals of late Arikareean age, about 21–19 Ma. These come primarily from a single locality, the Standing Rock Quarry at the type section of the Piedra Parada Member (Piedra Parada is Spanish for "standing rock") about 10 km (6 mi) southwest of San Ysidro (e.g.,

Galusha, 1966; Gawne, 1975; Tedford, 1981). The age assignment is primarily based on carnivore, rodent, lagomorph, and camel taxa shared with well-dated fossil mammal assemblages in Nebraska and Wyoming (Tedford, 1981; Tedford et al., 2004; Morgan, 2015).

Fossils recovered in the Chamisa Mesa through Cañada Pilares Members of the Zia Formation are correlated to species that lived in the early Hemingfordian North American Land Mammal Age. Fossil mammal localities in the middle of the Chamisa Mesa Member are assigned an early Hemingfordian age based primarily on taxa of carnivores, rodents, and lagomorphs shared with well-dated fossil mammal assemblages to the north (Gawne, 1975, 1976, 1981a, 1981b; Tedford, 1981). These localities correlate to the fossil mammals from the Nambé Member of the Tesuque Formation in the Española basin of northern New Mexico.

An early Hemingfordian age is corroborated by the presence of a volcanic ashes and a detrital sanidine age of 18.262 ± 0.029 Ma collected in its middle part (Fig. 2.33; Koning et al., 2026d). Both dates provide maximum depositional ages. Using these data and considering the age assignment of the overlying Cañada Pilares Member, Koning et al. (2026d) interpret that the upper half of the Chamita Mesa Member is probably 18.5 to 18.0 Ma, with the entire unit likely 19–18.0 Ma.

The Cañada Pilares Member is younger than the 18.10 ± 0.46 Ma and 18.36 ± 0.14 Ma ages shown in Figure 2.33 because the associated sampled ashes may have been reworked. Most of the Cañada Pilares Member yields few age-diagnostic fossil mammals (Gawne, 1981a, 1981b). Fossils found in the Cañada Pilares Member are mostly the small camel *Blickomylus galushai*. However, sand-filled channels near the top of the member have yielded a composite fauna indicative of an early Hemingfordian North American Land Mammal Age (18.9–17.5 Ma; Tedford and Barghoorn, 1999). Considering that the magnetic polarity of the Cañada Pilares Member and the constraints that its age needs to be >17.5 Ma (based on fossils) and <18.2 Ma (aforementioned detrital sanidine and ash data) gives the correlation to the global polarity time scale as shown



FIGURE 2.30. The Pilares fault at Station 4b. View is to the north. The fault juxtaposes reddish-brown clay-rich strata of the Cañada Pilares Member (left) against the lighter-colored, sandy Piedra Parada Member (right). The fault is partially annotated as a thick, black line; for adjoining text U = up and D = down. Immediately below the fault plane, in the Piedra Parada Member, is a 10–50-cm (4–20-inch)-thick inclined shear fabric that has been strongly cemented. The white and gray arrows point to a clay bed and a pink sand, respectively, of the Cañada Pilares Member that have been detached and brought into the fault zone. With continued slip, these would be expected to continue to shear and disaggregate and form the typical sandy-clayey mixture seen in the mixed zone of a fault in weakly lithified sediment.



FIGURE 2.31. Photograph of the footwall of the Pilares fault. Note the sand-deformation-band style of shear and the enhanced cementation observed near the blue pencil. View is to the north. As shown in the inset photo, there are linear features on the cemented part of the fault zone. Blue pencil for scale. These linear features look like slicken-striae but are actually small groundwater-cemented ridges.

in Figure 2.33 and an age of 18.0–17.5 Ma.

The age of the Cerro Conejo Formation is mostly 14.7–10 Ma in its type area and in this area (Connell et al., 1999; Connell, 2008a; Koning and Jochems, 2014; Koning and Rawling, 2017). Mammalian fossils found in the unit primarily correlate to the late Barstovian North American Land Mammal Age (Tedford and Barghoorn, 1999). A key fossil is a *Gomphothere*, which has only been collected in the Cerro Conejo Formation above a disconformity in its lowest strata (~30 m [~100 ft] above its base; Figs. 2.33 and 2.36). This age range is generally consistent with a detrital sanidine age of 14.87 + 0.04 Ma obtained from ~45 m (150 ft) above its basal contact in unit 3 (Fig. 2.33). Synthesizing these data with the paleomagnetic data of Tedford and Barghoorn (1999) gives an age range of 14.8 to ~9 Ma for the majority of the Cerro Conejo Formation, but 17.5–16.6 Ma for the lower ~30 m (~100 ft) underlying the cryptic disconformity (Figs. 2.33 and 2.34; Koning et al., 2026d).

Middle Miocene unconformity: allostratigraphic versus lithostratigraphic?

Based on available age control, no fossils from the early Barstovian North American Land Mammal Age have been collected along the Ceja del Rio Puerco, meaning an unconformity exists between the Cerro Conejo and Zia Formations—the former has late Barstovian fossils and the latter has Hemingfordian fossils (see summary in Connell, 2004). The location of this unconformity in the stratigraphic section is not obvious. Instead of one disconformity, there may be several or a condensed section. Based on the aforementioned faunal distribution and detrital sanidine data, a disconformity appears to lie somewhere between 30–45.2 m (100–148 ft) above the base—between the top of the cross-stratified sandstones (containing late Hemingfordian fossils per Tedford and Barghoorn, 1999) and the location of the 14.867 ± 0.041 Ma detrital sanidine age in the Arroyo Benavdiez-02 stratigraphic section (Fig. 2.33). But the obvious choice for a lithostratigraphic contact is the top of the mudstone-rich Cañada Pilares Member (Figs. 2.33 and 2.34) and identifying a mappable contact ~30–45 m (~100–150 ft) above these mudstones proved difficult (as stated in Tedford and Barghoorn, 1999), especially to the south. This presents the mapper with the dilemma of reconciling lithostratigraphy (rock-based contacts) with allostratigraphy (unconformity-based boundaries). Typically, the two coincide where lacunae are sufficiently large and extensive, but in this case they do not, and the North American Stratigraphic Code (NACSN, 2005) states that formation-related contacts should be based on lithologic criteria. The lead author chose the obvious lithostratigraphic contact in mapping, but this results in an allostratigraphic contact with a ~2 My lacuna being present ~30–45 m (100–150 ft) above the base of the Cerro Conejo Formation or possibly a condensed section in the lower ~30–45 m (100–150 ft) of the formation. This results in a broader age range of 17.5–9.5 Ma for the Cerro Conejo Formation instead of the more focused 14.8–9.5 Ma (see Connell, 2008b, for constraints on the age of the upper contact).

Paleoclimate Interpretations

As part of a National Science Foundation (NSF)-funded project focused on Miocene paleoclimates in New Mexico, several of the authors and students at Colorado State University have collected samples of authigenic carbonate and clay from the Santa Fe Group to investigate paleoclimate and paleoenvironments of central and northern New Mexico. Initial findings—particularly as they relate to the relationship between local and global climate during the Miocene Climate Optimum in the Española Basin—have been published in Spaur et al. (2025). The Miocene presents a potentially valuable analogue to future Earth system states. Much of the Miocene, and particularly the Miocene Climate Optimum (MCO), is characterized by higher atmospheric CO_2 levels (400–800 ppm) and global temperatures that were 5–8°C warmer than preindustrial global temperatures (Steinthorsdottir et al., 2021; CenCO2PIP, 2023).

Several major, outstanding questions revolve around how climate and ecosystems in the modern-day southwestern United States will respond to current warming and rising atmospheric CO_2. There remains substantial uncertainty about how both the North American Monsoon and wintertime moisture will change in the future (Seager and Vecchi, 2010). Consequently, past climates present an opportunity to potentially constrain

future climates in the Southwest. Whereas models tend to suggest drying as the world warms, during the middle Pliocene (~3.2 Ma), the Southwest appears to have hosted lakes, which require an increase in effective moisture (Ibarra et al., 2018; Menemenlis et al., 2022). This increase in precipitation has been attributed to either the existence of a permanent El Niño-state (also called "El Padre") in the tropical Pacific (Molnar and Cane, 2002; Winnick et al., 2013; Ibarra et al., 2018) or to an increase in North American Monsoonal moisture caused by exceptionally warm sea-surface temperatures off the coast of California (Bhattacharya et al., 2022; Fu et al., 2022).

Rugenstein et al. (2026) present new stable isotope data from the Albuquerque Basin. Samples were collected from the upper Piedra Parada Member of the Zia Formation through the middle Cerro Conejo Formation (~20–17 Ma and 17–12 Ma), the upper Arroyo Ojito Formation (7.2–6.3 Ma), and the petrocalcic paleosol (5–4 Ma) on the Rincones paleosurface. Figure 2.33 shows stable isotope data for the Zia Formation through lower Cerro Conejo Formation. Sampling targeted authigenic carbonates such as rhizoliths, root casts, nodules, paleosol calcic (Bk) horizons, and sandstone cements. The $\delta^{18}O$ of carbonate is thought to reflect regional precipitation trends in $\delta^{18}O$, which in turn reflects moisture source (i.e., North American Monsoon or wintertime westerly moisture; Spaur et al., 2025). The $\delta^{13}C$ in authigenic carbonate, in turn, reflects the balance between atmospheric pCO_2 and soil respiration, which is related to plant productivity.

We summarize $\delta^{18}O$ and $\delta^{13}C$ isotope trends with respect to the stratigraphy and the implications for seasonality of moisture and plant productivity on the landscape. For more detailed information, we refer the reader to Rugenstein et al. (2026). The combination of relatively low $\delta^{13}C$ in the uppermost Piedra Parada and Chamisa Mesa Members, combined with relatively high atmospheric CO_2, means that plant productivity was fairly high and likely higher than today (Fig. 2.33). There are no notable shifts in $\delta^{18}O$ and $\delta^{13}C$ between the uppermost Piedra Parada and Chamisa Mesa samples. This is consistent with the notion that the shift from the eolinite facies of the Piedra Parada Member to the basin floor/distal piedmont facies of the Chamisa Mesa Member may have been driven by changes in sand supply rather than a shift in climate (Koning et al., 2026d).



FIGURE 2.32. Relatively massive medium-lower to coarse-lower sand of the Piedra Parada Member at Station 6. East-facing cross-stratification is locally observed (white arrow), but in most places this stratification is obscured due to a thin brownish film of muddy sand on the outcrop face.

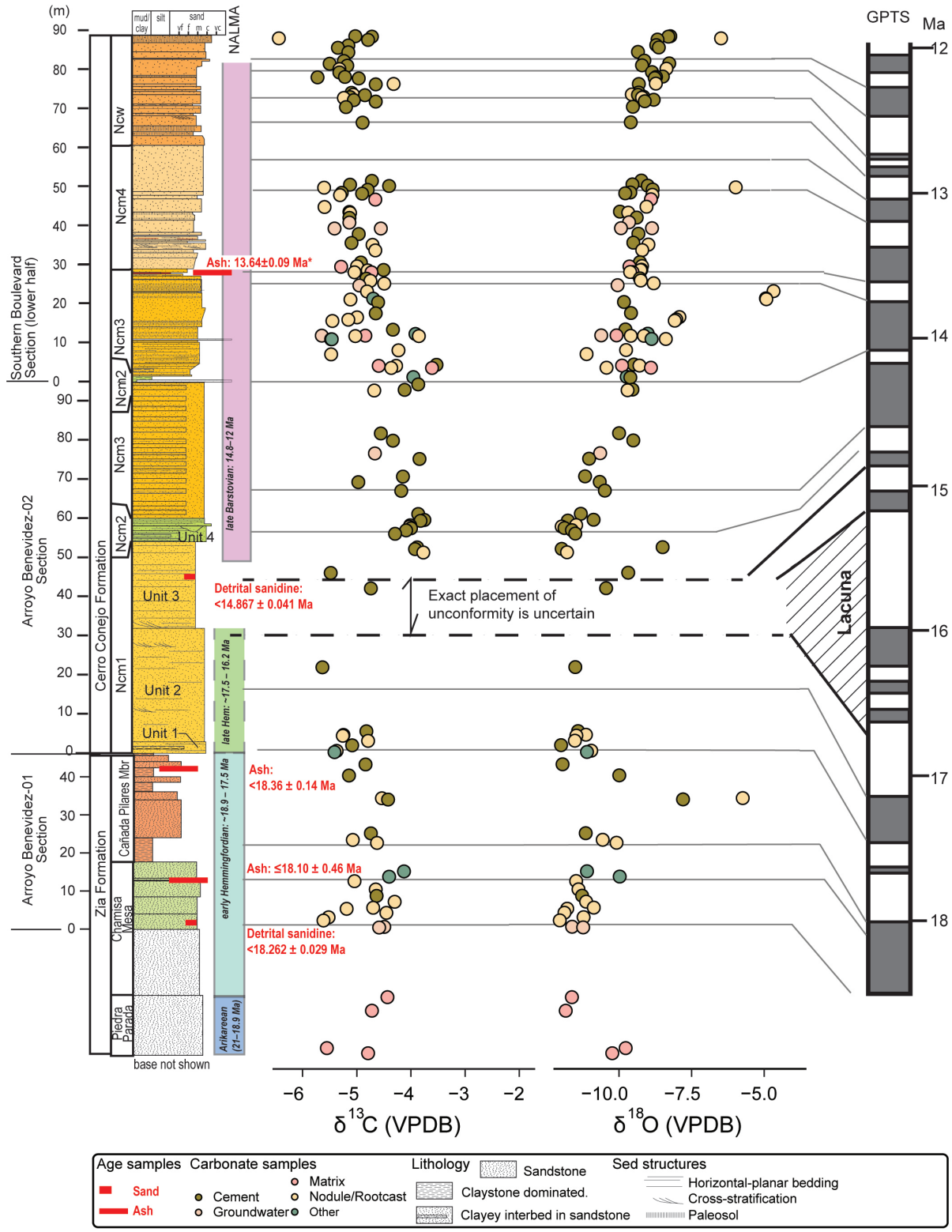


FIGURE 2.33. Stratigraphic section (left) correlated to the Global Polarity Time Scale (right) using the magnetostratigraphic data of Tedford and Barghoorn (1999). Radiometric age control shown in red; asterisk denotes age control from an ash at a similar stratigraphic position in Tedford and Barghoorn (1999). Informal lithofacies of the Cerro Conejo Formation are labeled Ncm1 through Ncm4 and Ncw (Koning et al., 2026d). The four stratigraphic units seen at Station 6 (Fig. 2.34) are labeled units 1 through 4. Circles in the middle of the figure show the $\delta^{13}C$ and $\delta^{18}O$ stable isotope data of Rugenstein et al. (2026). Both $\delta^{13}C$ and $\delta^{18}O$ values are relatively low and steady throughout deposition of the Zia Formation (the two high $\delta^{18}O$ values occur in the middle of the Cañada Pilares Member and may reflect evaporation of surface water in a playa lake). Samples in the lower Cerro Conejo Formation correspond temporally to the very beginning of the MCO. These samples exhibit particularly low $\delta^{13}C$ and $\delta^{18}O$, suggesting a high proportion of winter precipitation and relatively high plant productivity. In the overlying Cerro Conejo Formation, a period of heavier $\delta^{13}C$ values occurs at 14.8–14 Ma. After 14.8 Ma, note how the $\delta^{18}O$ data steadily increase, likely due to a long-term increase in the proportion of summer precipitation.

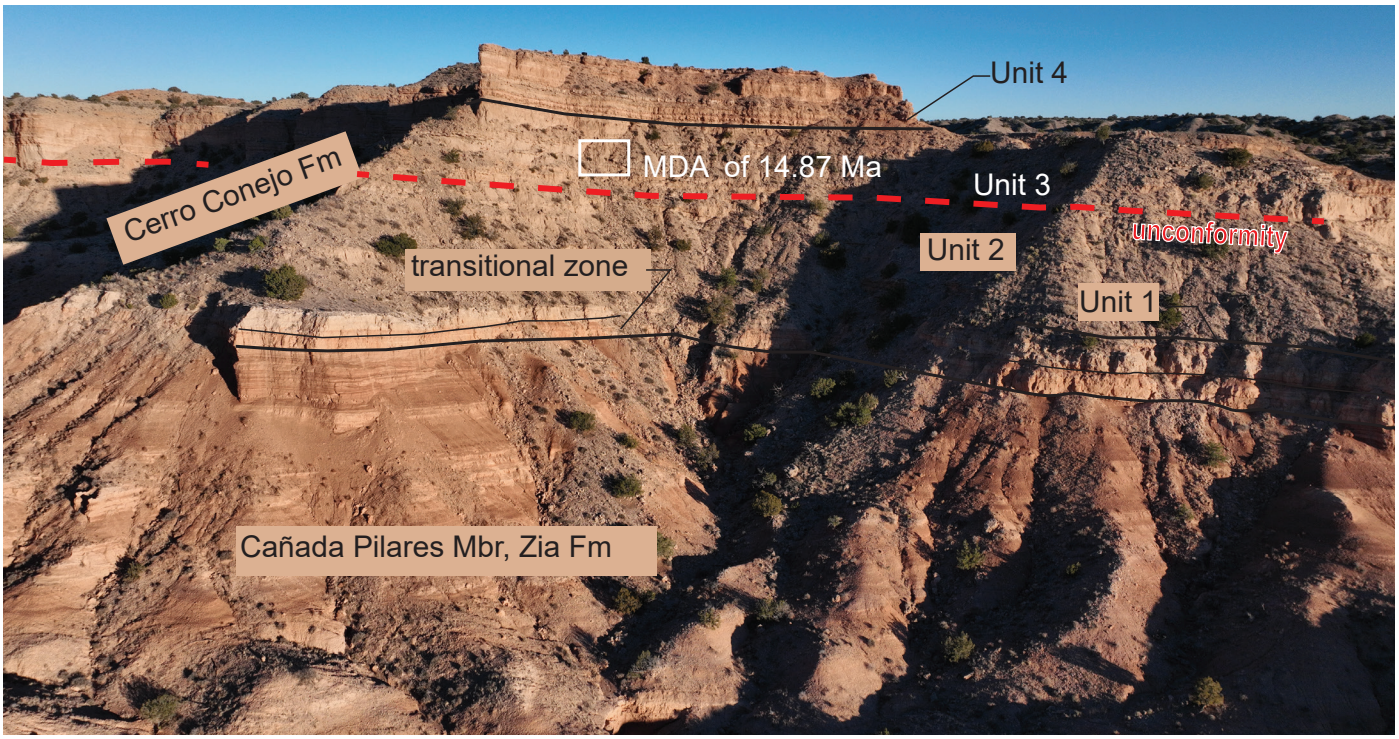


FIGURE 2.34. Annotated photograph of the steep terrain located 300 m (1,000 ft) east of Station 6. View is to the east. Units 1 through 4 are from the Arroyo Benavidez-02 stratigraphic section (Koning et al., 2026d) and summarized in the road log text. Approximate position of a major unconformity (lacuna of ~16.7–14.8 Ma) is indicated by the dashed red line. The contact between the Cañada Pilares Member and the lower Cerro Conejo Formation alternates between scoured and gradational in this area, and the associated transitional zone is labeled. The detrital sanidine sample that gave a maximum depositional age of 14.87 Ma is correlated into view from 350 m (1,150 ft) to the south.

Within the Cañada Pilares Member, $\delta^{13}C$ data are similar to those within the Chamisa Mesa Member. However, several authigenic carbonate samples have high $\delta^{18}O$ values (2.5–5‰ higher than average). Such high values, particularly when these are several standard deviations different than the majority of the data, are thought to indicate evaporative conditions in a shallow lake or playa system (Detmann et al. 2003), consistent with our sedimentological interpretation.

The lacuna (or possible condensed section) within the lower Cerro Conejo Formation means that few samples are available to test whether the exceptionally high CO_2 of the MCO resulted in a major change in $\delta^{13}C$ and plant productivity. However, the few samples at the beginning of the MCO exhibit low $\delta^{13}C$ and, combined with the high atmospheric CO_2 at the time, suggest that plant productivity was high. Above the lacuna, carbonate $\delta^{13}C$ is high and then steadily declines through the measured Cerro Conejo Formation. This decline in $\delta^{13}C$ may be a result of declining atmospheric CO_2 as the world cooled following the MCO, or possibly it reflects an increase in C3 plant productivity (Rugenstein et al., 2026). C3 plants include mainly shrubs and trees that utilize an older and more widespread form of photosynthesis. C4 plants include mainly summertime grasses that use a more water-efficient photosynthetic pathway that most recently originated in the late Paleogene or early Neogene (Edwards et al., 2010).

Carbonate $\delta^{18}O$ generally increases through the lower-middle Cerro Conejo Formation and is comparably higher than in the Zia Formation. There is a particularly rapid increase above the lacuna in the Cerro Conejo that may represent a shift away from low-$\delta^{18}O$ wintertime precipitation following the conclusion of the MCO toward high $\delta^{18}O$ summertime precipitation. A similar shift post-MCO was found by Spaur et al. (2025) in the Española Basin and may be attributed to increasing proportions of summertime moisture. Overall, these data support the interpretation that the Albuquerque Basin was semiarid during the Miocene but may have sustained greater plant productivity. This greater productivity may have been due to higher atmospheric CO_2 that drove CO_2 fertilization, and semiarid environments should be particularly susceptible to changes in productivity driven by changes in CO_2, facilitated by adjustments in plant water use efficiency (Donohue et al., 2013). Alternatively (or perhaps in addition to), the greater fraction of moisture received in the winter may have sustained higher groundwater tables in the basin, promoting greater standing biomass. Such a relationship between wintertime moisture and standing biomass is observed across the western United States today (Kukla et al., 2022, and references therein).

Fault zones and groundwater flow

Faults can control groundwater flow in two ways. First, the clay cores and enhanced cementation of damaged and mixed zones can act as barriers to subhorizontal flow (Rawling et al., 2001; Caine and Minor, 2009). The enhanced cementation is a result of initially high permeability, especially in the vertical direction, because of vertical disruption (shear) of the original sedimentary fabric, which can be anisotropic at the grain scale (Rawling and Goodwin, 2006). As deformation progresses with subsequent rupture events, more clay, sourced from the

host rock, becomes entrained into the mixed zone via smearing and/or injection (Rawling and Goodwin, 2006). Cement often continues to accumulate from subvertically oriented groundwater flow parallel to the fault plane, but this cementation may be subjected to continued syn-rupture disruption followed by reprecipitation (Williams et al., 2016). Over time cementation of formerly more porous (sandy to gravelly) sediments in the damaged and mixed zones commonly increases and the clay core widens and/or becomes more continuous. The net effect is that faults developed in poorly lithified sediments of the Santa Fe Group are likely to be barriers to both horizontal and vertical groundwater flow (Rawling et al., 2001).

Second, faults can juxtapose a low permeability unit against a high permeability unit. If the lower permeability unit is downgradient (in terms of groundwater flow) across a fault and the higher permeability unit is upgradient of the fault, this juxtaposition would result in a seal being created across the fault. Across the three-dimensional extent of the fault plane in the subsurface, higher permeability units might be juxtaposed against one another, creating local groundwater flow "windows" (Connell, 2011, 2026). **Return to parked vehicles, following the way we walked in (Fig. 2.12).**

End Stop 1 Walking Tour

Turn vehicles around and drive the county road back east to the top of the escarpment (Ceja del Rio Puerco), about 1.2 mi east of the Stop 1 parking area.

Waypoint 2.26 [N35.2940°, W106.8575°]

14.9 **Drive through the gate marking the boundary of the Santa Ana Pueblo and REZERO THE ODOMETER. Proceed east on network of dirt roads.** *0.05*

0.05 **Turn right (south) on the wide dirt road (Sixtieth Street) immediately east of the north-trending powerlines.** *0.55*

0.6 Pass the north end of the TAG Solar array field. *0.8*

1.4 Intersection of Sixtieth Street and the west end of Northern Boulevard (unsigned). Continue straight. *0.3*

1.7 Tilled area to the left (east) of Sixtieth Street. *0.8*

2.5 Intersection of Sixtieth Street and the west end of Sandia Boulevard (unsigned). Continue straight. *1.0*

3.5 Pass concrete bunker-like communications facility. *0.1*

3.6 **Waypoint 2.27 [N35.2416°, W106.8563°]**
Intersection of Sixtieth Street and Southern Boulevard. **Continue south on Sixtieth Street.** Views of Sandia Mountains and Manzanita Mountains to the east and southeast, respectively (Fig. 2.37). *1.0*

4.6 **Waypoint 2.28 [N35.2312°, W106.8579°]**

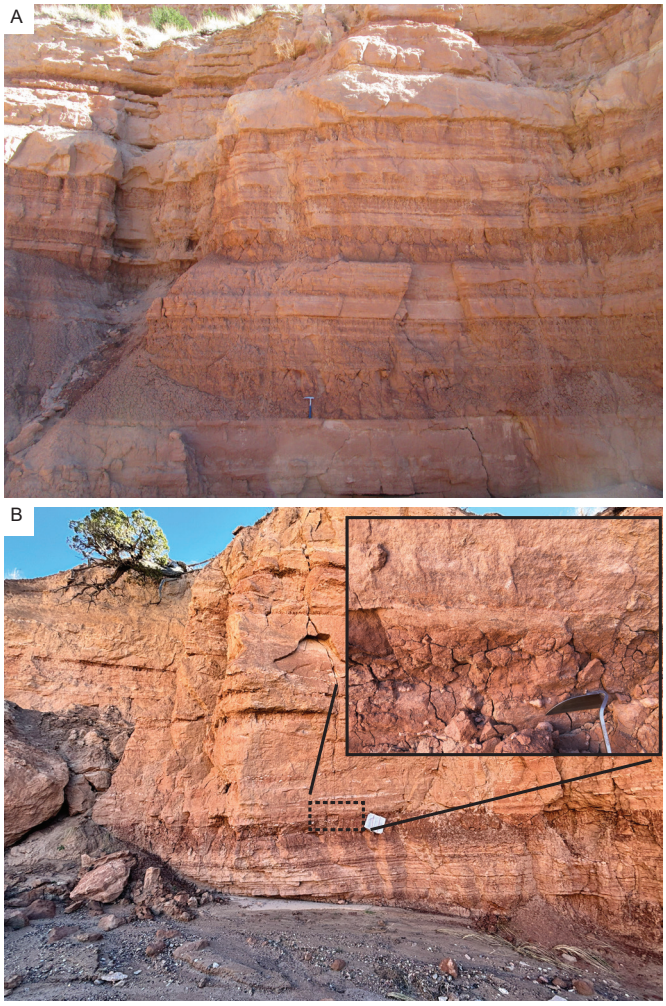


FIGURE 2.35. Photographs illustrating the gradational nature of the Zia–Cerro Conejo Formation contact in Arroyo Benavidez. Compare this with the scoured sharp contact seen at Station 3 of Stop 1.

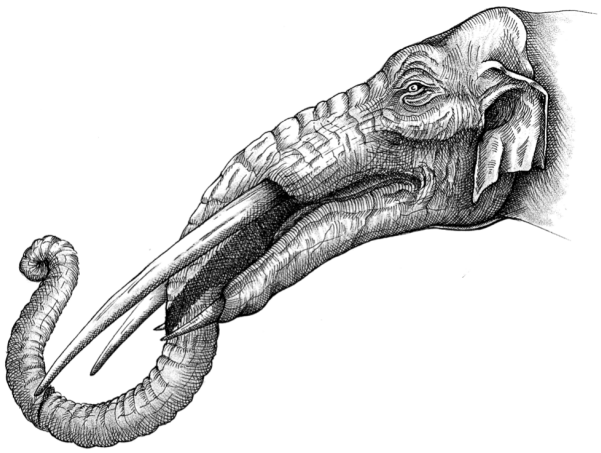


FIGURE 2.36. The first North American proboscideans belonged to the genus *Gomphotherium*, a stocky browser characterized by its very long lower jaw and possession of four tusks, among other features. These proboscideans (elephants and their allies) originated in Africa during the Eocene and made it to Eurasia by the early Miocene. They then emigrated on to the Americas, reaching the American Southwest about 14.5 Ma. This genus is a diagnostic species used to differentiate the late versus early Barstovian Land Mammal Ages (i.e., the late Barstovian has these proboscideans).

Turn right (west) on an unmarked west-east dirt road and park vehicles for Stop 2. *0.1*

STOP 2: Upper Santa Fe Group, Calabacillas Segment of the San Ysidro Fault Zone, and Quaternary Hanging-wall Wedge Deposits

Following 4-wheel drive roads, walk ~300 m (~1,000 ft) west from the parking area to the top of the ridge (dashed yellow line on Fig. 2.38). Once on this ridge, proceed northward ~50 m (~160 ft) to the highest part of the ridge, where it juts westward (Station 1).

Waypoint 2.29 [N35.2309°, W106.8627°]

Station 1: Upper Santa Fe Group, San Ysidro Fault, and Quaternary Hanging Wall Wedge Deposits

Geographic and tectonic setting

Stop 2 offers a view of the upper Santa Fe Group and the San Ysidro fault from a short westward spur of the Ceja del Rio Puerco (Fig. 2.38). The latter is the north-trending escarpment bounding the west side of the Llano de Albuquerque, where cliffy terrain is frequently formed in upper Santa Fe Group strata. To get there, we will hike about 0.4 km (0.25 mi) up a steep dirt track to the top of the hill (Station 1). After overview discussion, participants who wish to see a fault zone and associated faulted deposits can hike down a short, flagged-out path to Station 2 (be cautious of ledges and cliffs that can cause injury).

From here, we can view contrasting landscapes of the eastern Colorado Plateau to the west and the Albuquerque Basin to the east before focusing on the topographic amphitheater to our immediate north, where the traces of the Sand Hill fault and Calabacillas segment of the San Ysidro fault are within 0.5 km (0.3 mi) of each other. To the west is the Rio Puerco Valley, which is about 60 km (37 mi) east of Mount Taylor on the western skyline. Compared with Stop 1, we have a more expansive view of the Rio Puerco Valley, especially to the south. Eastward of us is a gently rolling grassy landscape that makes up the western side of the Llano de Albuquerque. The Llano de Albuquerque forms a prominent interfluve between the Rio Puerco and Rio Grande valleys. The Llano de Albuquerque represents maximum aggradation of the Ceja Formation of the Santa Fe Group and thus is a relict depositional surface. However, it has been modified by extensive arroyo incision, faulting, and eolian deposition. This geomorphic surface formed shortly after 1.8 Ma and before 1.3 Ma (Connell et al., 2013) due to incision and sediment bypass of southeastward-flowing Colorado Plateau drainages.

Fault influence on Santa Fe Group stratigraphy

The amphitheater to the north contains two major faults that juxtapose the Cerro Conejo, Arroyo Ojito, and Ceja Formations (Figs. 2.39–2.41). The two faults are the Sand Hill fault (west) and the San Ysidro fault (east), both of which are east-down normal faults (Cather et al., 1997; Rawling et al. 2001; Connell, 2008a). On the west (footwall) side of the Sand Hill fault lies markedly reddish, tabular, and thickly bedded sandstone of the upper red unit of the Cerro Conejo Formation (Fig. 2.40). Cerro Conejo sandstones are generally fine- to coarse-grained and exhibits weak paleosols (Koning et al., 2026d). Upper Cerro Conejo strata are interpreted to reflect a notable progradation of the western piedmont at 13–10 Ma, and



FIGURE 2.37. View to east of Sandia Mountains from the west end of Southern Boulevard. Sandy surficial unit consists of fine- to medium-grained eolian sand and locally reworked by sheetwash. This map unit is probably the most common surficial unit in the basin.

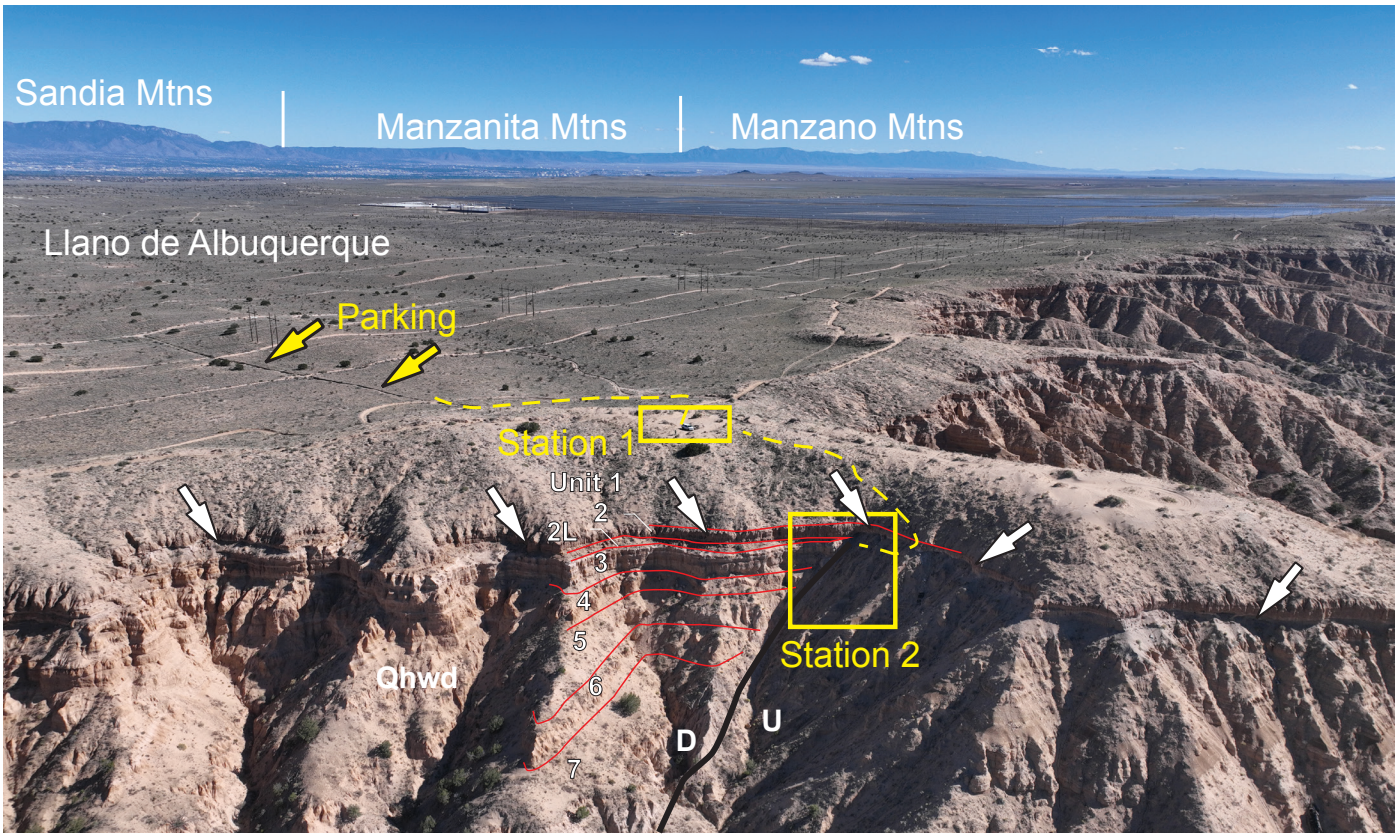


FIGURE 2.38. View to southeast, illustrating the locations of Stations 1 and 2 at Stop 2. Dashed yellow line is the walking route. The black line is the San Ysidro fault (U = up; D = down). Provisionally labeled stratigraphic units are described in the text and in Connell et al. (2026), and make up a hanging wall wedge deposit (Here, a map unit called Qhwd). White arrows denote a well-developed petrocalcic paleosol (Stage III carbonate morphology) in unit 2. Overlying unit 2 is the eolian dune sand of unit 1. Note that both units 1 and 2 extend westward across the San Ysidro fault and onto the footwall.

grade westward laterally into gravelly strata of the Benavidez Member of the Arroyo Ojito Formation (Koning et al., 2026d).

Between the Sand Hill and San Ysidro fault zones are tan sandstone and pebbly sandstone mapped as the Navajo Draw Member of the Arroyo Ojito Formation (Fig. 2.41). The Navajo Draw Member consists of >60 m (>200 ft) of sandstone interbedded with minor pebble-conglomerate beds and 1–5% mudstone beds. Gravel composition is approximately 30–50% tan and fine-grained Mesozoic sandstone, 15–30% dark gray to black to brown chert, 10–40% Pedernal chert, 10% red granite, 1–5% quartzite, 1% gray intermediate-volcanic rocks, 0.5% mudstone rip-up clasts, and trace lithic-rich sandstone. Arroyo Ojito Formation sandstone is mostly fine- to coarse-grained and cross-laminated (up to 50 cm [20 inch]-thick foresets) or horizontal-planar laminated (Koning and Jochems, 2014). These strata lack the characteristic yellowish colors of the Navajo Draw Member and the red to brown colors of the Loma Barbon Member of the Arroyo Ojito Formation, but the gravel composition is more similar to the Navajo Draw Member and it has been mapped as such in Connell (2008b). The presence of variously colored cherts and sandstones is similar to those of other paleodrainages derived from the Colorado Plateau (compare to Connell et al., 1999; Koning et al., 2002). However, the high proportion of Pedernal Chert, coupled with 10% granite, indicates the associated paleodrainage was also partly sourced

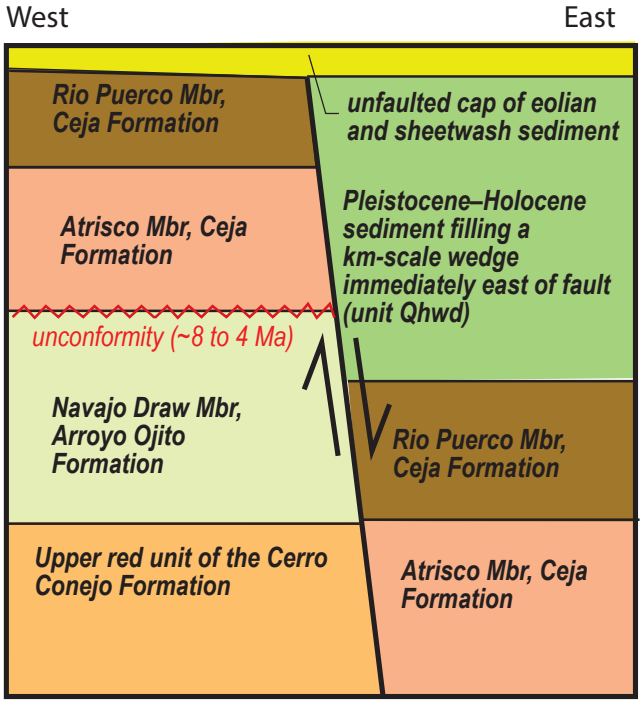


FIGURE 2.39. Diagram illustrating the general stratigraphy on either side of the San Ysidro fault in the vicinity of Stop 2. Note the unconformity that separates the Ceja and Arroyo Ojito Formations (red line and text), corresponding to the Rincones paleosurface of Connell (2008b).

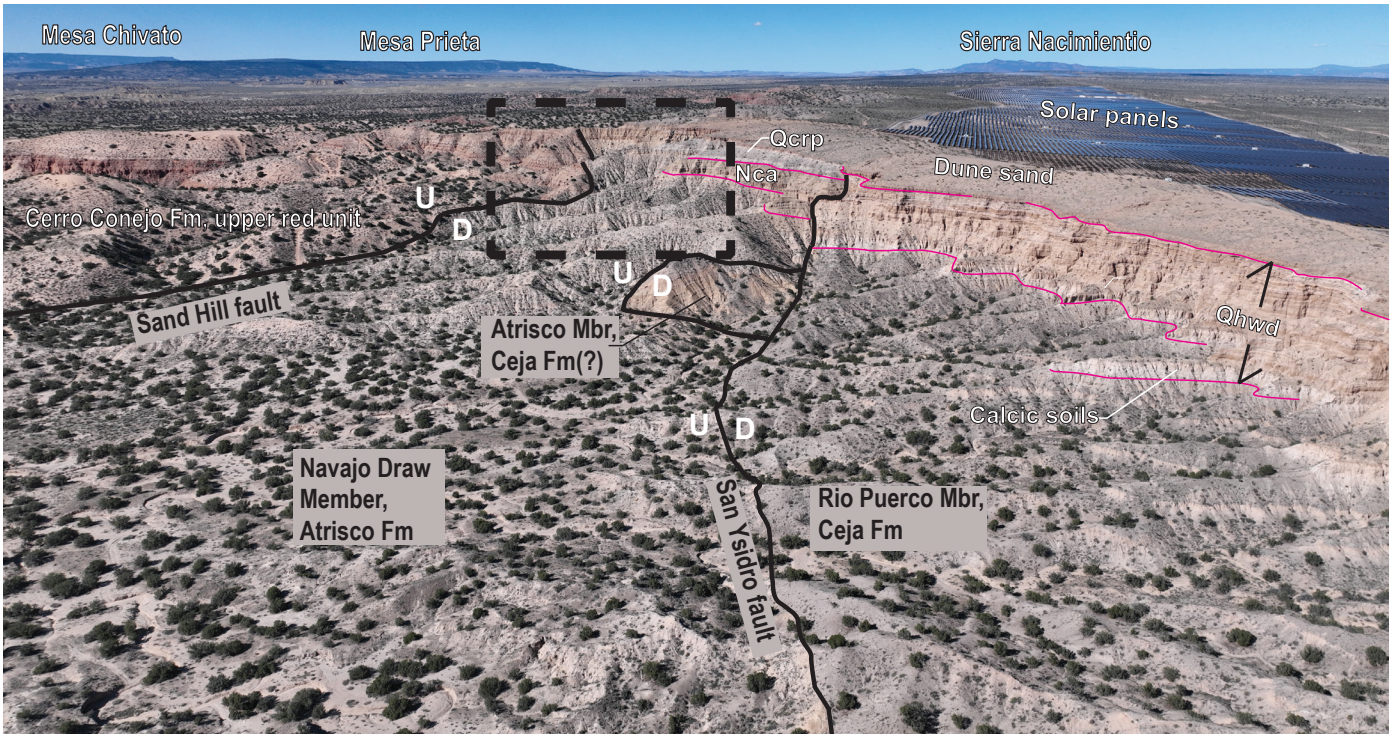


FIGURE 2.40. Photograph to the north across the amphitheater north of Stop 2. The black lines denote the traces of the Sand Hill and San Ysidro faults. The upper red unit of the Cerro Conejo Formation is on the footwall of the Sand Hill fault. The lighter-colored sandy Navajo Draw Member is exposed the between the Sand Hill and San Ysidro faults. The younger conglomeratic Rio Puerco Member (Ceja Formation) is exposed on the hanging wall (east side) of the San Ysidro fault. Above the Rio Puerco Member are eolian and sheetwash deposits that form Qhwd and that collectively occupy a wedge-shaped area created by post-Ceja Formation displacement on the San Ysidro fault. The thick, dashed line denotes the area captured in Figure 2.41. Qcrp = Rio Puerco Member of Ceja Formation; Nca = Atrisco Member of Ceja Fm.

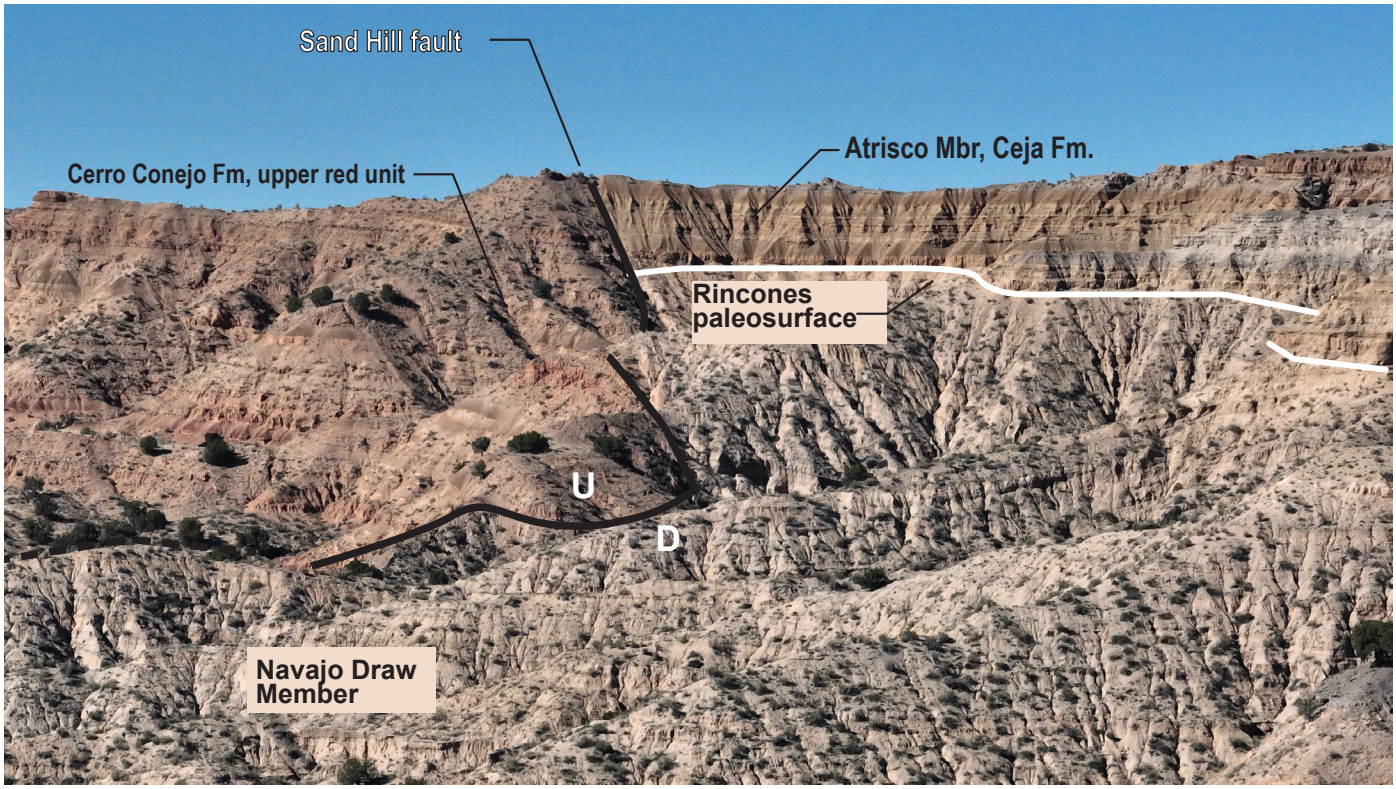


FIGURE 2.41. Photograph of offset strata on either side of the Sand Hill fault on the north side of the topographic amphitheater at Stop 2. The photographed area approximately corresponds to that within the thick, dashed line of Figure 2.40. The Rincones paleosurface, shown as a white line, represent a major disconformity dividing Miocene and Pliocene strata. Navajo Draw Member strata form a syncline on the hanging wall of the Sand Hill fault, where the Rincones paleosurface is locally expressed as an angular unconformity.

from the western flank of the Nacimiento Mountains (Brandes, 2002; Connell, 2004).

Two members of the Ceja Formation are exposed in this amphitheater. Between the Sand Hill and San Ysidro faults, the brownish, mudstone-prone unit overlying the whitish sediment is correlated to the Atrisco Member of the Ceja Formation (Figs. 2.39–2.41). A sharp, planar contact separates this sediment from the underlying Navajo Draw Member of the Arroyo Ojito Formation. This contact corresponds to a major unconformity correlated to the Rincones paleosurface (Connell, 2008a). The grayish gravelly strata on the lowest exposed part of the hanging wall (east side) of the San Ysidro fault are correlated to the Rio Puerco Member of the Ceja Formation (Fig. 2.40). In unfaulted exposures, the Rio Puerco Member overlies the Atrisco Member, such as in the fault block between the Sand Hill and San Ysidro faults (Figs. 2.39 and 2.40), so on the hanging wall (east side) of the San Ysidro fault, the Atrisco Member lies beneath the Rio Puerco Member in the subsurface (see Connell, 2004, 2008a, 2008b).

The younger unconformity is best preserved on the footwall (west side) of the San Ysidro fault (Fig. 2.42). There, it consists of a ~1-m (~3-ft)-thick petrocalcic paleosol (Stage III carbonate morphology) that separates late Pleistocene to Holocene strata (generally not faulted) from older, faulted Ceja Formation.

Stratigraphy of unit Qhwd

An approximately 35–50-m (115–160-ft)-thick succession of eolian, sheetwash, and colluvial sediment overlies the grayish Rio Puerco Member of the Ceja Formation. Hanging-wall wedge deposits (Qhwd) form a kilometer-scale, wedge-shaped unit created by filling of localized depressions, primarily generated by faulting, on the proximal hanging walls of intrabasinal normal faults in the Albuquerque Basin (Figs. 2.38, 2.42–2.44). This site has the best exposure of Qhwd in the Albuquerque Basin. Qhwd sediment is tan to reddish-yellow and composed of very fine- to medium-grained sand, locally with coarse-grained sands and pebbles, that is commonly bounded by calcic and/or cambic paleosols. These paleosols give the outcrop a horizontally striped appearance (Fig. 2.44). Qhwd units are mapped from the fault exposure below Station 1 to as far as 1 km (0.6 mi) distant (Figs. 2.40 and 2.44).

Eight stratigraphic units within Qhwd are provisionally recognized in the proximal hanging wall of the San Ysidro fault. Connell et al. (2026) provide sedimentologic details of these units for exposures below Station 1. Unit 1 is the uppermost stratigraphic unit and it consists of relatively loose, fine- to medium-grained sand. At Station 1, we view an exposure of the uppermost part of the unit (Fig. 2.45). Here, it is massive to vaguely laminated (horizontal-planar to low-angle). Unit 1 corresponds to eolian sand that accumulated on the top of the Rio Puerco escarpment. Prevailing winds are to the northeast, and sand was transported uphill via saltation and suspension. Wind-flow paths diverge after passing over the crest of the escarpment and turbulence is created, causing sand to be deposited onto a relatively thick dune on the ridge immediately above the escarpment. This sand wedges (thins) to the east, as reflected in the modern topography. Unit 1 exhibits no soil development and is likely Holocene in age. This unit extends

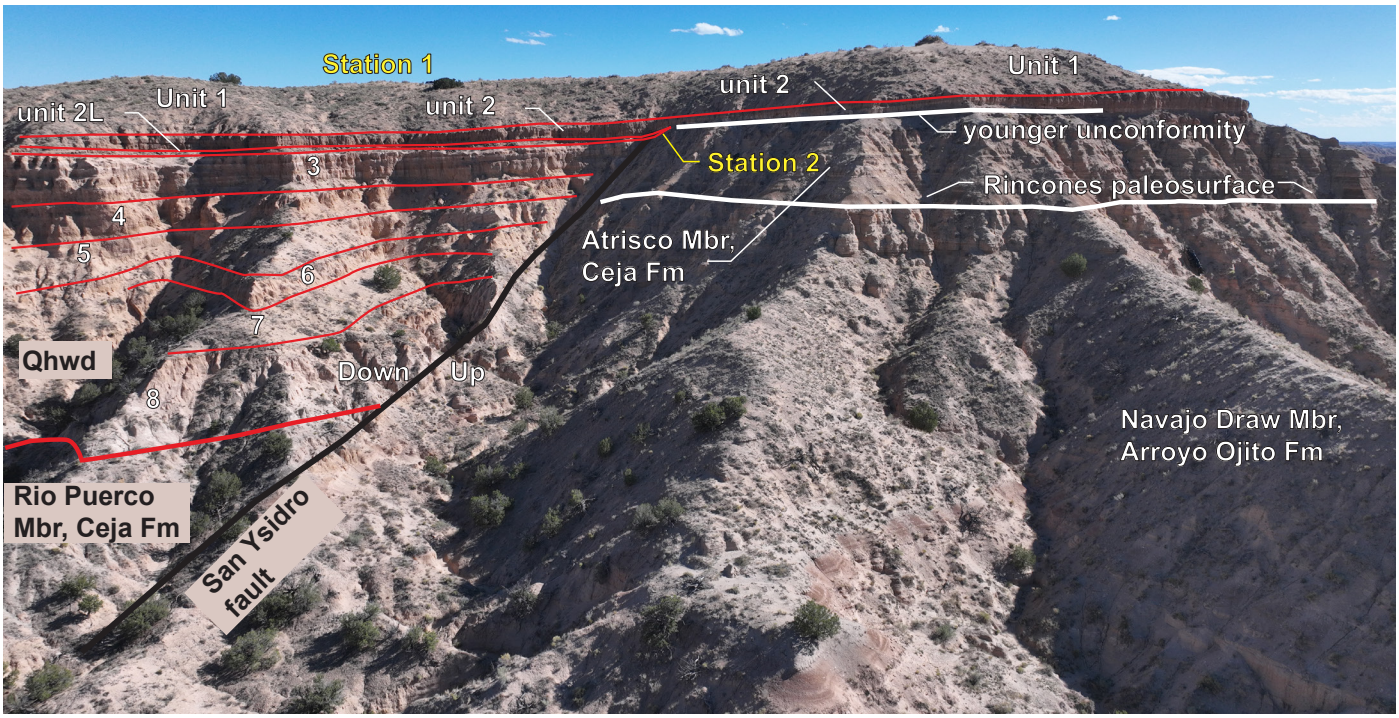


FIGURE 2.42. View to SSE of strata and fault on the north side of the spur ridge at Stop 1. The lower white line corresponds to a disconformity (Rincones paleosurface) separating the Ceja and Arroyo Ojito Formations. The lower thick red line east of the San Ysidro fault is the contact separating the Ceja Formation from overlying hanging wall wedge deposits (Qhwd). For this area immediately adjacent to the San Ysidro fault, the Qhwd units are provisionally labeled units 1 through 8 (top to bottom). Units 2 through 8 are collectively 24 m (79 ft) thick, and overlying eolian dune sand (unit 1) is approximately 12–15 m (40–50 ft) thick. Qhwd consists of eolian sand, sheetwash, and minor colluvium (including colluvium from paleo fault scarps) that filled in a depression created by movement along the San Ysidro fault (Connell et al., 2026).

well onto the fault footwall and thus may not technically be part of Qhwd.

Unit 2 is a distinctive 3–4 m (10–13 ft)-thick ledge that lies below unit 1 and above the distinctly striped unit 3 (Figs. 2.42–2.44). It corresponds to cumulic paleosols composed of slightly silty and clayey, very fine- to medium-grained sand. Paleosol are stacked and exhibit Stage I to I+ pedogenic carbonate morphology. Near the fault is a poorly exposed lower subunit (2L) composed of sand with pebbles (Fig. 2.42).

Unit 3 is a 4–5-m (13–16-ft)-thick ledge below unit 2. Unit 2 sediment is composed of well-bedded, very fine- to medium-grained sand with multiple calcic horizons (Stage III morphology), which give the outcrop a distinctive striped appearance.

Units 4 through 6 consists of medium- to thickly bedded, very fine- to medium-grained sand with scattered pebbles. This sequence contains stacked calcic paleosols that exhibit Stage II to III carbonate morphology. The top and bottom of the sequence (units 4 and 6, respectively; Figs. 2.42 and 2.43) corresponds to a light-orange sand that contains cambic, illuviated clay, and calcic horizons (Stage I to II pedogenic carbonate morphology). These two units are difficult to map 1 km (0.6 mi) to the northeast. Collectively, units 4 through 6 is 10–12 m (33–40 ft) thick.

Unit 7 is a grayish, loose pebbly sand that is ~2 m (~6 ft) thick. It is inferred to have been deposited by a strike-parallel paleodrainage on the immediate hanging wall of the San Ysidro fault. It appears to pinch out about 1 km (0.6 mi) to the northeast this stop.

The lower ~10 m (~30 ft) of Qhwd consists of a whitish compound unit containing about 8 calcic paleosols (Stage I to II morphology) with reddish-yellow to yellowish-brown cambic horizons and locally illuviated-clay horizons. The sediment is mainly fine- to medium-grained sand.

Waypoint 2.30 [N35.2314°, W106.8631°]

Station 2: San Ysidro Fault Zone and Proximal Hanging-Wall Wedge Deposits

Station 2 is an optional hike that involves a descent town a steep hill to an exposure of the San Ysidro fault (Fig. 2.38),

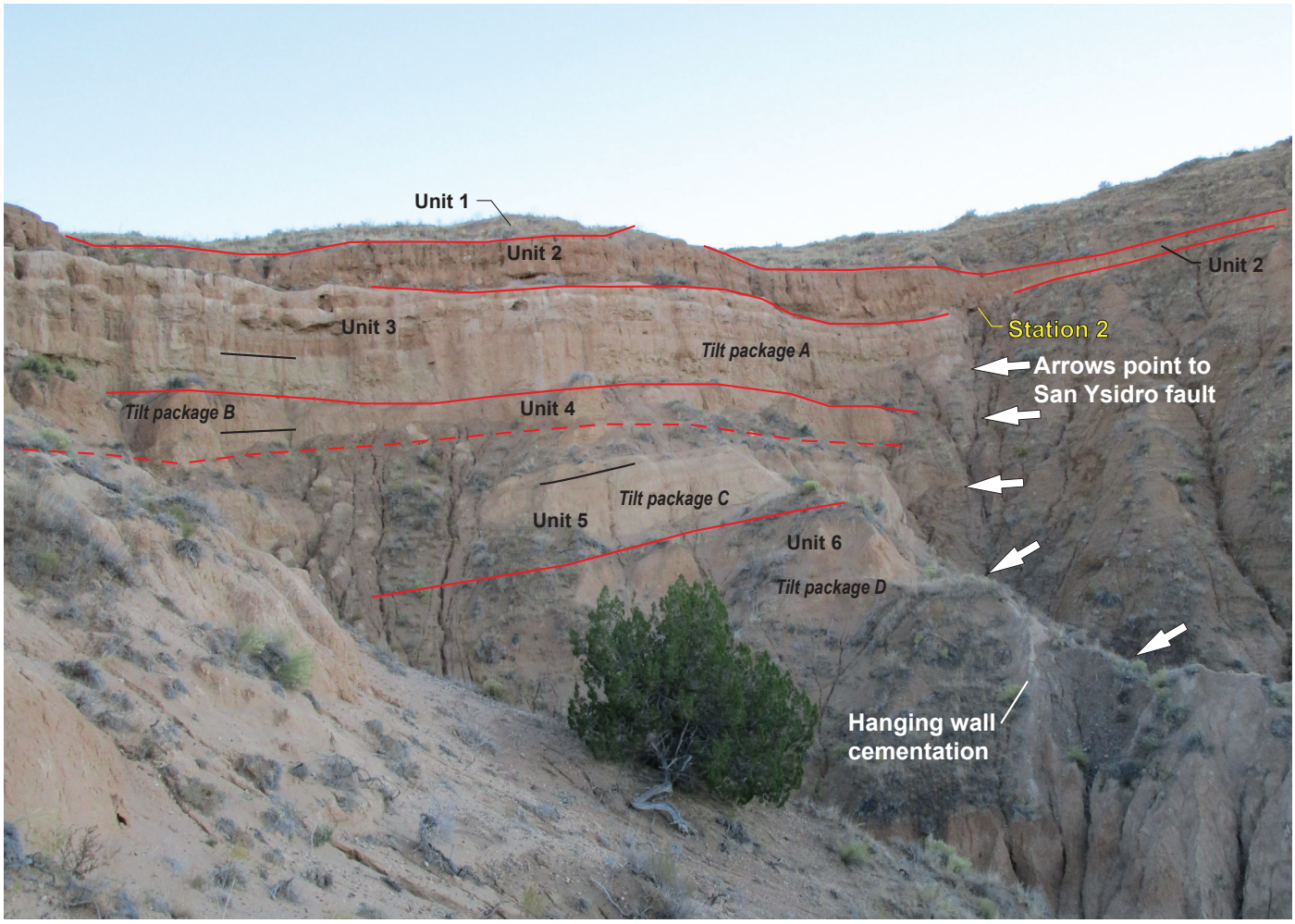


FIGURE 2.43. Photograph looking southward at the stratigraphy on the immediate hanging wall of the San Ysidro fault (white arrows). Stratigraphic divisions of Qhwd (units 1 through 8) are provisional and only apply to the area adjacent to the fault; these units are summarized in the text. Four tilt packages (A, B, C, and D) are tentatively proposed based on apparent angular relations, corresponding respectively to units 3, 4, 5, and 6.

where participants can (1) determine what strata are offset and those that are not; (2) identify and compare soil-bounded colluvial wedges associated with a fault scarp versus soil-bounded units that may not be directly related to fault movement; and (3) inspect the details of the San Ysidro fault zone and compare this zone with the Pilares fault (Stop 1, Station 4). Be careful in descending and follow the flags, since there is only one safe passage past a ledge. Going any other way may result in injury.

The study of paleoseismology concerns itself with the earthquake record over geologic time. It commonly involves closely inspecting faulted Quaternary sediment and using various dating methods and cross-cutting relations to decipher the ages and displacements associated with past rupture events (McCalpin, 1996). The upper diagram of Figure 2.46 illustrates what happens on the surface after a large seismogenic rupture on a normal fault in weakly cohesive to unconsolidated deposits. A fault scarp is created that soon erodes to deposit colluvium in the proximal hanging wall of the fault. Shortly after the quake, the fresh scarp (which may be steeper than the angle of repose) erodes relatively quickly, depositing colluvium and sandy sheetwash deposits. But erosion rates for the scarp face lessen as the scarp's slope decreases (Wallace, 1977). Eventually soil formation occurs on the top of the fault-scarp colluvium during a time of quasi-geomorphic stability (Fig. 2.46, top).

Annotated photographs show the stratigraphic relations at Station 2 (Figs. 2.42, 2.47, and 2.48). Note how rim-dune sand extends across the San Ysidro fault with no change in thickness or obvious vertical displacement. In contrast, unit 2 thins (tapers) appreciably westward across the San Ysidro fault, but there is no sign that it has been offset by the fault (Figs. 2.47 and 2.48). At the base of unit 2 is a strong calcic horizon a few decimeters thick (unit 2 calcic marker soil; Figs. 2.47 and 2.48). East of the fault, the interval of calcic paleosols broadens and becomes more diffuse; evidently, more accommodation allowed higher sedimentation rates and more diffuse precipitation of calcium carbonate. The unit 2 marker soil is not notably offset by the fault.

Unit 2L is offset by the fault (white arrows in Fig. 2.48). Unit 2L consists of sand with 10–15% pebbles, with the latter being scattered or in thin beds that are inclined toward the fault. We interpret unit 2L as younger fault-scarp colluvium and slope wash because of its coarse-grained texture and the fact that it appears to wedge out a short distance west of the fault. Unit 2L continues a couple hundred meters to the northeast (away from the fault) before pinching out. Similar-textured sand with pebbles below unit 2L (at the top of unit 3) is interpreted as older fault-scarp colluvium and slopewash (Fig. 2.47). After this older sediment was deposited, there was a sufficient duration of stability to overprint the top of unit 3 with soil development. However, the wedge-shaped nature of the older colluvium (top of unit 3) is not obvious.

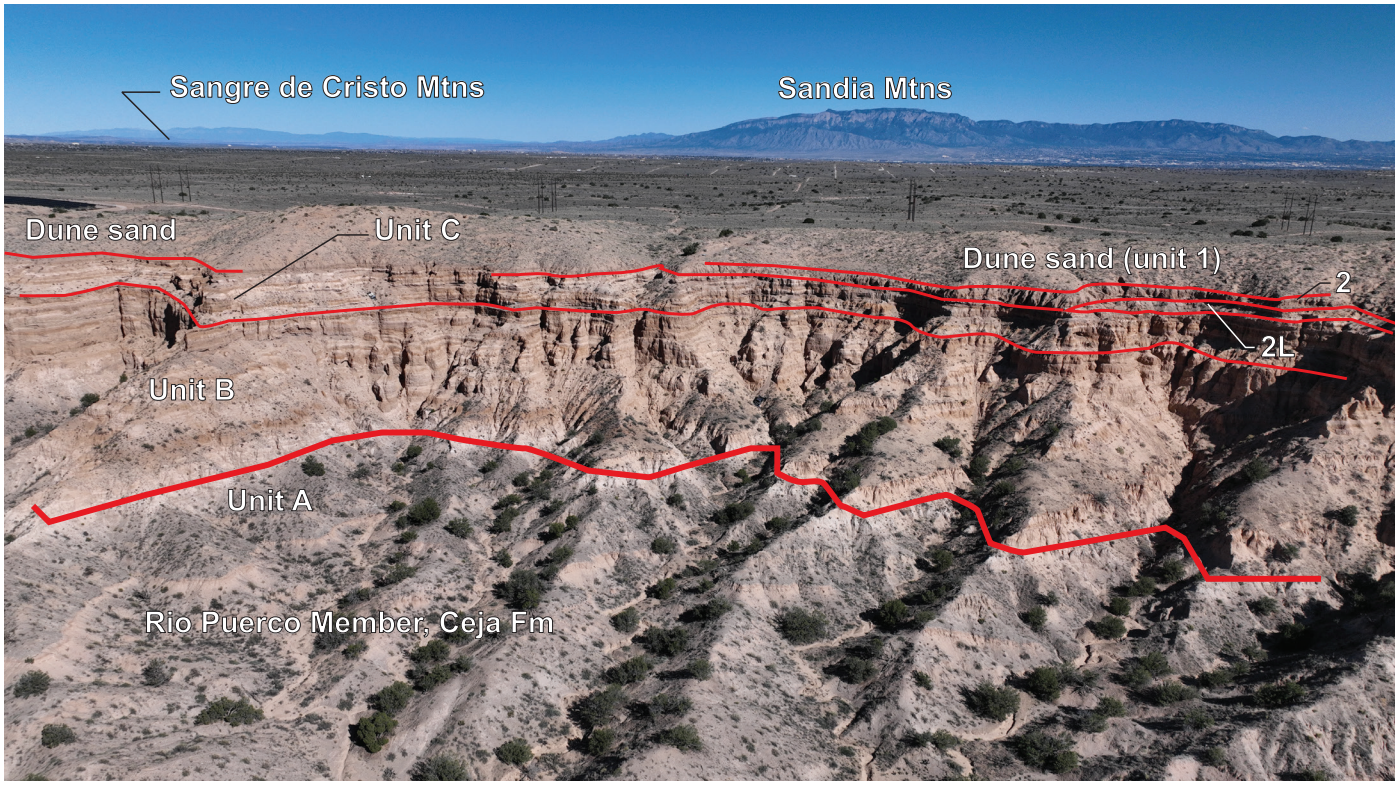


FIGURE 2.44. View of southeast side of the Stop 1 amphitheater. The lower, thick red line separates the Ceja Formation from overlying brownish to reddish sediment of unit Qhwd. Three units of Qhwd (Connell et al., 2026) are separated by thinner red lines and labeled in white text. These units approximately correlate to those adjacent to the fault (Figs. 2.42 and 2.43) as follows: Units A (base of unit 8 and underlying Ceja Formation), B (units that are remainder of unit 8 through unit 6), and C (units 1 through 5). At the top of unit A is the strongly developed calcic soil underlying the Llano de Albuquerque, but its burial here by Qhwd means that its minimum age is notably older than the minimum age of the Llano de Albuquerque surface. Cumulic paleosol development in unit 2 made it resistant to erosion and a laterally extensive ledge former.

Using these observations, a preliminary interpretation of the latest activity on the San Ysidro fault is as follows:

1. Generation of a fault scarp and deposition of the older colluvium (upper unit 3);
2. Geomorphic stability occurred and a Stage II+ soil formed at the top of unit 3 (there may still have been a paleoscarp to the immediate west);
3. Another rupture event occurred followed by erosion of the steep fault scarp that deposited pebble-bearing sand, forming unit 2L;
4. The last rupture was relatively small, creating an offset of only a few decimeters in pebble lenses of unit 2L (Fig. 2.48);
5. The fault scarp stabilized sufficiently that a Stage III calcic soil formed on top of unit 2L (i.e., the unit 2 calcic marker soil); a Stage III calcic horizon typically corresponds to late Pleistocene ages, and probably takes few to several tens of thousands years to form (Bachman and Machette, 1977; Gile et al., 1981);
6. The remainder of unit 2 accumulated via eolian and sheetwash sedimentation but at a slow rate, allowing a cumulic soil to form consisting primarily of cambic (Bw) horizons; this likely occurred in the latest Pleistocene to early Holocene;
7. Drier conditions in the Holocene resulted in the accumulation of dune sand along the rim.

Personius and Mahon (2003) recognized that eolian sand sheets are commonly seen in exposures of faulted middle and upper Quaternary sediment. They posited that eolian sheets on the hanging wall of a normal fault in a sandy rift setting are preferentially formed after an earthquake event. Thus, the age of the eolian sheet would be close to the age of a rupture event. However, Connell et al. (2026) emphasize that in the Albuquerque Basin paleoclimate-controlled depositional events can occur at a higher frequency than earthquake events, which



FIGURE 2.45. Eolian sediment of unit 1observed at Station 1 (blue book is 20 cm [8 inch] long). Inset photograph illustrates the massive to vaguely laminated sand typical of the unit.

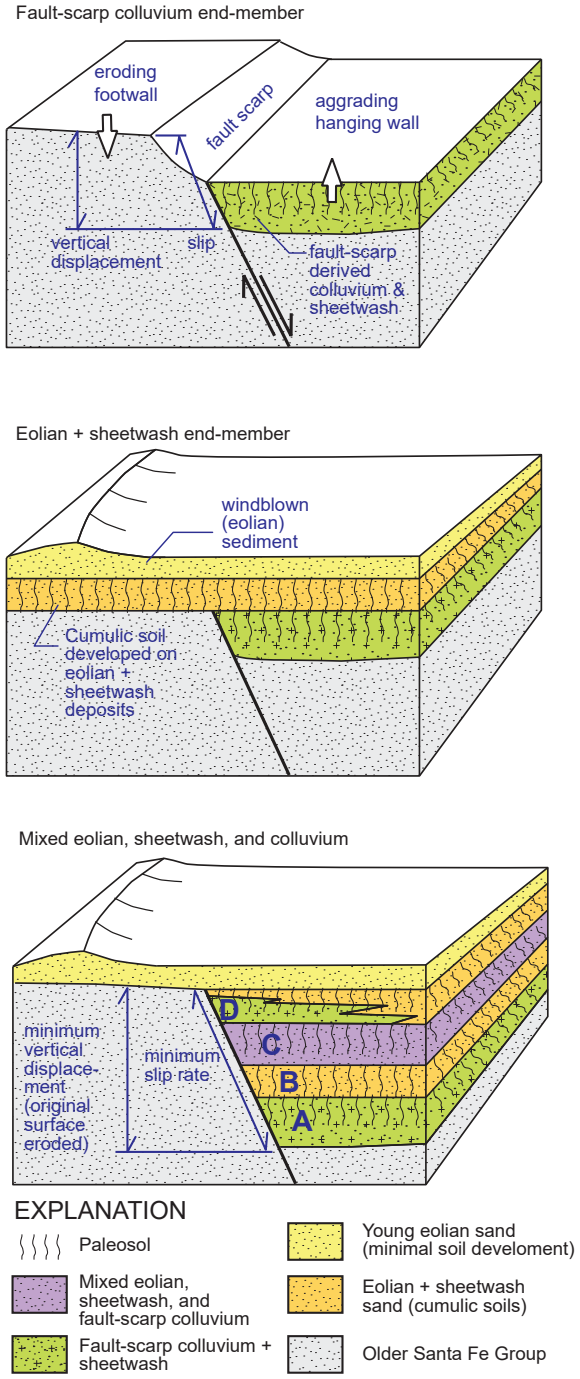


FIGURE 2.46. Three-dimensional block diagrams illustrating a schematic geomorphic history of Qhwd. Top diagram: Sediment derived from erosion of the fault scarp shortly after a rupture event. Middle diagram: Orange and yellow units are formed by eolian sedimentation that initially extends across the fault. If rates of eolian deposition are sufficiently low, then soils can form. Bottom diagram: Summary of the different types of sedimentation comprising soil-bounded units of Qhwd: (A) strata consist primarily of colluvium and sheetwash deposits sourced from the fault scarp; this is directly related to rupture along the fault; (B) eolian deposits; these deposits were reworked by sheetwash, not directly related to a rupture event but later preserved (downthrown) by a rupture event; (C) eolian and colluvial deposition occurred synchronously and partly related to a rupture event; and (D) fault-scarp derived colluvium interfingers with eolian sediment (including eolian sediment reworked by sheetwash). The colluvium is related to the rupture event, but the overlying eolian and sheetwash sediment may not be.

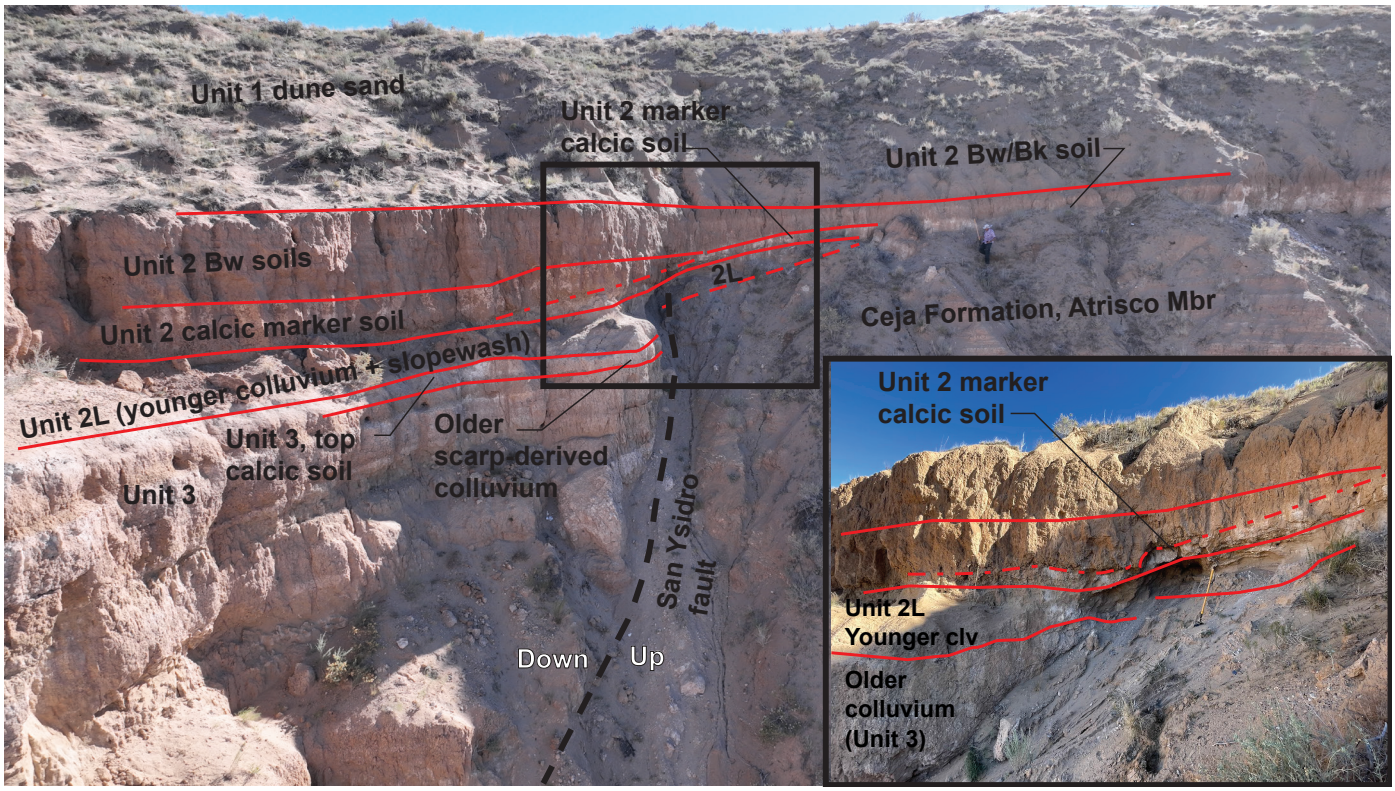


FIGURE 2.47. View to south-southwest illustrating stratigraphic relations at Station 2 (Stop 2). Units are separated by red lines. The dashed-dotted line illustrates a leftward gradation from the calcic horizon to the right (unit 2 marker calcic soil) to thicker calcic horizons with less concentrated calcium carbonate precipitation. Note how units 1 and 2 of Qhwd extend across the San Ysidro fault without being offset, although unit 2 tapers notably to the west on the fault footwall. This westward tapering probably reflects paleotopography that existed during unit 2 deposition. Initially, slow eolian-driven sedimentation completely filled in the originally lower topographic surface that existed immediately east of the paleoscarp. The paleoscarp was then buried by unit 1. Unit 2L is probably colluvium and slopewash directly eroded from the paleoscarp, with minimal eolian input. The upper part of unit 3, immediately adjacent to the fault, is pebbly and inferred to be colluvial detritus shed from an older buried scarp.

greatly complicates efforts to interpret the paleoseismicity of a given fault.

At Station 2, we can observe such complexity using the stratigraphy at and above the fault exposure. Note how eolian and sheetwash sand sheets can drape over the fault (units 1 and 2; Fig. 2.42), even where a scarp is present. These two units are not directly related to fault movement but probably are influenced by paleoclimate change near the last glacial-interglacial boundary. If a large earthquake were to occur, units 2 and basal unit 1 would likely be down-dropped and juxtaposed against the uppermost Atrisco Member (one can use Fig. 2.47 to mentally recreate this scenario), but their age would not align to that rupture age or the previous rupture age. Extending this concept means that not every soil-bounded unit on the hanging wall of the San Ysidro fault at Stop 2 corresponds to a unique earthquake event, although in the long term these eolian and sheetwash are preserved due to subsidence of the fault hanging wall. Rather, one needs to delineate scarp-derived colluvial wedges to identify individual rupture events. Recognizing the two separate deposit types (eolian and sheetwash versus colluvium and sheetwash) is challenging. We posit that the presence of pebbles and overall wedge-shaped geometry of deposits on the proximal hanging wall (i.e., thickest adjacent to fault but tapering or interfingering away from the fault) may be criteria for identifying past ground-rupturing events.

Notwithstanding these difficulties in interpretating lithofacies and event stratigraphy, this exposure provides a long-term record of paleoseismic activity along the San Ysidro fault over the past 1.8 Ma. Assuming each major slip event involves 0.5 m (~1.5 ft) of throw (maximum range based on McCalpin et al., 2011), then the ~27–28 m (~88–92 ft) of Qhwd sediment

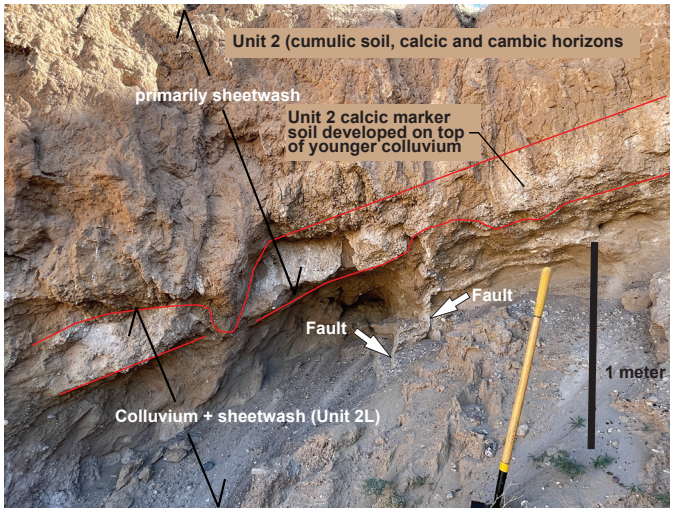


FIGURE 2.48. View to south of cross-cutting relations across the San Ysidro fault (white arrows).

buttressed by the fault (units 2L through 8) indicate approximately 54–56 events since Ceja deposition less than 1.8 Ma ago. A long-term throw rate can be calculated of 0.02 mm/year, but this is a minimum because the top of the Ceja Formation on the corresponding footwall may been eroded (Fig. 52, lower block). However, this slip rate compares favorably with the 0.01–0.03 mm/yr interpreted by McCalpin (2025) using upper Pleistocene strata. Note that slip rates of 0.02–0.2 mm/yr are typical for most large, middle–late Quaternary faults in the Rio Grande rift (Personius et al., 1999; Wong et al., 2004; van Wijk et al., 2018; McCalpin, 2025).

Lastly, we turn our attention to the capping massive sand (Figs. 2.42 and 2.47). It is relatively massive, but vague laminations can locally be seen (Fig. 2.45). The fact that such thick eolian sands are not recognized in the paleosol-bounded succession of Qhwd may possibly be ascribed to (1) tectonic subsidence per earthquake event <1 m (<3 ft) so only the basal part of the ridge-top sand dune can be preserved; and (2) the ridge-line sand dune may have only arrived here in the late Pleistocene after the last earthquake event on the San Ysidro fault. The latter reason invokes a conceptual model that this unusual Holocene thickness is due to the eastward migration of the top of the escarpment to this area in the last few tens of thousands of years (Fig. 2.49). Eolian sand sheets and dunes are particularly thick on top of the crest of the Ceja del Rio Puerco. Prevailing western winds deflate sand from the sandstone-dominated Santa Fe Group and transport this sand (via saltation and suspension) eastward to the top of the ridge. But turbulence on the immediate leeward side of the ridge (due in part to diverging wind flow paths) causes these sand particles to drop out and form a ridge-line sand dune. Maybe eastward slope retreat of the escarpment resulted in the ridge-top dune only migrating here in the past few tens of thousands of years (Fig. 2.49). **Return to vehicles.**

End Stop 2

4.7 **Turn right (north)** on the dirt road under the powerlines. *1.0*

5.7 **Waypoint 2.31 [N35.2416° W106.8563°]**
Return to the west end of Southern Boulevard. Turn right and drive east along Southern Boulevard. *9.0*

14.7 **Waypoint 2.32 [N35.2312°, W106.6969°]**
Intersection of Southern and Unser Boulevards. **Turn right (south) on Unser Boulevard.** *19.4*

34.1 **Waypoint 2.33 [N35.1016°, W106.6662°]**
Return the way we came to the New Mexico Museum of Natural History.

End of Day 2 Road Log

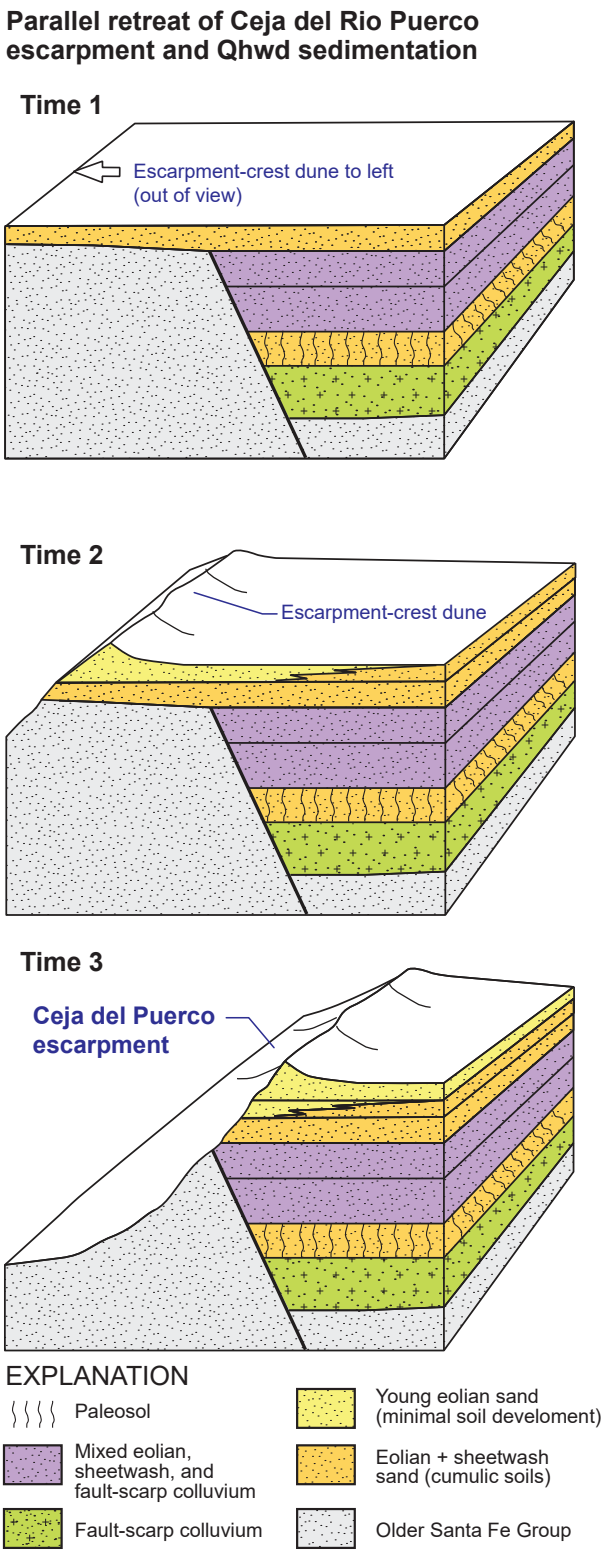


FIGURE 2.49. Block diagrams illustrating the eastward migration of the Ceja del Rio Puerco escarpment and preservation of thick eolian sands in the stratigraphic record. Successive blocks represent progressively younger time (from top to bottom).